

# The Institute of Paper Chemistry

Appleton, Wisconsin

## Doctor's Dissertation

Light Scattering in Fibrous Sheets

Edwin W. Arnold

June, 1962

LOAN COPY  
To be returned to  
EDITORIAL DEPARTMENT

# LIGHT SCATTERING IN FIBROUS SHEETS

A thesis submitted by

Edwin W. Arnold

S.B. 1957, Massachusetts Institute of Technology  
M.S. 1960, Lawrence College

in partial fulfillment of the requirements  
of The Institute of Paper Chemistry  
for the degree of Doctor of Philosophy  
from Lawrence College,  
Appleton, Wisconsin

June, 1962

# TABLE OF CONTENTS

	Page
STATEMENT OF THE PROBLEM	1
INTRODUCTION	2
Light Scattering in a Fibrous Sheet	2
Review of the Kubelka-Munk Theory of Light Scattering	3
Summary of the Previous Work Relating the Optical Properties of Paper to Individual Fiber Properties	5
LIGHT SCATTERING BY SMALL PARTICLES	10
THE RELATIONSHIP BETWEEN THE SPECIFIC SCATTERING COEFFICIENT AND THE LIGHT BACK-SCATTERED FROM A UNIT LENGTH OF FIBER	24
DETERMINATION OF THE BACK-SCATTERED LIGHT FROM A UNIT LENGTH OF FIBER	25
EXPERIMENTAL	27
Preparation and Characterization of the Fibers	27
Glass Fibers	27
Nylon Fibers	30
Orlon Fibers	32
Preparation of the Sheets	33
Measurement of the Scattering and Absorption Coefficients	36
Summary of Fiber Characteristics	43
Effect of Fiber Length on the Specific Scattering Coefficient	44
Effect of Basis Weight on the Specific Scattering Coefficient	46
Specific Scattering and Absorption Coefficients of the Synthetic Fibers	46
Glass Fibers	46
Nylon Fibers	49
Orlon Fibers	49
Comparison of the Scattering Power of Pulp Sheets Determined on the Normal GERS and on the Modified GERS	58

	Page
DISCUSSION OF RESULTS	60
Theoretical Results	60
Discussion of the Experimental Results for Nylon and Orlon Sheets	73
Discussion of the Optical Techniques Used to Determine Individual Fiber Properties	80
SUMMARY AND CONCLUSIONS	84
ACKNOWLEDGMENTS	86
NOMENCLATURE	87
LITERATURE CITED	89
APPENDIX I. DETAILS OF THE NUMERICAL INTEGRATION PROCEDURE	91
APPENDIX II. SCATTERING DIAGRAMS	94
APPENDIX III. THE DISTRIBUTION OF LIGHT REFLECTED FROM A SINGLE FIBER	137

## STATEMENT OF THE PROBLEM

The reflectance and transmittance properties of paper have been extensively studied in the past. Two reasons for this are: (a) The reflectance and transmittance properties are important in many end uses to which paper is put. (b) There have been repeated attempts to relate the reflectance and transmittance behavior of paper to individual fiber properties.

These studies have been handicapped by the lack of a theoretical relationship between the reflectance and transmittance properties of the sheet and the optical properties of the individual fibers. The present investigation was undertaken to formulate such a relationship. The relationship that was found was tested with the use of synthetic fibers, which more closely approach the assumptions used in the development than pulp fibers do. From these equations and from the data which were collected, it is possible to form a critical evaluation of the bases used to determine individual fiber properties from the optical properties of the sheet.

## INTRODUCTION

### LIGHT SCATTERING IN A FIBROUS SHEET

Light scattering may be defined as the deflection of a ray of light due to the presence of a particle or optical discontinuity in the vicinity of the light ray. The mechanism by which light is scattered may be considered reflection and refraction at the air-solid surface, refraction due to optical discontinuities, and diffraction of the light around the boundaries of the solid object. Since light is an electromagnetic wave, the propagation of the electric and magnetic fields can be rigorously described by the Maxwell equations.

A sheet of paper made from pulp fibers is a very complex material on a microscopic scale. There may be more or less whole pulp fibers, fiber fragments, inorganic pigments and fillers, and various adhesives present in the sheet which are distributed in a nonuniform and unknown manner. The boundary conditions for the Maxwell equations would be very complex for this type of structure. The structure could be simplified considerably by using only whole pulp fibers in the sheet. However, neither the optical properties nor the shapes of the fibers are adequately known to allow one to set up the proper boundary values for the Maxwell equations.

About the simplest structure which still resembles a pulp sheet is a sheet composed of uniform, transparent fibers whose cross sections are circular and which are arranged randomly in the plane of the sheet. This type of structure is still not amenable to a rigorous analysis based upon the complete solution to the Maxwell equations for the sheet as a whole. The reason for this is that once the proper boundary conditions were found, there is little chance that the Maxwell equations could be solved.

This type of structure can be analyzed if the assumptions are made that each unit length of fiber is illuminated with the same light distribution and that each unit length of fiber scatters independently from adjacent fibers.

The use of these assumptions allows one to relate the optical properties of the fibers to the optical properties of the sheet.

#### REVIEW OF THE KUBELKA-MUNK THEORY OF LIGHT SCATTERING

Kubelka and Munk (K-M) (1) in 1931 developed a theory in which the reflectance and transmittance properties of a paper sheet could be calculated if the thickness and the scattering and absorption coefficients were known. The K-M theory has been described in detail by Steele (2). Using the modification suggested by Van den Akker (3) that the basis weight rather than thickness be used, the theory can be summarized as shown below.

A sheet of basis weight  $\underline{W}$  is illuminated diffusely from above. The term "diffuse" will be used to indicate unpolarized light coming from all directions. If the light intensity coming from each direction is equal, it will be called isotropic illumination. Let us imagine a layer of differential basis weight,  $d\underline{W}$ , in the interior of the sheet and parallel to the surfaces. Let the light moving downward onto the differential layer be called  $\underline{i}_T$  and the light moving upward from the layer,  $\underline{i}_R$ , as shown in Fig. 1.

The specific scattering coefficient,  $\underline{s}$ , may be defined as the fraction of the light which is incident on a differential layer that is back scattered per unit basis weight, and the specific absorption coefficient,  $\underline{k}$ , may be defined as the fraction of light which is absorbed by a differential layer per unit

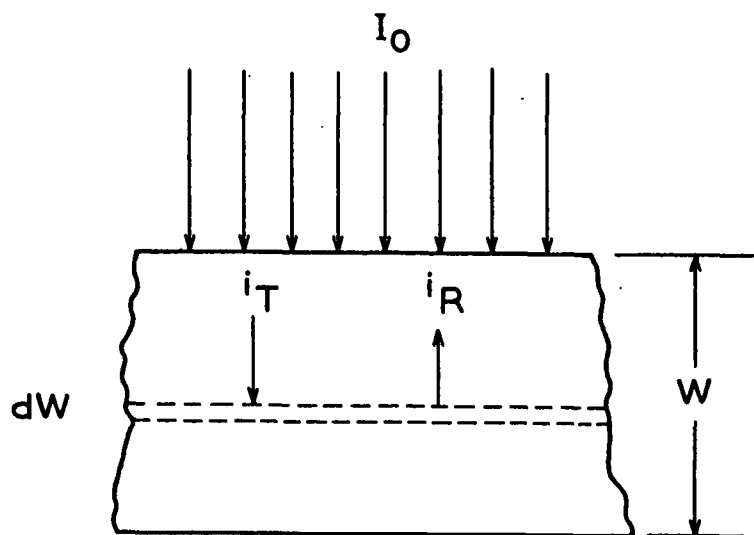


Figure 1. Development of the Kubelka-Munk Theory

basis weight. With these definitions, the changes in  $\underline{i_T}$  and  $\underline{i_R}$  as the light passes through the differential layer are given by:

$$-di_T = -(s + k)i_T dW + si_R dW \quad (1)$$

$$di_R = -(s + k)i_R dW + si_T dW \quad (2).$$

Equations (1) and (2) can be solved if the boundary conditions for the reflectance of the backing material in contact with the lower surface,  $\underline{R_g}$ , and the total basis weight,  $\underline{W}$ , are known. When this is done, the reflectance and transmittance of a sheet of paper can be calculated as a function of  $\underline{W}$ ,  $\underline{s}$ , and  $\underline{k}$ . Kubelka (4) gives an extensive list of the solutions to the equations for various types of backing materials.

Judd (5) has critically examined the K-M theory and experimentally verified its applicability to paper sheets. This has been confirmed by some further work by Judd (6) and by Stenius (7-11). These men found small differences between the



optical properties predicted from the K-M theory and the experimental values. The order of magnitude of the differences was about 1% difference between the experimental and the theoretical values.

The excellent agreement between theory and experiment indicates that the assumptions in the K-M theory are very nearly correct. The basic assumption used by Kubelka in order to solve Equations (1) and (2) is that the specific scattering and absorption coefficients are uniform throughout the sheet. This means either that the light distribution incident on each layer of the sheet is constant or that the scattering and absorption coefficients are independent of the light distribution.

Later in the thesis, it will be necessary to compare the scattering coefficients of fibrous sheets composed of fibers of different densities. It is convenient to define a volume scattering coefficient,  $\underline{s}_v$ , for these comparisons which is defined as the product of the specific scattering coefficient times the density of the fibers,  $\rho_f$ . For the same reason, the specific surface,  $\underline{A}_v$ , is defined as the surface area per cubic centimeter of fiber.

#### SUMMARY OF THE PREVIOUS WORK RELATING THE OPTICAL PROPERTIES OF PAPER TO INDIVIDUAL FIBER PROPERTIES

As early as 1940, Davis (12) suggested that the specific scattering coefficient was proportional to the surface area per unit mass of particles in the sheet. Parsons (13) used this concept to find the relative bonded area in a sheet of paper. He found experimentally that  $\underline{s}$  was linearly related to the external specific surface of a pulp which he determined by means of the silvering technique. He also found that the linear curve extrapolated to a positive intercept on the  $\underline{s}$  axis at zero specific surface. Ratliff (14) used the technique of

Parsons and found a linear relationship between  $\underline{s}$  and specific surface determined by the silvering method. Ratliff, however, found that his curve of  $\underline{s}$  versus specific surface extrapolated to a zero intercept. Leech (15), in similar experiments, also found a straight-line relationship between  $\underline{s}$  and specific surface.

Haselton (16) compared  $\underline{s}$  with the specific surface of pulp fibers measured by means of the nitrogen adsorption of the fibers. He found a linear relationship which extrapolated to a slightly negative value of  $\underline{s}$  at zero specific surface.

Some later work by Ingmanson and Thode (17) and Swanson and Steber (18) has cast doubt on the linearity of the curve of  $\underline{s}$  versus specific surface, at least for certain types of pulps. Part of the data of Ingmanson and Thode, from their Fig. 3, is replotted in Fig. 2. Ingmanson and Thode indicate that there is a great deal of scatter in their data, so the fact that the curves are nonlinear may not be statistically significant. There are also the complications associated with solvent exchanging the handsheets with acetone and finally with butanol which may have caused a loss of fines to an unknown and uncontrolled extent. However, their data do indicate that  $\underline{s}$  versus specific surface may be nonlinear in certain situations. Ingmanson and Thode found that the scattering coefficient of their pulps decreased as the wavelength of light used to determine  $\underline{s}$  increased.

Swanson and Steber correlated the specific scattering coefficient with the specific surface as measured by the nitrogen adsorption method for sheets made from three different pulps: (a) Weyerhaeuser bleached sulfite pulp, (b) Coosa bleached gum pulp, and (c) Bloedel unbleached kraft pulp. They varied both the degree of refining and the amount of wet pressing in order to produce handsheets of widely different surface areas and scattering coefficients. It is instructive to replot their data for Weyerhaeuser bleached sulfite pulp. This has been done

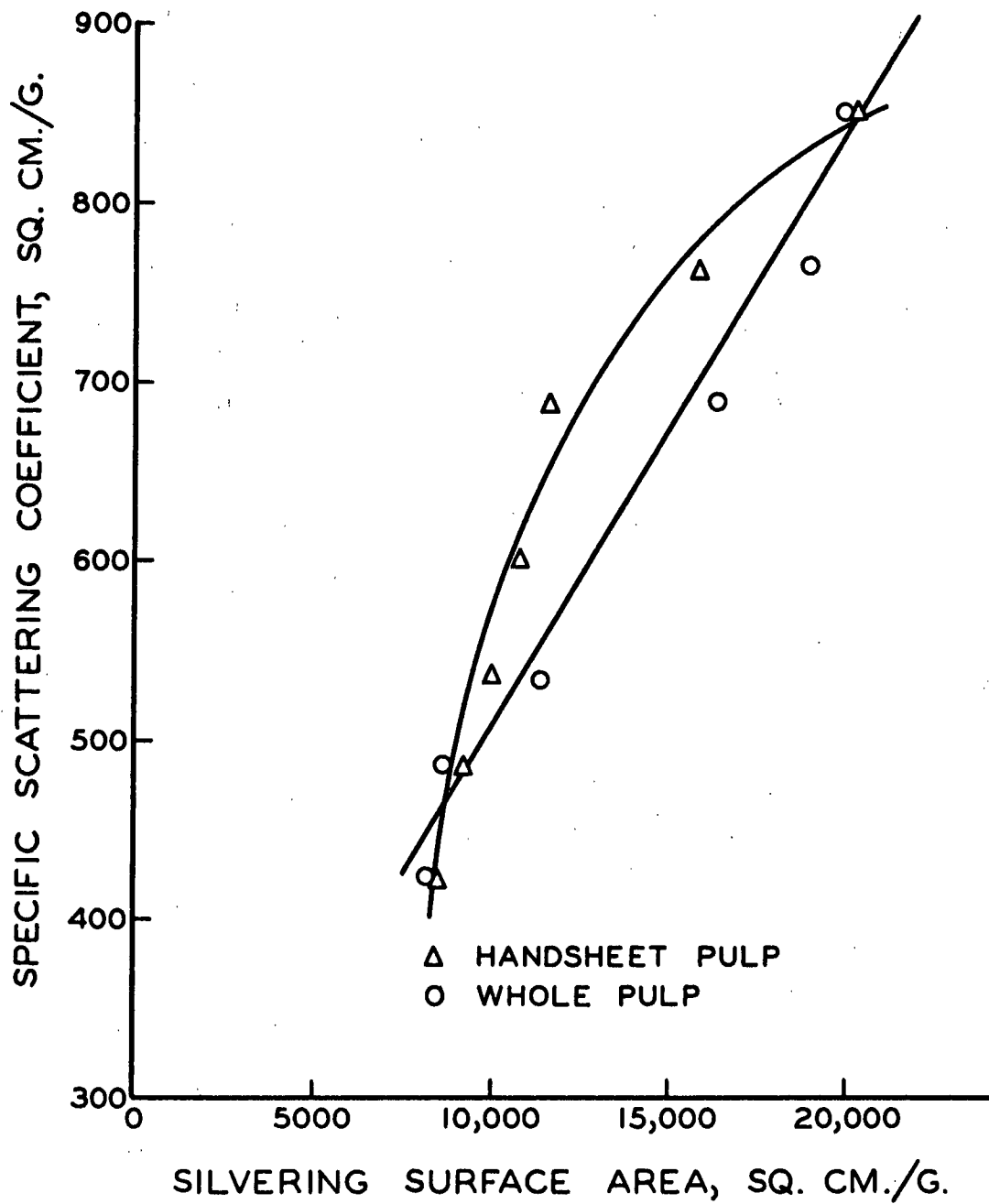


Figure 2. Butanol Specific Scattering Coefficient versus Surface Area from the Data of Ingmanson and Thode

in Fig. 3. It will be noticed that each beating interval plots as a separate, curved line. The data for the other two pulps were not as complete nor as consistent, so it is impossible to draw any conclusions concerning the linearity of the  $\underline{s}$  versus specific surface relationship from the behavior of these pulps. Swanson and Steber also found that the scattering coefficient for the Weyerhaeuser bleached sulfite pulp decreased with increasing wavelength; in the case of the Coosa bleached gum pulp the scattering coefficient was almost independent of wavelength, and with the Bloedel unbleached kraft pulp the scattering coefficient increased with increasing wavelength.

From this previous work, it is apparent that the scattering process in a sheet of paper must be more complex than the simple linear correlation,  $\underline{s} = \underline{KA}$ , would indicate, where  $\underline{K}$  is a proportionality constant. The causes of the non-linearity of the  $\underline{s}$  versus  $\underline{A}$  curves and the differences between the curves for pulps refined to different extents have never previously been studied. Also, the reasons for the apparently anomalous variation of  $\underline{s}$  with wavelength observed by Swanson and Steber have not been investigated.

The present study was undertaken in an attempt to find the reasons for these scattering phenomena and, in general, to examine the mechanism of light scattering in a fibrous sheet.

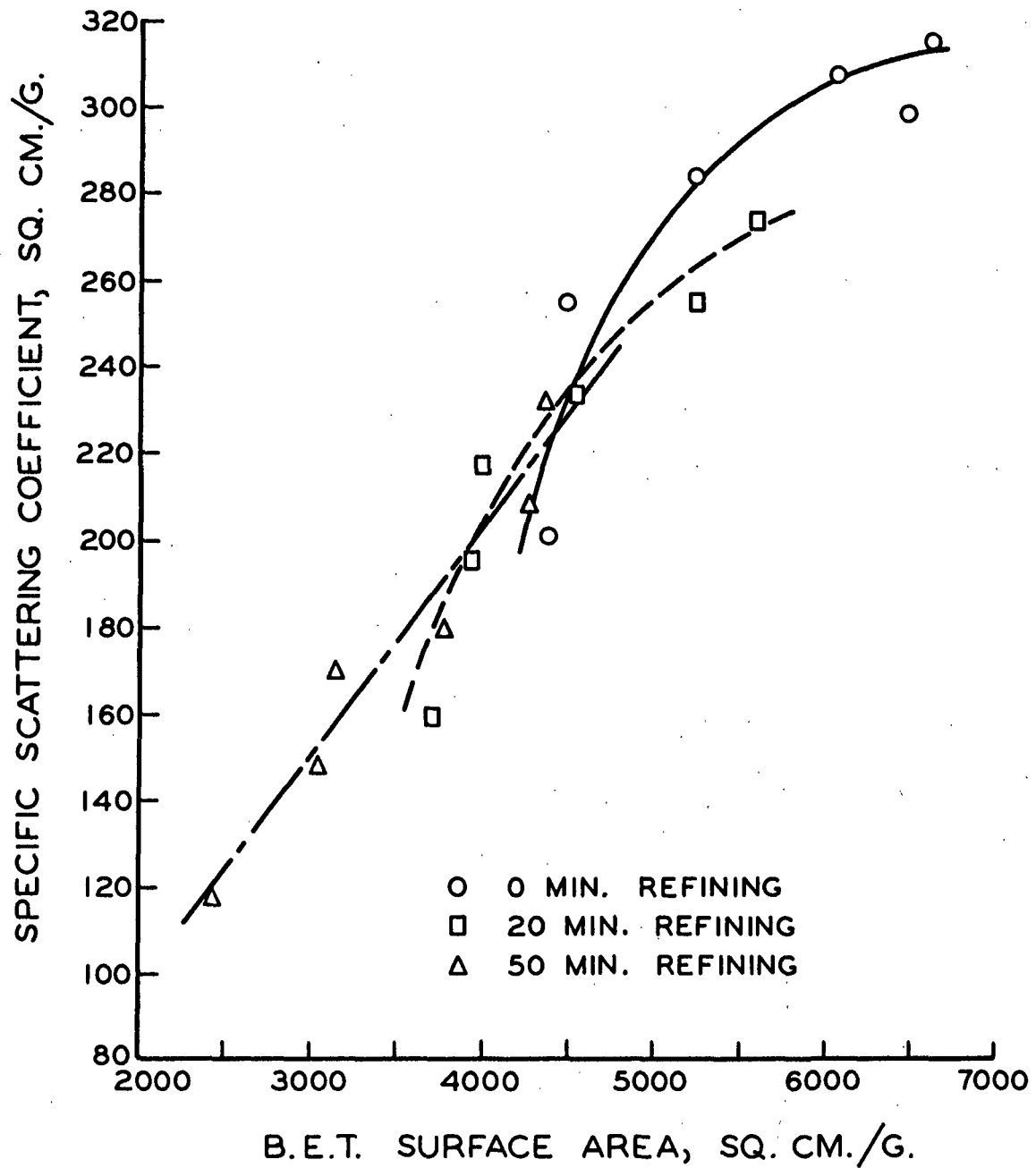


Figure 3. Specific Scattering Coefficient versus B.E.T. Surface Area from the Data of Swanson and Steber

## LIGHT SCATTERING BY SMALL PARTICLES

The scattering and absorption of electromagnetic radiation can be completely described by the Maxwell equations if the electrical and magnetic properties of the scattering body and the surrounding medium are known. In practice, the Maxwell equations are very difficult to solve, and it has been done only for certain limited situations. The form of the solution is often very complex and requires laborious numerical calculations to extract practical results. Because of the difficulty in obtaining numerical results from the complete electromagnetic equations, many workers have attempted to find approximations which are valid over certain ranges of particle sizes and optical properties.

One of the earliest approximations was that given by Rayleigh for very small particles whose largest dimension is much less than the wavelength of light. The approximation was extended to somewhat larger particles and is often called the Rayleigh-Gans theory of scattering. For particles much larger than the wavelength of light, the laws of geometric optics are approximately valid. The scattering from particles in the size range from about 0.5 to about 20 wavelengths of light requires the use of the complete electromagnetic equations to accurately describe the scattering, although the ray optics approximations begin to be valid for much of the scattering diagram when the particle size is above about 10 wavelengths of light. The glass fibers used in this investigation ranged from about  $5.7 \mu$  to about  $13.7 \mu$ . This corresponds to a diameter-to-wavelength ratio of from 8 to about 30 for visible light. Thus, it would be expected that the geometric optics approximations would describe many of the features of the scattering diagram for the larger fibers which were used.

No complete review of the literature of light scattering by small particles will be given here. The reader is referred to a review by Bouwkamp (19) and a book by Van de Hulst (20) for a more complete discussion of small particle scattering.

The model of a sheet which was chosen for analysis was an assemblage of circularly cylindrical fibers arranged so that their major axes were randomly oriented in the plane of the sheet. The light in a sheet of paper is diffused so the light strikes each fiber from all angles. Therefore, in order to find the total scattering from a unit length of fiber, it was necessary to find the scattering when light was incident on the fiber from any direction.

The complete electromagnetic equations have been solved for a plane wave incident on a dielectric cylinder at any angle of incidence by Wait (21), Burberg (22), and Wilhelmsson (23). The solutions are similar in each case. The solution given by Wait was used for the numerical computations since it was in a slightly simpler form than the others. The solution given by Wait is shown below.

Let a plane wave of light of wavelength  $\lambda^0$  be incident on a dielectric cylinder of radius  $a$ , as shown in Fig. 4. The light scattered is given by:

#### Polarization 1

$$\mathcal{E}_z = \sum_{n=-\infty}^{\infty} a_n H_n^{(2)}(\lambda_2 \rho) F_n \quad (3)$$

$$\mathcal{H}_z = \sum_{n=-\infty}^{\infty} b_n H_n^{(2)}(\lambda_2 \rho) F_n \quad (4)$$

#### Polarization 2

$$\mathcal{H}_z = \sum_{n=-\infty}^{\infty} c_n H_n^{(2)}(\lambda_2 \rho) F_n \quad (5)$$

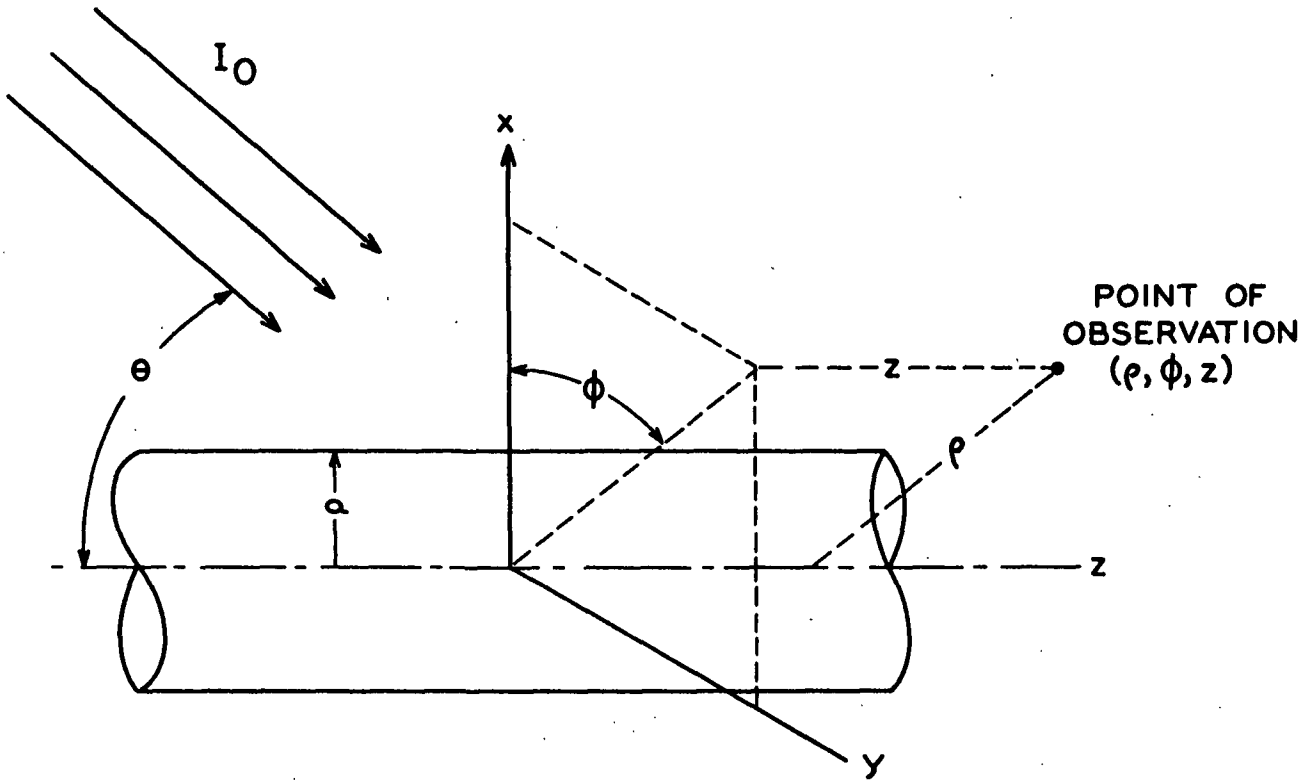


Figure 4. Light Incident on a Cylinder

$$-\mathcal{E}_z = \sum_{n=-\infty}^{\infty} a_n H_n^{(2)}(\lambda_2 \rho) F_n \quad (6)$$

where Polarization 1 represents an incoming plane wave linearly polarized in a plane defined by the fiber axis and the incident direction, and Polarization 2 represents a wave linearly polarized perpendicular to Polarization 1.

In Equations (3) through (6),  $H_n^{(2)}(\lambda_2 \rho)$  is a Hankel function of the second kind of order  $n$  and argument  $(\lambda_2 \rho)$ .

$$a_n = \mathcal{E}_0 (\sin \epsilon) i^n \left[ -\frac{J_n(v)}{H_n^2(v)} - \frac{2i \left( \frac{H_n^{(2)'}(v)}{v H_n^2(v)} - \frac{K J_n'(u)}{u J_n(u)} \right)}{\pi v^2 [H_n^2(v)]^2 D} \right] \quad (7)$$



$$b_n = \frac{\beta_2}{\mu_2 \omega} \mathcal{E}_0 (\sin \epsilon) i^n \left[ \frac{2}{\pi v^2} \left( \frac{1}{u^2} - \frac{1}{v^2} \right) \frac{n \cos \theta}{[H_n^{(2)}(v)]^2 D} \right] \quad (8)$$

$\underline{c}_n$  = similar to  $\underline{a}_n$  except  $\epsilon$  and  $\mu$  are interchanged, and

$\underline{\mathcal{E}}$  is replaced by  $\mathcal{H}$  and  $\mathcal{H}$  is replaced by  $-\underline{\mathcal{E}}$ .

$\underline{d}_n$  = similar to  $\underline{b}_n$  except  $\epsilon$  and  $\mu$  are interchanged and

$\underline{\mathcal{E}}$  is replaced by  $\mathcal{H}$  and  $\mathcal{H}$  is replaced by  $-\underline{\mathcal{E}}$ .

$$D = \left( \frac{H_n^{(2)'}(v)}{v[H_n^{(2)}(v)]} - \frac{KJ_n'(u)}{uJ_n(u)} \right) \left( \frac{H_n^{(2)'}(v)}{vH_n^{(2)}(v)} - \frac{N^2 J_n'(u)}{KuJ_n(u)} \right) - \left( \frac{1}{v^2} - \frac{1}{u^2} \right)^2 n^2 \cos^2 \theta \quad (9)$$

$J_n(\underline{Z})$  = Bessel's functions of the first kind of order  $\underline{n}$  and argument  $\underline{Z}$ .

Primes indicate derivatives of the Bessel's and Hankel's functions with respect to the argument.

$\mathcal{H}$  = magnetic amplitude vector component

$\underline{\mathcal{E}}$  = electric amplitude vector component

$\underline{F}_n = e^{-in\phi} e^{-i\beta_2 \underline{z}} \cos \theta e^{i\omega \underline{t}}$

$\underline{a}$  = fiber radius, microns

$\underline{m}$  = index of refraction

$\lambda^\circ$  = wavelength in vacuum (surrounding medium), microns

$\lambda_1 = (\beta_1^2 - \beta_2^2 \cos^2 \theta)^{1/2}$

$\lambda_2 = \beta_2 (\sin \theta)$

$\beta_1 = 2\pi \underline{m} / \lambda^\circ$

$\beta_2 = (\epsilon_2 \mu_2)^{1/2} \omega = 2\pi / \lambda^\circ$

$\underline{u} = \lambda_1 \underline{a}$

- $\underline{v} = \lambda_2 \underline{a}$   
 $\underline{N}^2 = \beta_1^2 / \beta_2^2$   
 $\underline{K} = \mu_1 / \mu_2$ , assumed to be 1.0 in the calculations  
 $\omega$  = angular frequency of incident light, radians/sec.  
 $\rho, \phi, z$  = cylindrical co-ordinates,  $z$  axis along fiber axis,  
the  $\phi = 0$  plane is the incident plane  
 $\theta$  = angle between fiber axis and incident direction  
 $\epsilon, \mu$  = inductive capacities  
subscript  $1$  = cylinder properties  
subscript  $2$  = surrounding medium properties

The far field approximations of Equations (3) through (6) can be formed by replacing the Hankel functions by their asymptotic expressions which are valid as the argument gets very large. An asymptotic expression for the Hankel function of the second kind is (24):

$$H_n^{(2)}(\lambda_2 \rho) = \sqrt{\frac{2}{\pi \lambda_2 \rho}} e^{-i(\lambda_2 \rho - \frac{2n+1}{4} \pi)} \quad (10)$$

It is convenient to define new coefficients in place of the ones used by Wait:

$$A_n = \frac{a_n}{i^n E_0 \sin \theta}, \quad B_n = \frac{b_n \mu_2 \omega}{i^n E_0 \sin \theta \beta_2} \quad (11, 12)$$

and similarly for  $C_n$  and  $D_n$ . Substituting Equations (10) through (12) into Equations (3) and (4) gives:

$$E_z = E_0^G \sin \theta \sqrt{\frac{1}{\pi \lambda_2 \rho}} \sum_{n=-\infty}^{\infty} A_n i^{2n} e^{-in\phi} (1+i) \quad (13)$$

$$\mathcal{H}_z = \frac{E_0^G \sin \theta \beta_2}{\mu_2 \omega} \sqrt{\frac{1}{\pi \lambda_2 \rho}} \sum_{n=-\infty}^{\infty} B_n i^{2n} e^{-in\phi} (1+i) \quad (14)$$

where 
$$G = e^{-i\lambda_2 \rho} e^{-i\beta_2 z \cos \theta} e^{i\omega t} \quad (15).$$

It should be noted that:

$$G \cdot G^* = 1 \quad (16)$$

where \* indicates the complex conjugate of the quantity. Let the coefficients  $\underline{A}_n$  and  $\underline{B}_n$  be split into their real and imaginary parts:

$$A_n = a' + ia'', \quad B_n = b' + ib'' \quad (17, 18).$$

The series in Equations (13) and (14) can be separated into a real and an imaginary series,  $\underline{P}$  and  $\underline{Q}$ , respectively. Using the relation

$$e^{-in\theta} = \cos n\theta - i \sin n\theta \quad (19),$$

the real and imaginary parts are found to be:

$$P_a = \sum_{-\infty}^{\infty} (-1)^n [a'(\cos n\theta + \sin n\theta) - a''(\cos n\theta - \sin n\theta)] \quad (20)$$

$$Q_a = \sum_{-\infty}^{\infty} (-1)^n [a''(\cos n\theta + \sin n\theta) + a'(\cos n\theta - \sin n\theta)] \quad (21)$$

$$P_b = \sum_{-\infty}^{\infty} (-1)^n [b'(\cos n\theta + \sin n\theta) - b''(\cos n\theta - \sin n\theta)] \quad (22)$$

$$Q_b = \sum_{-\infty}^{\infty} (-1)^n [b''(\cos n\theta + \sin n\theta) + b'(\cos n\theta - \sin n\theta)] \quad (23).$$

An examination of the definitions of  $\underline{A}_n$  and  $\underline{B}_n$  shows that:

$$A_n = A_{-n} \quad (24)$$

$$B_n = -B_{-n} \quad (25).$$

Thus, the sine terms drop out of Equation (20) and (21), and the cosine terms drop out of Equations (22) and (23) except for the terms when  $n\phi = 0$ . When  $n\phi$  is zero, the series reduce to:

$$P_b = b_o' - b_o'' \quad (26)$$

$$Q_b = b_o' + b_o''$$

The series may now be written:

$$P_a = a_o' - a_o'' + 2 \sum_{n=1}^{\infty} (-1)^n (a_n' - a_n'') \cos n\phi$$

$$P_b = b_o' + b_o'' + 2 \sum_{n=1}^{\infty} (-1)^n (b_n' + b_n'') \sin n\phi \quad (27)$$

$$Q_a = a_o' + a_o'' + 2 \sum_{n=1}^{\infty} (-1)^n (a_n' + a_n'') \cos n\phi$$

$$Q_b = b_o'' - b_o' + 2 \sum_{n=1}^{\infty} (-1)^n (b_n'' - b_n') \sin n\phi$$

The electric and magnetic vectors in these units are related by:

$$\mathcal{H}_o = \mathcal{E}_o \frac{\beta_2}{\mu_2 \omega} \quad (28).$$

Equations (13) and (14) may now be written, omitting the complex variable  $\underline{G}$ :

$$\frac{\mathcal{E}_z}{\mathcal{E}_o} = \sqrt{\frac{1}{\pi \lambda_2^o}} (\sin \theta) (P_a + i Q_a) \quad (29)$$

$$\frac{\mathcal{H}_z}{\mathcal{H}_o} = \sqrt{\frac{1}{\pi \lambda_2^o}} (\sin \theta) (P_a + i Q_a) \quad (30)$$

The scattered wave is cylindrical in nature, so the intensity decreases as  $1/\rho$ . However, the direction of propagation of the scattered wave makes an angle  $\theta$  with the  $z$ -axis of the fiber as shown by Wait for the far field approximation. This is sketched diagrammatically in Fig. 5.

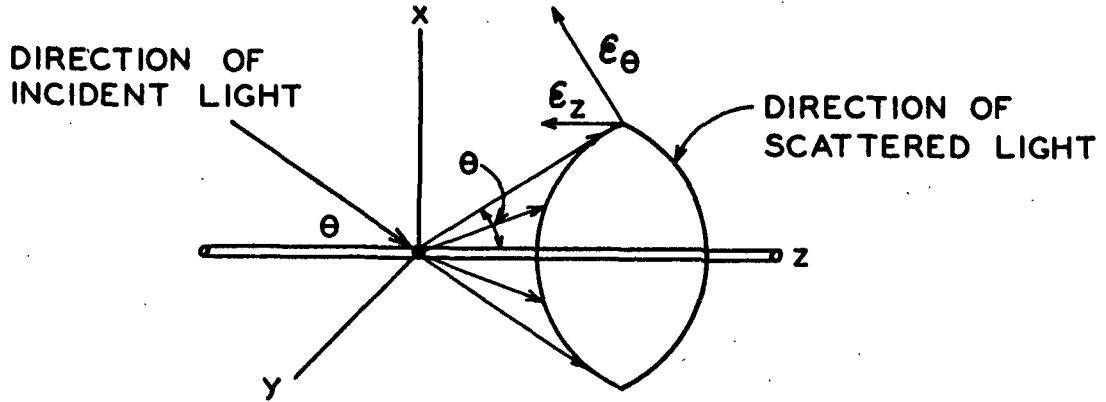


Figure 5. Diagram of the Scattered Wave

Since there is no component of the  $\mathcal{E}$  vector in the direction of propagation, it can be seen from Fig. 5 that  $\mathcal{E}_\theta$  is related to  $\mathcal{E}_z$  by:

$$\mathcal{E}_\theta = \mathcal{E}_z / \sin \theta \quad (31)$$

and similarly:

$$\mathcal{H}_\theta = \mathcal{H}_z / \sin \theta \quad (32).$$

From Equations (29) and (30) we find that:

$$\frac{\mathcal{E}_\theta}{\mathcal{E}_0} = \sqrt{\frac{1}{\pi \lambda_2 \rho}} (P_a + i Q_a) \quad (33)$$

$$\frac{\mathcal{H}_\theta}{\mathcal{H}_0} = \sqrt{\frac{1}{\pi \lambda_2 \rho}} (P_b + i Q_b) \quad (34)$$

The radiant energy per second in the scattered wave passing through a unit area of a cylinder surrounding the fiber at a distance  $\rho$ ,  $I_{(\theta, \phi)}$ , is:

$$\frac{I(\theta, \phi)}{I_0} = \frac{1}{\pi \lambda_2^2} \sin^2 \theta (P_a^2 + Q_a^2 + P_b^2 + Q_b^2) \quad (35)$$

and since  $\lambda_2 = 2\pi \sin \theta / \lambda^\circ$

$$\frac{I(\theta, \phi)}{I_0} = \frac{\lambda^2}{2\pi^2 \rho} (P_a^2 + Q_a^2 + P_b^2 + Q_b^2) \quad (36)$$

A similar expression may be derived for Polarization 2. The total scattered radiation for unpolarized incident light is:

$$\frac{I(\theta, \phi)}{I_0} = \frac{\lambda^2}{4\pi^2 \rho} (P_a^2 + Q_a^2 + P_b^2 + Q_b^2 + P_c^2 + Q_c^2 + P_d^2 + Q_d^2) \quad (37)$$

This is the expression for the light scattered from a unit length of fiber at an angle  $\phi$  when a dielectric cylinder is illuminated by a plane wave at an angle  $\theta$  from the fiber axis. This is the correct representation of the scattered light intensity at a distance many fiber diameters from the fiber but still close enough that the ends of the fiber alter the calculated scattered intensity a negligible amount. These expressions are in complete agreement with the far field approximations given by Wait.

Van de Hulst (20) has developed a similar equation for the scattering from a dielectric cylinder which is illuminated with a plane wave perpendicular to the fiber axis. He also reported some numerical results for small cylinders,  $2\pi a / \lambda^\circ \leq 6.0$ . These equations were useful for checking the accuracy of the numerical computations from Wait's equations. The equations given by Van de Hulst are:

Polarization I:

$$I_z = \frac{2}{\pi \rho k} |T_1(\phi)|^2 I_0 \quad (38)$$

Polarization II:

$$I_{\emptyset} = \frac{2}{\pi \rho k} \left| T_2(\emptyset) \right|^2 I_0 \quad (39)$$

$$T_1(\emptyset) = b_0 + 2 \sum_{n=1}^{\infty} b_n \cos n\emptyset \quad (40)$$

$$T_2(\emptyset) = a_0 + 2 \sum_{n=1}^{\infty} a_n \cos n\emptyset \quad (41)$$

$$b_n = \frac{m J_n'(y) J_n(x) - J_n(y) J_n'(x)}{m J_n'(y) H_n^{(2)}(x) - J_n(y) H_n^{(2)'}(x)} \quad (42)$$

$$a_n = \frac{J_n'(y) J_n(x) - m J_n(y) J_n'(x)}{J_n'(y) H_n^{(2)}(x) - m J_n(y) H_n^{(2)'}(x)} \quad (43)$$

where:

$$x = 2\pi a/\lambda \quad (44)$$

$$y = mx \quad (45).$$

These equations accurately describe the light scattered from a dielectric cylinder of infinite length which is illuminated by a plane wave. Since the cylinder is assumed to be infinitely long, the scattered wave is cylindrical in nature so that the intensity decreases as  $1/\rho$ . The assumption was also made in the computations that the cylinder was composed of a nonabsorbing dielectric.

The intensity of light scattered at any angle,  $\emptyset$ , and for various angles of incidence,  $\theta$ , were calculated. The detailed description of these computations is given on page 91. The scattering diagrams, scattering intensity at any angle,  $\emptyset$ , are tabulated in Tables XV and XVI, and scattering diagrams are plotted in Fig. 25 and 26 for certain angles of  $\theta$  (see Appendix II).

The total scattered light per unit geometrically obstructed light has often been called the efficiency factor,  $\underline{Q}$ . For the case of no absorption,  $\underline{Q}$  is an oscillating function of the parameter  $\underline{x} = 2\pi a/\lambda^\circ$ . For circular cylinders illuminated by a plane wave perpendicular to the fiber axis, the value of  $\underline{Q}$  is zero at  $\underline{x} = 0$ , increases to about 4 at  $\underline{x} = 4$ , decreases again to about 1.5 at  $\underline{x} = 6$ , and continues oscillating with decreasing amplitude as  $\underline{x}$  gets larger. The value of  $\underline{Q}$  approaches 2.0 as  $\underline{x}$  goes to infinity. This value of  $\underline{Q}$  is approached regardless of the angle of incidence of the oncoming plane wave. The amount of light geometrically obstructed decreases as the sine of the angle of incidence,  $\theta$ , so the total amount of light scattered also decreases as the sine of the angle for the limit of very large particles.

One way to visualize the reason for this factor of two to one is to notice that all of the light which is geometrically obstructed would be scattered due to refraction and reflection at the air-dielectric boundaries. Superimposed on this is the diffraction pattern of the light which is disturbed by the edges of the object. The total scattered intensity is, then, the sum of the diffracted part plus the refracted and reflected part. This is merely a simplified picture of the scattering; the actual phenomena are more complex.

These diffraction effects can be seen in Fig. 25 and 26 where the scattering at nearly forward angles,  $\pi$  radians, has the shape typical of the diffraction pattern from an opaque body in a beam of coherent light. The rest of the diagram is more typical of what would be expected from reflection and refraction. The total scattered light is simply twice the area under the scattering diagrams. Dividing by the geometrically obstructed light gives  $\underline{Q}$ . For perpendicular incidence with the 9.02  $\mu$  diameter fiber at 700  $m\mu$ , it is interesting to note that the scattered light from  $-173^\circ$  to  $+173^\circ$  per unit geometrically obstructed light



is about 1.0 and the light scattered in the remaining  $14^\circ$  interval is about 0.8; so the efficiency factor is 1.8. This indicates that the diffraction part of the scattered light is contained primarily in the interval  $7^\circ$  each side of the forward direction.

The efficiency factors for the  $5.69 \mu$  and the  $9.02 \mu$  diameter fibers at  $700 \text{ m}\mu$  were calculated. The  $Q$  factors are shown in Fig. 6 as a function of the angle of incidence,  $\theta$ . It can be seen from Fig. 6 that the efficiency factor is not 2.0 at all angles of  $\theta$ , which indicates that the fibers are not behaving as very large bodies in respect to light scattering.

These expressions have been derived for the light scattered at large distances from the fiber. From an examination of Fig. 7 it is evident that the fibers are not separated by large distances. The distance at which the scattering pattern is calculated will affect primarily the diffraction portion of the scattering diagram, unless one is within a few fiber diameters of the fiber. Close to a fiber, the diffraction pattern would be roughly similar to a shadow; and, as the distance from the fiber was increased, the diffraction pattern would assume a configuration more and more similar to the far field case. Thus, it is likely that the intense forward scattering due to diffraction would be unobservable at the distance at which many of the fibers are separated in the sheet.

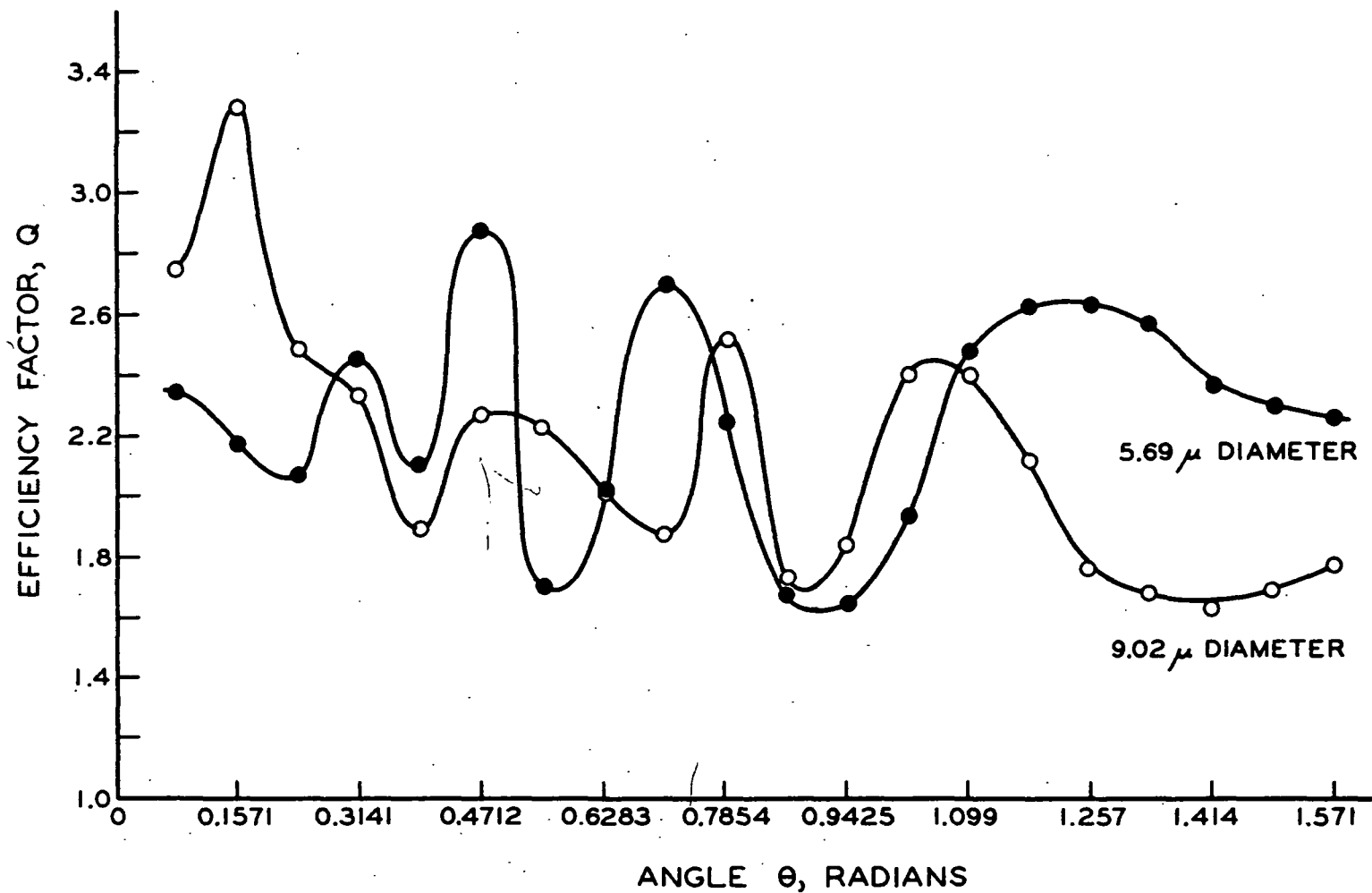


Figure 6. Efficiency Factor as a Function of the Angle  $\theta$

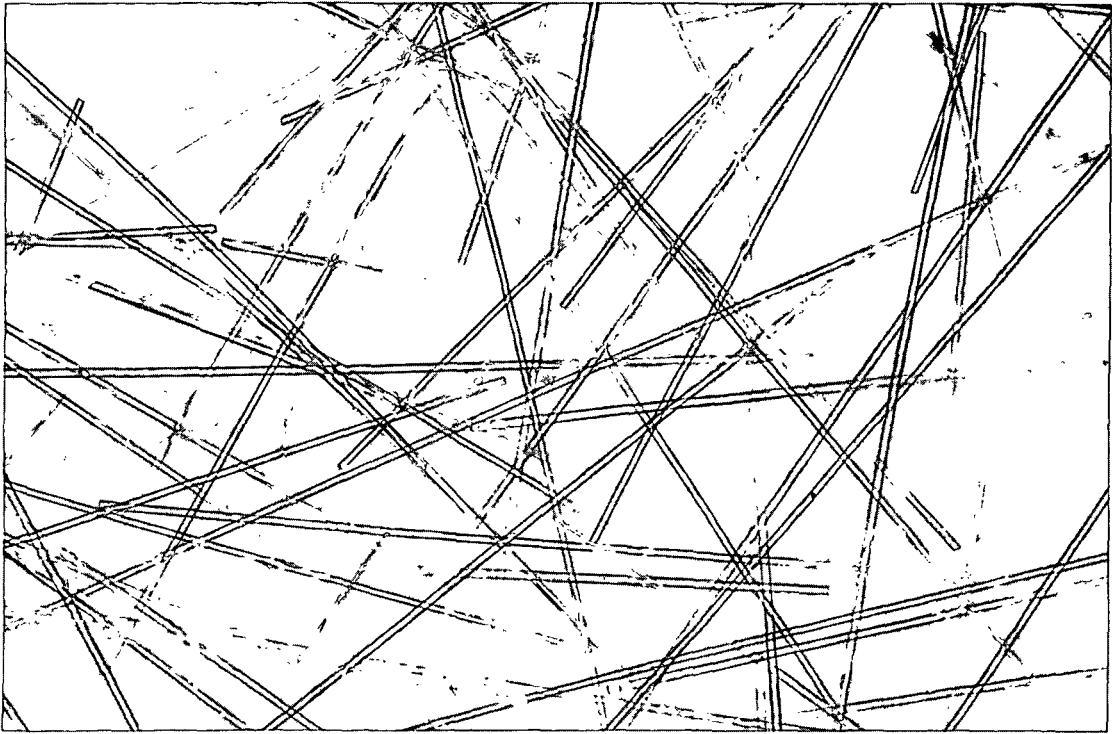


Figure 7. Photograph of a Glass Fiber Sheet

THE RELATIONSHIP BETWEEN THE SPECIFIC SCATTERING COEFFICIENT  
AND THE LIGHT BACK-SCATTERED FROM A UNIT LENGTH OF FIBER

The incident light intensity was defined in the following manner. Consider a differential cone of light oriented at some angle  $\alpha$  from the normal to the sheet. The radiant energy striking a unit area of the sheet per second from the differential cone of light is  $\underline{I}_0 f(\alpha) \cos\alpha d\omega$  where  $f(\alpha)$  is a dimensionless weighting factor used to describe the light distribution incident on the sheet, and  $d\omega$  is the solid angle in the cone. For isotropic illumination,  $f(\alpha) = 1$  and the irradiance of the sheet is simply  $\pi \underline{I}_0$ . The quantity  $\underline{I}_0$  has the units joules/sq. cm./steradian.

Let  $\underline{I}_B$  equal the total light intensity scattered backward from a unit length of fiber. If  $\underline{L}$  is the length of fiber per gram of fiber, the value of  $\underline{L}$  can be given by:

$$\underline{L} = \frac{1}{\pi a^2 \rho_f} \quad (46)$$

where  $\rho_f$  is the fiber density and  $a$  is the fiber radius. The angle between the normal to the sheet and the angle of incidence of a pencil of light will be called  $\alpha$ . The distribution of the light at any plane in the sheet will be given by  $\underline{I}_0 f(\alpha)$  where, for isotropic illumination,  $f(\alpha) = 1$ . This assumes that the light distribution is constant from point to point in the sheet. The scattering coefficient is given by:

$$s = \frac{\underline{I}_B}{\pi a^2 \rho_f \underline{I}_0} \frac{1}{\int_0^{\pi/2} f(\alpha) 2\pi \sin\alpha \cos\alpha d\alpha} \quad (47).$$

For isotropic illumination, the scattering coefficient can be written:

$$s = \frac{\underline{I}_B}{\pi^2 a^2 \rho_f \underline{I}_0} \quad (48).$$

# DETERMINATION OF THE BACK-SCATTERED LIGHT FROM A UNIT LENGTH OF FIBER

Wait's equations were solved for the scattering diagrams at various angles of incidence. These were integrated numerically, the details of which are shown in Appendix I. The integrations were based upon the following analysis.

The angles,  $\phi$ ,  $\Phi$ , and  $\theta$ , were defined as shown in Fig. 8. The light distribution which is given by  $I_0 f(\alpha)$  was drawn in Fig. 8 for the case where  $f(\alpha)$  equalled 1. The illumination, in this case, can be represented by a hemisphere.

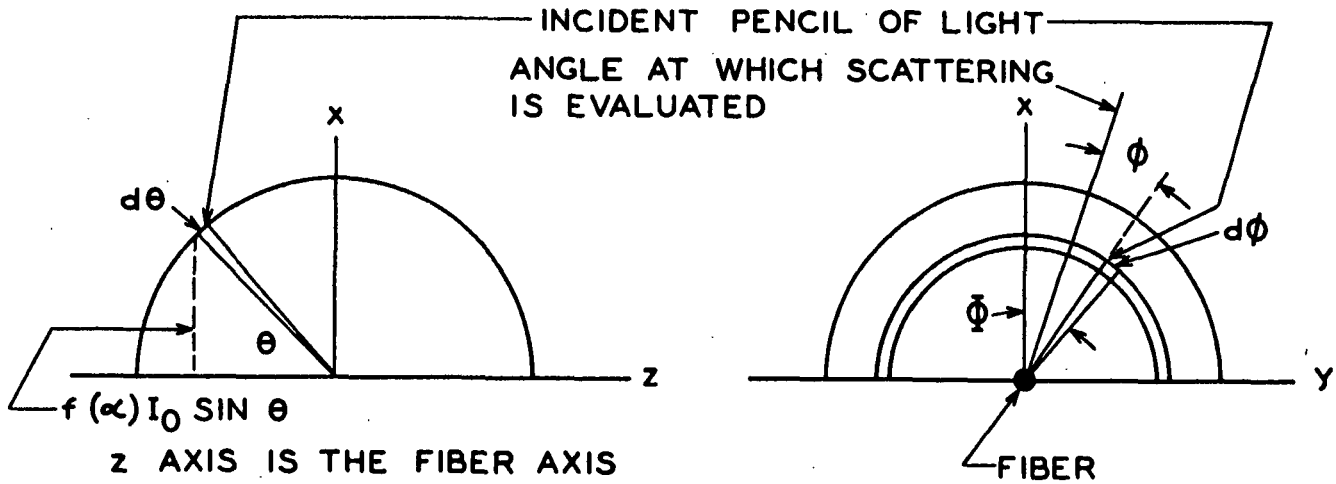


Figure 8. Diagram of Integration Procedure

The light incident on the fiber at angles  $\theta$  and  $\phi$  contained in the increments  $d\theta$  and  $d\phi$  is  $I_0 f(\alpha) \sin \theta d\theta d\phi$ . The back scattered light from a unit length of fiber due to the light incident between angles  $d\theta$  and  $d\phi$  is given by:

$$d^2 I_b = \int_{\phi = \Phi - \pi/2}^{\phi = \Phi + \pi/2} \frac{I(\phi, \theta)}{I_0} \rho I_0 f(\alpha) \sin \theta d\theta d\phi \quad (49)$$

where  $\frac{I(\phi, \theta)}{I_0} \rho$  is the light scattered into an angle increment  $d\phi$  at a distance  $\rho$  from the  $\underline{z}$ -axis and at an angle  $\phi$  when illuminated at angle  $\theta$  from the  $\underline{z}$ -axis.

These are simply the scattering diagrams from Equation (37). It should be noted that the scattered light is of the nature of a cylindrical wave, so the back-scattered light was found by the one integration indicated above.

The total back-scattered light was found by the integration of Equation (49) over the angles  $-\pi/2 \leq \theta \leq \pi/2$  and  $-\pi/2 \leq \phi \leq \pi/2$ . Since the scattering diagrams and the incident distributions are symmetrical, the integrated equation can be written:

$$\frac{I_B}{I_0} = 4 \int_0^{\pi/2} \int_0^{\pi/2} \int_{\phi = \phi - \pi/2}^{\phi = \phi + \pi/2} \frac{I(\phi, \theta)}{I_0} \rho f(\alpha) \sin \theta d\phi d\theta d\phi \quad (50)$$

## EXPERIMENTAL

### PREPARATION AND CHARACTERIZATION OF THE FIBERS

#### GLASS FIBERS

The glass fibers were supplied by Owens-Corning Fiberglas Corp. The three samples used were labeled by Owens-Corning with the following designations:

K 37 1/0 0.7z 630  
TRT .040  
ASH

D450 1/0 5z 630  
HUNT

G150 1/0 1z 630  
ASH

The fibers are called Samples K, D, and G, respectively, throughout this thesis.

The fibers were supplied in the form of a continuous filament yarn composed of several hundred individual filaments twisted together and bound with an organic adhesive. In order to form the fibers into sheets, it was necessary to cut the yarn into short lengths and to remove the organic binder.

Both the glass and the nylon fibers were cut in the same way. A cutter was constructed from single-edged razor blades. About 30 to 50 blades were arranged parallel to each other and equally spaced by means of washers, and the entire assembly was bolted together with three bolts.

The fiber yarn was wound on the periphery of an octagonally shaped wheel about two feet in diameter which had been covered with chipboard. A bundle of fibers about one inch wide and about 1/8th inch thick was wound onto the cardboard. The bundle was secured with Duco cement at each of the corners of the

octagon; and, when the glue was dry, the fiber bundles and cardboard were cut from the wheel leaving the bundle glued at each end to a cardboard strip. A sheet of aluminum foil was placed over the fiber bundle to aid in the subsequent removal of the fibers from the cutter. The cutter was then placed over the fibers and forced through the bundle by means of a hydraulic press.

The organic coating on the glass fibers was removed by treatment in 30% hydrogen peroxide. A sample of fiber sufficient for one sheet, about one gram, was placed in a 250-ml. filter flask. The fibers were covered with peroxide and a vacuum was applied to remove air from the bundles of fibers. The reaction was allowed to proceed overnight. The peroxide was then filtered off; the fibers were washed with dilute hydrochloric acid and finally with deionized water.

The anthrone test (25) for carbohydrate materials was run on the fibers before and after cleaning. A strong color reaction was produced with the uncleaned fibers; no reaction was observed with the cleaned fibers. This indicates that the organic coating was essentially completely removed from the fibers by the peroxide treatment.

The cleaned fibers were then transferred to 4-1. flasks with about 0.3 g. in each flask. The flasks were filled with deionized, deaerated water, and the fibers were dispersed with a mechanical zig-zag stirrer. The fibers were then poured into the 30-gallon forming tank which had been filled with filtered, deaerated water. The complete sheet-forming apparatus and procedure are described on page 33.

The fiber diameters were measured microscopically by means of an eyepiece micrometer calibrated with a stage micrometer. About 200 fibers were counted



from each sample. Table I shows the distribution of fiber diameters for the glass fibers as well as the average value for each of the three samples.

TABLE I  
FIBER DIAMETERS

	Midpoint of Interval, $\mu$	Percentage of Fibers Counted Whose Diameters are in the Interval
Sample K	11.9	3.1
	12.4	5.2
	12.9	16.7
	13.4	29.0
	13.9	20.8
	14.4	13.5
	14.9	10.4
	15.5	2.1
	16.0	0.0
Average	13.7 (192 fibers counted)	
Sample G	7.73	2.0
	8.25	15.4
	8.76	37.4
	9.28	26.1
	9.79	13.8
	10.3	4.6
	10.8	0.5
Average	9.02 (195 fibers counted)	
Sample D	4.64	1.4
	5.15	23.1
	5.67	49.5
	6.19	20.2
	6.70	4.6
	7.22	0.6
Average	5.69 (173 fibers counted)	

The density of the glass fiber K was measured pycnometrically. The density determination was run in triplicate and gave values of 2.54, 2.55, and 2.56 g./cc. Jones (26) has found that similar glass fibers of different diameters have the same density, and the density he determined was 2.56 g./cc.

The refractive index of the fibers was measured microscopically using fluids of known refractive index. These fluids were purchased from R. P. Cargille Laboratories, New York 6, N. Y. The index of refraction of the fluids at the wavelength of the D line of sodium as well as a measure of the dispersion was given by Cargille. The fluids were assumed to have a linear variation of refractive index with wavelength over the visible spectrum.

Cleaned glass fibers were placed on microscope slides. The fibers were immersed in the fluids and were observed under a microscope with monochromatic illumination from a Bausch and Lomb double-prism monochromator. The wavelength was varied until the fibers disappeared, indicating that the refractive indices of the fiber and the fluid were the same. Using various fluids, the refractive index of the fibers could be measured over the whole visible spectrum. The results of this determination are shown in Fig. 9. The fibers were sufficiently transparent and uniform in their optical properties that all the fibers in the field of view disappeared completely when the indices of refraction were matched.

#### NYLON FIBERS

The nylon fibers used in this thesis were supplied by E. I. du Pont de Nemours & Co., Inc. The designations on the samples were as shown:

40-34-1/2-Z-200	(about 1.5 denier per filament)
40-13-1/2-Z-200	(about 3 denier per filament)
15-1-0-200	(about 15 denier per filament).

Nylon fibers have been found to shrink in a longitudinal direction when treated with hot water. During the sheet formation, the fibers were dispersed in hot, deaerated water. In order to remove any uncertainty in the fiber diameter

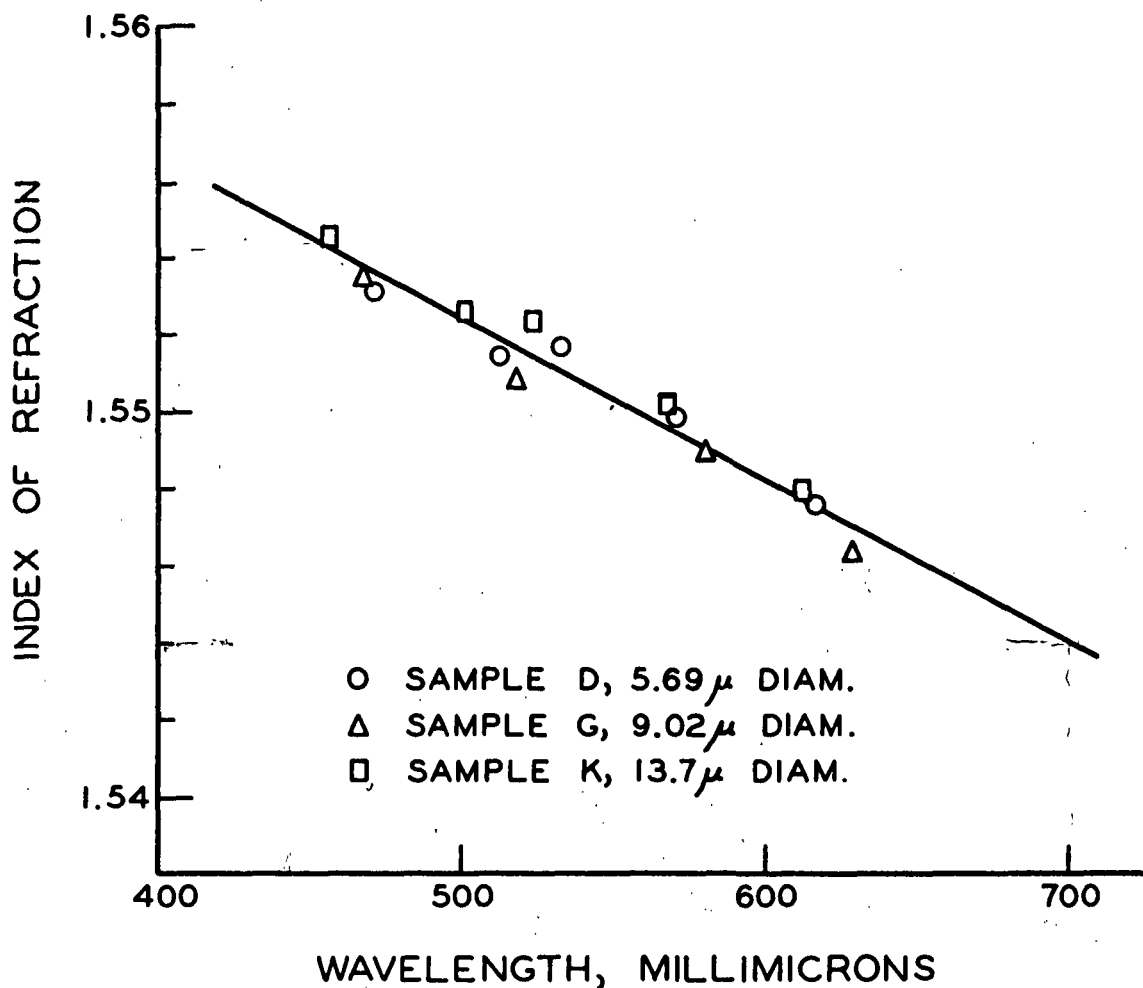


Figure 9. Index of Refraction of Glass Fibers

measurements due to shrinkage, the diameters were measured on fibers from the sheets which were used for scattering coefficient determinations. The results of the measurements are shown in Table II.

These nylons contained an inorganic pigment which was readily visible under the microscope. Johnson (27) has found that the pigment was essentially all titanium dioxide. The amount of pigment in these nylon samples was determined by ashing at 750°C. All three nylon samples were found to have an ash content of 0.33%. The reproducibility of the determinations was about  $\pm 0.005\%$ . The

density of the nylon has been reported (28) to be 1.14 g./cc. and the refractive index (29) about 1.55.

TABLE II  
DISTRIBUTION OF NYLON FIBER DIAMETERS

	Center of Size Interval, $\mu$	Number of Fibers
15 Denier	47.1	30
	48.2	1
	Average diameter	47.1
3 Denier	18.8	2
	20.0	39
	21.2	95
	22.4	4
	23.6	1
	Average diameter	20.8
1.5 Denier	11.7	20
	12.9	105
	14.1	1
	Average diameter	12.7

#### ORLON FIBERS

Two samples of orlon fibers were obtained from E. I. du Pont de Nemours & Co., Inc. These samples were labeled:

100% Orlon Acrylic Staple  
Semi-dull Type 42  
1.5 denier

100% Orlon Acrylic Staple  
Semi-dull Type 42  
2.0 denier

Samples of the orlon fibers were embedded in an epoxy embedding compound and microtome sections were prepared to show the fiber cross sections. The cross

sections are shown in Fig. 10 for the two samples. The pigment filler is readily visible in the 1.5-denier sample, but only an occasional fiber appears to be filled with pigment in the 2.0-denier fiber.

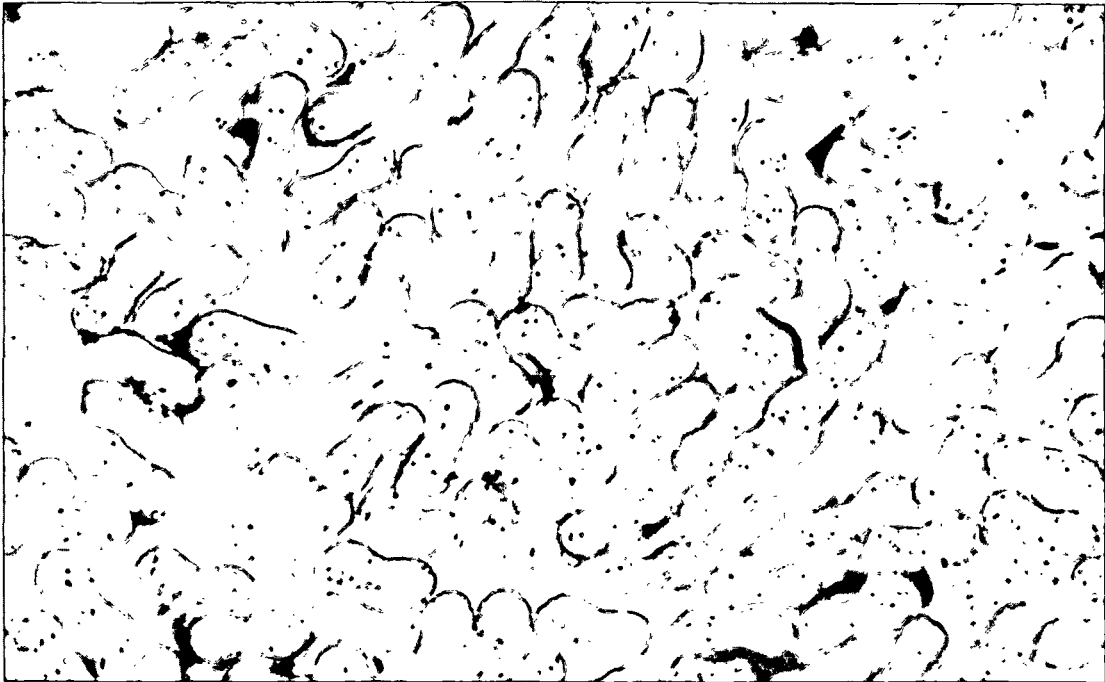
The samples were ashed in a manner similar to that used for the nylon. The ash content was found to be 0.55% for the 1.5-denier fiber and 0.21% for the 2.0-denier fiber. This confirms the observation that the amount of pigment was much lower in the 2.0-denier sample than in the 1.5-denier sample.

The specific surface of the orlon fibers was determined by measuring the area of the cross sections in the photomicrographs by means of a planimeter. The perimeters were measured by projecting the pictures on a chalk board, tracing the outlines of the fibers, and measuring the outlines with a small mileage measuring instrument designed for computing distances on maps. The specific surface areas of the two samples were found to be 3760 sq. cm./cc. for the 1.5-denier sample and 3200 sq. cm./cc. for the 2.0-denier sample.

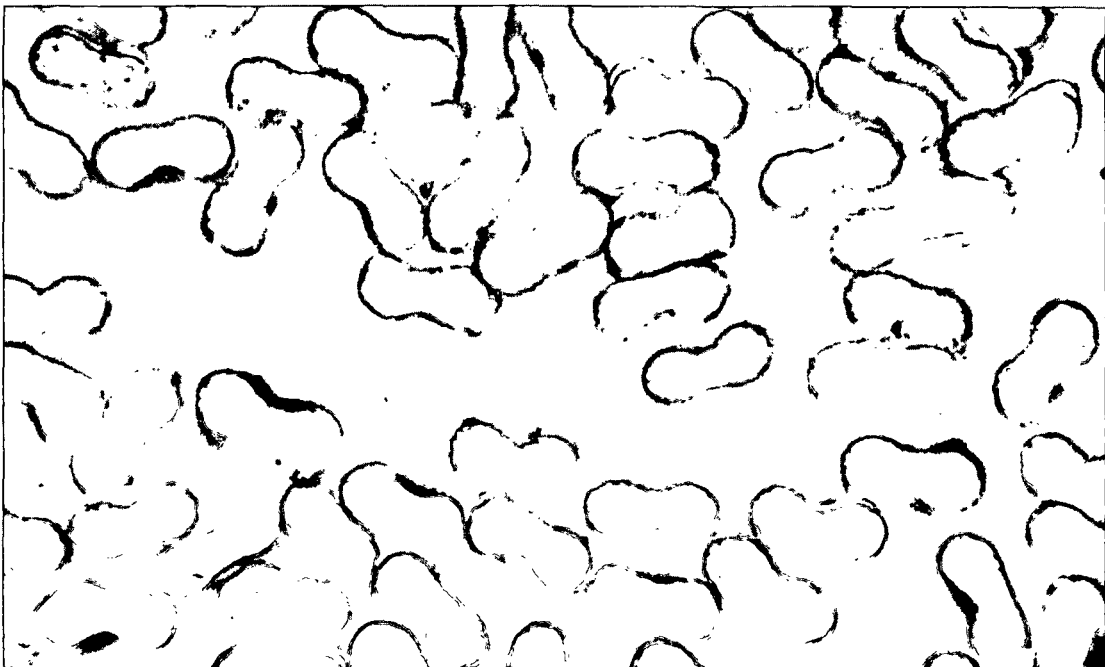
The values of the index of refraction and the density of the orlon were taken from the literature. The density was 1.14 (28) and the refractive index was about 1.51 (29).

#### PREPARATION OF THE SHEETS

The sheets were formed in the apparatus shown in Fig. 11. The fibers, dispersed mechanically in 4-l. filter flasks, were added to the slurry tank which had been filled with about 30 gallons of deaerated, filtered water. The forming tube was filled from below to force out any entrapped air. The appropriate valves were opened and the pump was started. The flow rate was adjusted with the pump by-pass valve until the highly turbulent flow in the forming tube was confined to the upper



1.5 Denier Orlon



2.0 Denier Orlon

Figure 10. Cross Section of the Orlon Fibers

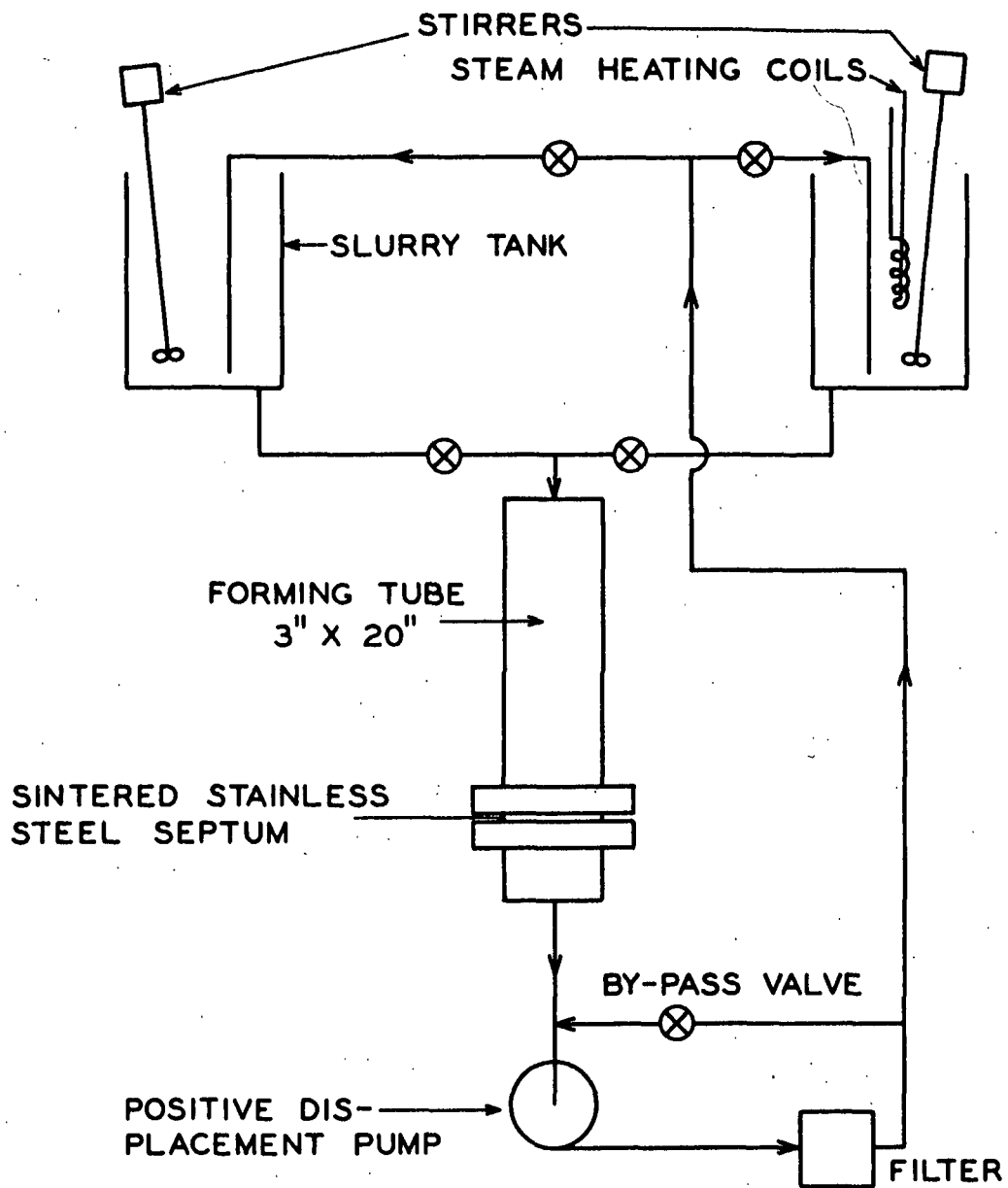


Figure 11. Sheet Forming Apparatus

two-thirds of the tube. When sufficient fiber had been deposited on the septum, the valve from the slurry tank was closed and air was allowed to enter the flow tube until air was sucked through the sheet. The pump was then stopped and the sheet was carefully removed from the septum. The wet sheet was placed on a clean glass plate to dry at room temperature.

#### MEASUREMENT OF THE SCATTERING AND ABSORPTION COEFFICIENTS

The sheets composed of synthetic fibers were almost completely unbonded. For this reason, the strength of the sheets was very low and they had to be supported between glass plates while the scattering determinations were being performed. A holder was constructed as shown in Fig. 12. The holder adequately supported the sheets and allowed the degree of compression of the sheets to be varied by adjusting the bolts.

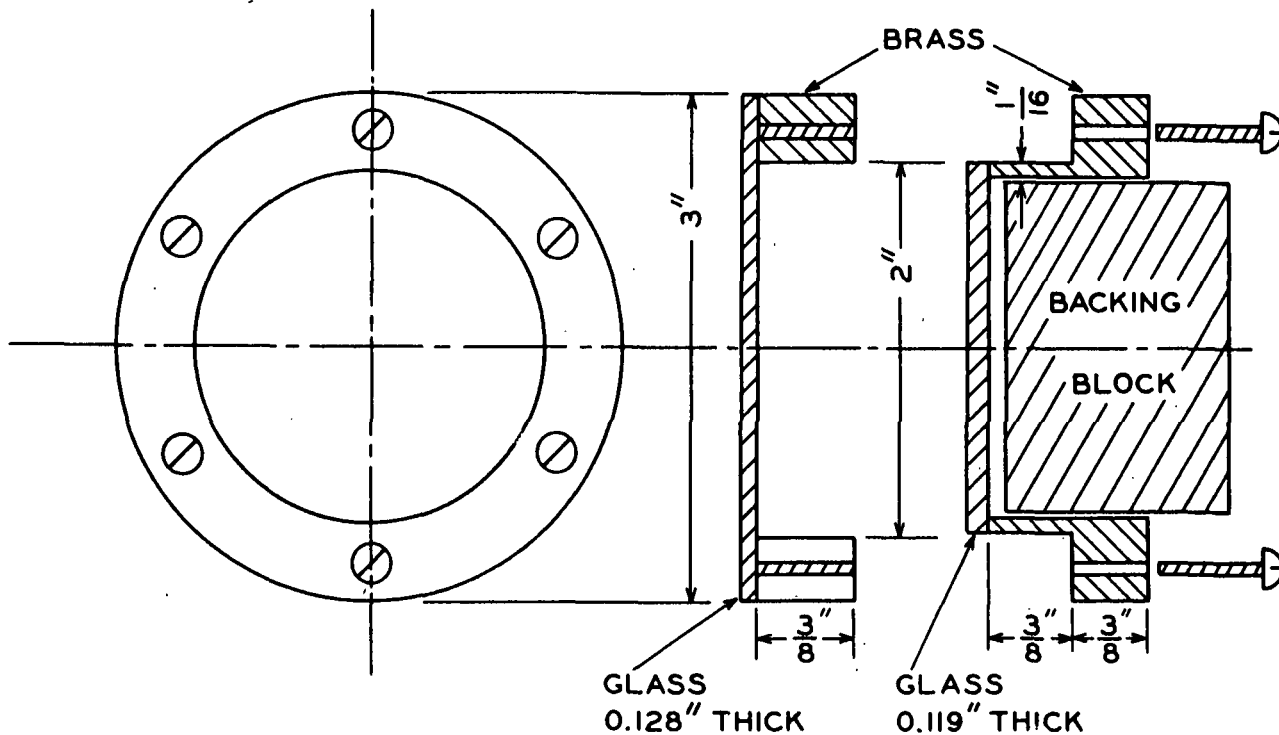


Figure 12. Sample Holder



The sheets were formed at a diameter of 3 inches. A punch was constructed to punch the central 2 inches from the sheet to fit into the sample holder.

The basis weight of the sheets was measured by weighing the samples from the holder. The diameter of the punch was used as the diameter of the sheet in order to calculate the basis weight. The sheets were quite thick, up to 0.5 cm., and very loose in structure. It was impossible to punch precisely sheets of this type due to deformation of the sheets as they were punched. This no doubt contributed a great deal to the scatter in the experimental results.

It was initially proposed to measure the reflectances of the samples in the holder on a General Electric Recording Spectrophotometer (GERS) (30) when the sample was backed by a black backing block and by a white backing block. Through proper calibration of the glasses in the sample holder with papers of known scattering and absorption properties, the scattering and absorption coefficients of the sample could be calculated. The black backing block was a cardboard cavity lined with black velour paper. This fitted snugly into the holder behind the back glass and contacted the glass only around the edges of the glass. The white backing block was a piece of opal glass cut to fit flush against the back glass of the holder. A brass block was glued to the opal glass to provide a handle for ease in manipulation. The reflectance of the opal glass glued to the brass block was measured on a brightness tester to be 85.1% using the number 1 brightness filter (457 mμ centroid wavelength).

The effect of the front glass was determined directly by measuring the reflectances of various samples without the front glass and then with the front glass at each of the four wavelengths used in this thesis--440, 500, 600, and 700 mμ. For example, a sheet of paper which had a reflectance of, say, 60% without

the front glass might have a reflectance of only 55% with the front glass. In this manner, a correction factor was found which could be added to or subtracted from the reflectances of the samples in the holder in order to find the reflectances the samples would have had if there had been no front glass present.

The back glass and the white or the black backing body were considered as a single unit having a reflectance  $\underline{R}_W$  and  $\underline{R}_B$ , respectively. Kubelka (4) gives the relationship between the absolute reflectance of a single sheet backed by a black body,  $\underline{R}_O$ , the reflectance of an infinite pad of the material,  $\underline{R}_\infty$ , the backing reflectance,  $\underline{R}_g$ , and the reflectance  $\underline{R}_{Rg}$  of a sheet with a backing of reflectance  $\underline{R}_g$ :

$$\underline{R}_{Rg} = \frac{\underline{R}_O - \underline{R}_g(2a\underline{R}_O - 1)}{1 - \underline{R}_O \underline{R}_g} \quad (51)$$

where

$$a = (1/\underline{R}_\infty + \underline{R}_\infty)/2 \quad (52).$$

Simple rearrangement gives:

$$\underline{R}_g = \frac{\underline{R}_{Rg} - \underline{R}_O}{\underline{R}_{Rg} \underline{R}_O - 2a\underline{R}_O + 1} \quad (53).$$

$\underline{R}_O$  and  $\underline{R}_\infty$  were measured on several sheets of the following types of papers: glassine, the uncoated base sheet for Thermofax paper, tracing paper, and a 14-lb. ledger paper. These same samples were then put into the sample holder, and the backing reflectances  $\underline{R}_W$  and  $\underline{R}_B$  were determined with the aid of Equation (53) after applying the correction for the front glass. Table III shows these results.

It will be noticed that the backing reflectances, which should have been the same for each type of paper, varied widely; so this technique was not suitable for determining the scattering coefficients of the glass fiber sheets.

TABLE III  
CALCULATED BACKING REFLECTANCES

Wavelength, mμ	$\underline{R}_W$	$\underline{R}_B$
Glassine		
400	0.678	0.078
500	0.797	0.084
600	0.793	0.084
700	0.712	0.079
Thermofax		
400	0.610	0.075
500	0.767	0.088
600	0.769	0.087
700	0.683	0.081
Tracing		
400	0.658	0.099
500	0.786	0.109
600	0.777	0.110
700	0.684	0.101
14-1b. Ledger		
400	0.625	0.097
500	0.780	0.088
600	0.796	0.108
700	0.679	--

The GERS illuminates the sample normal to the surface. The reflectance from the sample may or may not be isotropic, depending upon the thickness and type of sample used. Also, the light striking the back glass was not always isotropic, especially in the case of the glassine and Thermofax papers. The reflectance from a glass plate varies from about 16% for isotropic illumination to about 8% for normal illumination. It was thought that this probably accounted for the discrepancies.

The problem was solved by illuminating the sample with diffuse illumination and viewing the sample in the normal direction. A GERS was modified by removing

the phototube and amplifier from its usual position under the integrating sphere and placing it directly under the position which the lamp usually occupied. The lamp was removed and a prism inserted in its place to direct the light beam down into the phototube. The opening in the integrating sphere which the phototube normally occupied was covered with a brass disk painted white and smoked with magnesium oxide. A  $3/4$ -inch hole was cut in the top of the integrating sphere, centered laterally and just to the rear of the joint where the sphere may be disassembled. A beam of light from a lamp operated on direct current was directed through the hole into the sphere. The modified GERS illuminated the sample with the complete visible spectrum of light in a diffuse manner and viewed the sample along the normal. The usual optics of the GERS then split the light into individual wavelengths and recorded the reflectance of the sample on the usual read-out devices.

The Institute of Paper Chemistry maintains the day-to-day calibration of the normal GERS by means of an enameled tile which has been calibrated against absolute standards (31). This tile was used to calibrate a carefully surfaced magnesium carbonate block on the normal GERS. The carbonate block was then transferred to the modified GERS and another enameled tile was calibrated. This tile was then used to calibrate the reflectance of the reference material on all subsequent determinations made on the modified GERS.

The reflectances of various papers were checked on both the normal and the modified GERS. The paper samples were chosen so that they would have a minimum of fluorescence and would not have a high specular reflectance. The paper samples were a newsprint and two bond papers with a GE brightness of about 86 and 92%, respectively. Table IV shows a comparison of the five determinations for each sample between the normal GERS and the modified GERS. The two instruments are

in agreement to within 0.6%. The instrumental accuracy of the GERS is about 0.3%. Also, handling the samples while the determinations were being conducted could have caused a loss in reflectance. It may be concluded that the two instruments were essentially in agreement.

TABLE IV  
COMPARISON OF THE NORMAL GERS AND THE MODIFIED GERS

Wavelength, mμ	440	500	600	700
Reflectance Values				
Newsprint				
Normal GERS	0.582	0.718	0.847	0.900
Modified GERS	0.585	0.722	0.848	0.900
86 Brightness				
Normal GERS	0.877	0.903	0.859	0.917
Modified GERS	0.869	0.901	0.858	0.912
92 Brightness				
Normal GERS	0.928	0.947	0.962	0.966
Modified GERS	0.945	0.945	0.957	0.960

The sample holder was then recalibrated by the technique described previously. It was found that the backing reflectances were the same regardless of the type of paper samples used for calibration.

These values of the front glass corrections and the backing reflectances were then used to calculate the specific scattering and absorption coefficients of the synthetic fiber sheets from the equations given by Kubelka (4):

$$a = \frac{(R_W - R_{R_W})(1 + R_{R_B} R_B) - (R_g - R_{R_B})(1 + R_{R_W} R_W)}{2[R_B(R_W - R_{R_W}) - R_W(R_B - R_{R_B})]} \quad (54)$$

where

$$a = (1/R_{\infty} + R_{\infty})/2 \quad (55).$$

The specific scattering coefficients were calculated from the relationship (4):

$$sW = \frac{1}{b} \left[ \operatorname{ctgh}^{-1} \left( \frac{a - R_{\underline{R}}}{b} \right) - \operatorname{ctgh}^{-1} \left( \frac{a - R_{\underline{g}}}{b} \right) \right] \quad (56)$$

where

$$\underline{W} = \text{basis weight, g./sq. cm.}$$

$$b = (a^2 - 1)^{1/2} \text{ and} \quad (57)$$

$$k = (a - 1)s \quad (58).$$

The specific scattering and absorption coefficients were determined on all three glass fiber sheets. The sheets for fibers D and G were subjected to various degrees of compression as the determinations were carried out. It was found that  $\underline{R}_{\underline{W}}$  and  $\underline{R}_{\underline{B}}$  for these samples did not vary as the sheets were compressed. However, Sample K did show a variation in the reflectances as it was compressed. The specific scattering coefficient was found to vary from 55.0 sq. cm./g. to 57.8 sq. cm./g. for solid fractions of 0.033 and 0.13, respectively, at 440 mμ for one particular sheet.

The reason for this variation was thought to be that the thickness of the sheet allowed the light to be lost out of the edges of the sheet. The sheets from Fiber K were much thicker than those from Fibers G and D, so more light was lost. As the sheet was compressed, the light loss became less, accounting for the increased scattering coefficients at the higher compressions. The sample was observed in the holder placed on the sample opening of the modified GERS. The sample port of the GERS was 1-1/4 inches in diameter, and the sample size was 2 inches in diameter. The outline of the port could be seen through the back of

the holder as a fuzzy outline which increased in sharpness as the sample was compressed. A Densichron with a microprobe (about 1/16 in. diameter) was placed against the back glass to measure the apparent sample transmittance at various points across the sample. It was found that the apparent light transmittance increased continuously from the edge to the center of the sheet, with no area in the center with a constant transmission.

The difficulty was overcome by enlarging the sample port to 2 inches which equalled the size of the sample in the holder. The area viewed by the modified GERS was reduced to a rectangle approximately 1/4 by 5/8 in. by placing 9 diopter lenses in the openings in the front of the integrating sphere. The area viewed without the lenses was a circle about 3/4 in. in diameter. The transmittance was again measured with the Densichron equipped with the microprobe. The apparent transmittance still decreased slightly within 1/4 inch from the edge. However, the central area transmitted light nearly uniformly. The final check of the change in  $\frac{R_B}{R_W}$  and  $\frac{R_B}{R_W}$  with compression of the sheet indicated that the reflectances were unaffected, within the sensitivity of the GERS ( $\pm 0.1\%$ ), by varying the solid fraction of the sheet from about 0.035 to about 0.15.

The GERS, modified as described above, was used to determine all of the specific scattering and absorption coefficients of the synthetic fiber sheets.

#### SUMMARY OF FIBER CHARACTERISTICS

A summary of the pertinent fiber characteristics for the glass, nylon, and orlon fibers is given in Table V.

TABLE V  
SUMMARY OF FIBER CHARACTERISTICS

Fibers Denier	Glass			Nylon			Orlon	
	D	G	K	1.5	3	15	1.5	2.0
Av. diameter, $\mu$	5.69	9.02	13.7	12.7	20.8	47.1		
Surface area, sq. cm./g.	2800	1740	1140	2800	1700	750	3300	2800
Sp. surface, sq. cm./cc.	7150	4450	2910	3200	1940	860	3760	3200
Density, g./cc.		2.55			1.14		1.14	
Ref. index		Fig. 8			1.55		1.51	
Ash content, %					0.33		0.55	0.21
Cross-sectional shape		Circ.			Circ.		Dog-boned (See Fig. 9)	

#### EFFECT OF FIBER LENGTH ON THE SPECIFIC SCATTERING COEFFICIENT

Sheets were formed from the 13.7  $\mu$  diameter glass fibers prepared with cutters of three different blade spacings. The blade spacings were 2.78, 4.38, and 6.26 mm. The specific scattering and absorption coefficients were determined at each of the four wavelengths, 440, 500, 600, and 700 m $\mu$ . The results are tabulated in Table VI.

The standard deviation of the specific scattering coefficients estimated from the 4.38-mm. sample at 600 m $\mu$  was 3.7 sq. cm./g. The differences between the means of the fibers cut to different lengths was not statistically significant. The 90% confidence limits of the means were about  $\pm 2.5\%$ .

The differences between the absorption coefficients were not examined statistically, since the absorption coefficients were highly influenced by dirt contamination in the sheets. The contamination came primarily from impurities in the water from which the sheets were formed. A possible correlation between the



TABLE VI  
SPECIFIC SCATTERING AND ABSORPTION COEFFICIENTS FOR  
GLASS FIBER K, 13.7  $\mu$  DIAMETER

(s and k are given in sq. cm./g.)

Sheet No.	Wavelength, $\mu$								Basis Wt., g./sq. cm.
	440		500		600		700		
	<u>s</u>	<u>k</u>	<u>s</u>	<u>k</u>	<u>s</u>	<u>k</u>	<u>s</u>	<u>k</u>	
Fiber Length 2.78 mm.									
1	59.3	4.05	60.7	2.53	61.2	2.19	63.7	2.87	
2	51.9	3.83	53.9	2.76	54.4	2.39	55.6	2.93	
3	57.6	5.32	58.6	3.38	59.8	3.08	60.9	3.65	
4	56.8	3.91	58.0	2.55	58.9	2.20	59.7	2.77	
5	57.2	4.02	58.8	2.75	58.9	2.42	60.7	2.98	
6	<u>54.4</u>	4.74	<u>56.7</u>	3.28	<u>58.0</u>	2.73	<u>59.5</u>	3.35	
Average	56.2		57.8		58.7		60.0		
Fiber Length 4.38 mm.									
1	64.7	3.39	66.0	2.50	64.5	2.38	65.3	2.99	0.00841
2	61.6	2.94	62.1	2.18	61.4	2.05	62.4	2.58	0.01229
3	61.9	3.10	62.9	2.21	62.6	2.05	63.5	2.64	0.01508
4	54.3	2.82	55.0	2.11	54.4	1.92	54.9	2.39	0.01667
5	57.8	2.72	58.7	1.88	58.5	1.78	59.9	2.30	0.02327
6	53.8	2.60	53.9	1.78	53.4	1.65	54.5	2.17	0.02556
7	59.2	2.73	58.9	1.81	58.4	1.68	58.8	2.20	0.02836
8	<u>61.4</u>	2.78	<u>62.7</u>	1.83	<u>62.1</u>	1.68	<u>62.8</u>	2.24	0.03101
Average	59.3		60.0		59.4		60.3		
Fiber Length 6.26 mm.									
1	52.4	3.96	54.3	2.91	55.1	2.51	56.6	3.09	
2	56.6	3.84	58.2	2.57	59.3	2.20	60.9	2.86	
3	56.3	4.05	57.9	2.66	58.8	2.31	60.4	2.86	
4	59.0	4.22	60.7	2.77	62.4	2.42	63.7	2.92	
5	57.0	3.52	58.9	2.39	60.1	2.10	61.8	2.61	
6	<u>58.8</u>	3.94	<u>60.6</u>	2.67	<u>61.8</u>	2.23	<u>63.8</u>	2.83	
Average	56.6		58.4		59.6		61.2		
Grand av.	58		59		59		60		

specific scattering coefficients and the specific absorption coefficients was investigated. There was found to be no significant correlation between the two coefficients.

The sheets of different fiber lengths were formed at different times. It may be concluded that there was no statistical difference between sheets composed of different fiber lengths nor was there a significant difference between the scattering coefficients of sheets prepared at different times.

#### EFFECT OF BASIS WEIGHT ON THE SPECIFIC SCATTERING COEFFICIENT

Eight sheets were prepared from each of the three samples of glass fibers. The basis weights of the sheets were varied as shown in Table VI for Fiber K and in Table VII for Fibers G and D. The fiber length for Samples G and D was 4.38 mm. and for Sample K it was as indicated in Table VI.

It is evident from Tables VI and VII that there was no trend in the specific scattering coefficient as the basis weight was varied.

#### SPECIFIC SCATTERING AND ABSORPTION COEFFICIENTS OF THE SYNTHETIC FIBERS

##### GLASS FIBERS

The specific scattering and absorption coefficients for the glass fibers were tabulated in Tables VI and VII. The averages of the specific scattering coefficients for the glass fibers are summarized in Table VIII. The 90% confidence limits for the means are about  $\pm 4\%$  for Samples D and G and  $\pm 2.5\%$  for Sample K.

The variation of the specific scattering coefficient with wavelength is shown in Fig. 13.

TABLE VII

SPECIFIC SCATTERING COEFFICIENTS AND ABSORPTION COEFFICIENTS  
OF FIBERS G AND D

(s and k are given in sq. cm./g.)

Sheet No.	Wavelength, $\mu$								Basis Wt., g./sq. cm.
	440		500		600		700		
	<u>s</u>	<u>k</u>	<u>s</u>	<u>k</u>	<u>s</u>	<u>k</u>	<u>s</u>	<u>k</u>	
	Fiber G, 9.02 $\mu$ Diameter								
1	97.5	4.44	99.2	3.45	98.2	3.31	100	3.92	0.00640
2	85.5	3.46	87.7	2.55	88.5	2.54	90.6	3.14	0.00889
3	95.1	3.21	96.2	2.37	96.7	2.23	98.1	2.86	0.01296
4	96.4	3.46	97.8	2.41	97.7	2.27	98.7	2.83	0.01431
5	94.6	3.26	95.1	2.32	94.9	2.16	96.5	2.77	0.01664
6	103	3.30	104	2.28	104	2.13	107	2.78	0.02078
7	101	2.89	102	2.01	101	1.90	102	2.41	0.02482
8	<u>94.2</u>	2.88	<u>94.9</u>	2.00	<u>93.7</u>	1.85	<u>95.4</u>	2.45	0.02081
Average	96		97		97		99		
	Fiber D, 5.69 $\mu$ Diameter								
1	168	6.45	169	5.04	172	4.56	175	5.02	0.00660
2	175	5.91	177	4.36	178	4.00	182	4.67	0.01012
3	167	4.71	170	3.54	174	3.39	179	4.09	0.01212
4	184	4.88	185	3.54	188	3.47	193	3.99	0.01495
5	172	4.25	176	3.25	177	3.00	180	3.63	0.01866
6	178	7.27	181	5.12	182	4.91	185	6.29	0.02033
7	<u>187</u>	4.38	<u>184</u>	3.00	<u>188</u>	3.90	<u>189</u>	3.55	0.02502
Average	176		178		180		183		

TABLE VIII

SUMMARY OF SPECIFIC SCATTERING COEFFICIENTS, s,  
FOR GLASS FIBERS

(sq. cm./g.)

Fiber	Wavelength, $\mu$				
	440	500	600	700	
K, 13.7 $\mu$ diam.	58	59	59	60	30% $\rightarrow$ 54%
G, 9.02 $\mu$ diam.	96	97	97	99	30% $\rightarrow$ 44%
D, 5.69 $\mu$ diam.	176	178	180	183	47% $\rightarrow$ 54%

$\Delta n \approx .01$

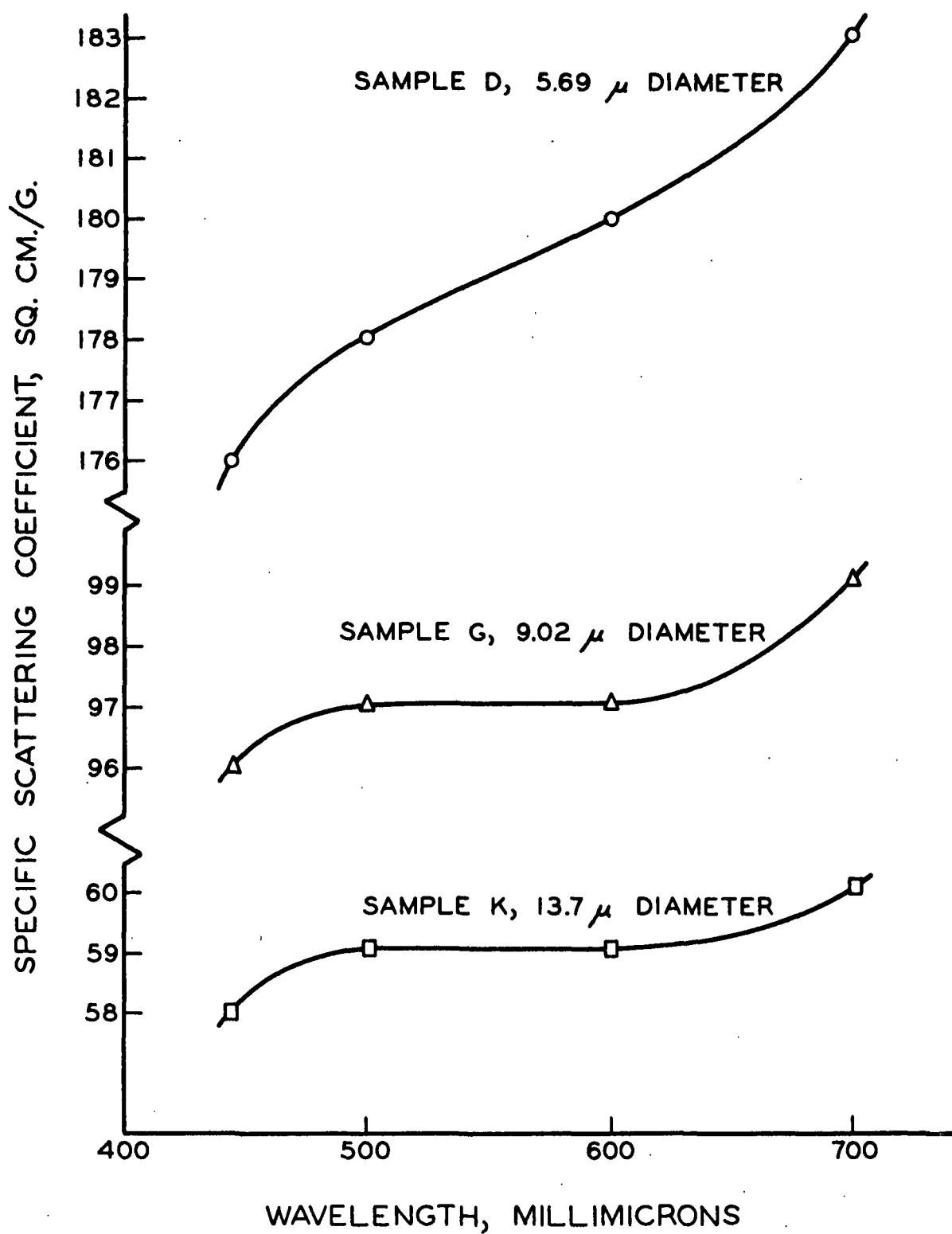


Figure 13. Specific Scattering Coefficient versus Wavelength for the Glass Fibers

## NYLON FIBERS

Sheets were prepared from each of the three samples of nylon fibers cut to a length of 6.26 mm. The specific scattering and absorption coefficients are tabulated in Table IX. The 90% confidence limits were about  $\pm 4\%$ .

The variation of the specific scattering coefficient with wavelength is plotted in Fig. 14.

## ORLON FIBERS

The orlon fibers were obtained as a precut staple about 1/4 inch in length. The two samples were made into sheets, and the scattering and absorption coefficients were measured. The results are shown in Table X. The 90% confidence limits of the means were about  $\pm 3\%$ .

The variation in the specific scattering coefficients with wavelength is shown in Fig. 15 for the orlon fibers.

The volume scattering coefficients were calculated from the average experimental values of the specific scattering coefficients for the glass, nylon, and orlon sheets. These data are plotted versus specific surface,  $\frac{A}{V}$ , in Fig. 16 through 19 for the four wavelengths used. The data for the nylon fibers were fitted by the method of least squares to a linear equation. The data show that the apparent curvature of the points is not statistically significant. It will be noticed that the line extrapolates to a positive intercept on the  $\frac{A}{V}$  axis. This is logical since, at zero surface area per unit volume of solid, there would still be scattering from the titanium dioxide particles within the volume of the nylon. The glass contained no pigment particles, so at zero surface area per unit volume there would be no scattering. Consequently, the curves for glass

TABLE IX

SPECIFIC SCATTERING AND ABSORPTION COEFFICIENTS FOR NYLON FIBERS

(s and k given in sq. cm./g.)

Sheet No.	Wavelength, $\mu$								Basis Wt., g./sq.cm.
	440		500		600		700		
	<u>s</u>	<u>k</u>	<u>s</u>	<u>k</u>	<u>s</u>	<u>k</u>	<u>s</u>	<u>k</u>	
.15 Denier, 47.1 $\mu$ Diameter									
1	67.2	2.24	63.4	1.36	57.1	1.14	52.0	1.06	0.01447
2	74.7	2.28	70.9	1.23	63.9	1.09	59.2	1.06	0.01329
3	75.4	2.17	71.8	1.39	63.9	1.05	59.1	1.04	0.01514
4	65.9	2.73	62.6	1.64	56.4	1.31	52.0	1.32	0.01026
5	73.8	2.75	69.5	1.72	62.2	1.34	57.2	1.26	0.01218
6	<u>68.8</u>	2.51	<u>66.0</u>	1.54	<u>59.0</u>	1.23	<u>54.8</u>	1.21	0.01242
Average	71		67		60		56		
3 Denier, 20.8 $\mu$ Diameter									
1	133.8	3.11	128.3	2.32	118.4	2.00	111.8	1.87	0.01177
2	131.4	3.52	126.1	2.43	115.3	1.99	109.5	2.16	0.00973
3	124.0	3.65	118.5	2.72	107.5	2.29	102.2	2.41	0.00979
4	123.3	2.81	115.2	1.80	106.0	1.62	100.1	1.46	0.01253
5	139.8	2.84	132.5	1.88	122.6	1.59	116.0	1.51	0.01617
6	125.5	5.20	119.4	3.94	108.6	3.33	103.5	3.03	0.01098
7	121.7	3.14	116.9	2.43	106.9	1.83	101.7	1.98	0.01609
8	<u>130.7</u>	3.43	<u>124.7</u>	2.56	<u>114.2</u>	1.98	<u>109.1</u>	1.97	0.01255
Average	129		123		112		107		
1.5 Denier, 12.7 $\mu$ Diameter									
1	165.1	8.44	159.9	5.79	151.3	4.75	145.0	4.73	0.00499
2	167.1	6.80	163.1	4.44	151.4	4.05	146.8	4.06	0.00448
3	156.7	4.68	152.8	3.29	142.7	2.41	137.4	2.23	0.00966
4	162.9	6.48	154.8	3.91	146.6	2.73	141.5	2.62	0.01383
5	186.6	7.80	181.8	5.41	170.6	4.49	162.9	4.35	0.00554
6	181.9	7.46	176.4	4.94	165.0	3.50	159.5	3.40	0.00821
7	176.4	9.18	169.5	5.61	161.6	4.15	154.9	4.09	0.00925
8	185.5	6.88	180.2	4.65	170.0	3.52	162.6	3.16	0.00601
9	<u>180.3</u>	4.71	<u>172.6</u>	3.00	<u>161.6</u>	2.19	<u>155.6</u>	2.12	0.01033
Average	174		168		158		152		

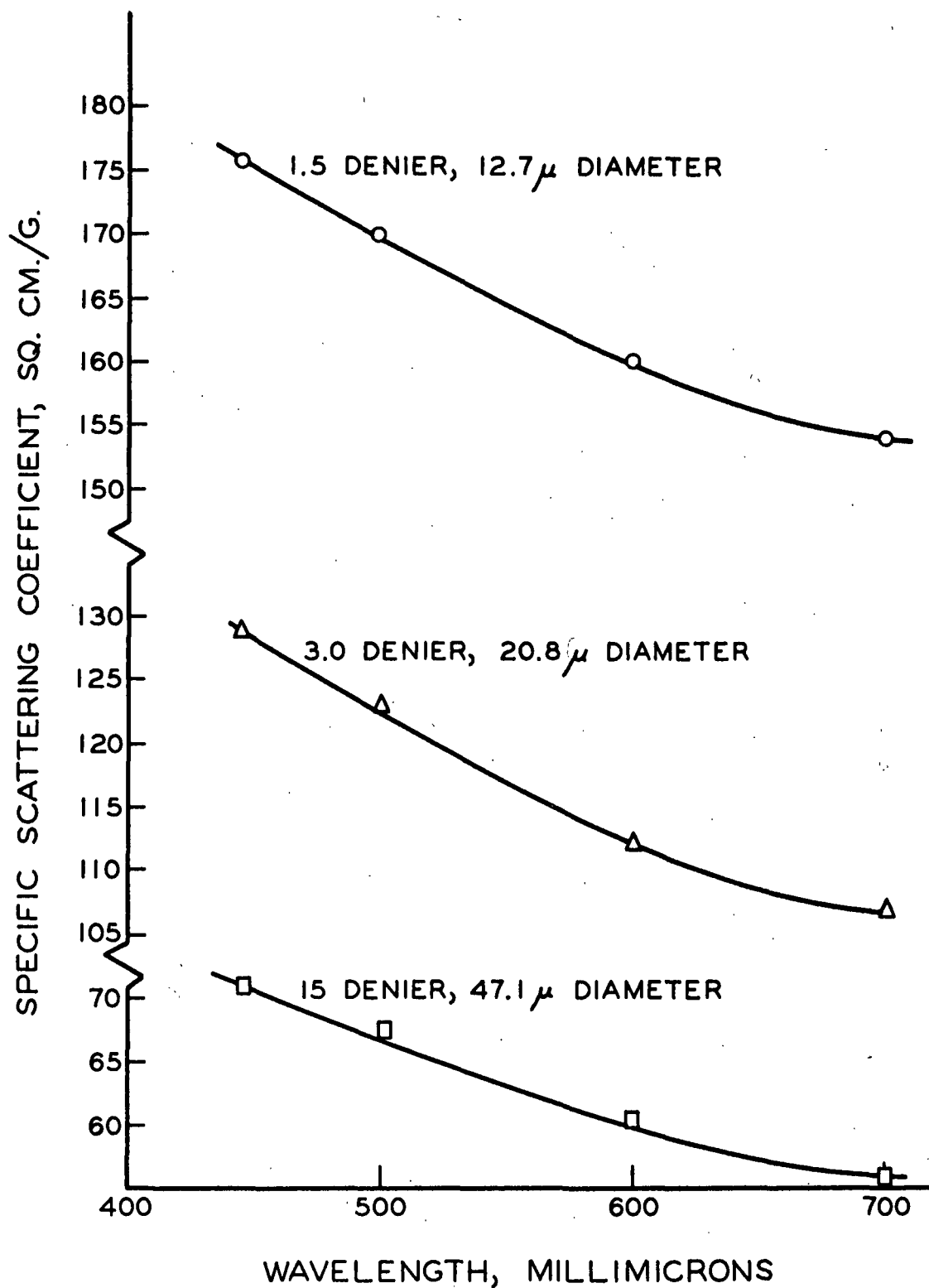


Figure 14. Specific Scattering Coefficient versus Wavelength for the Nylon Fibers

TABLE X

SPECIFIC SCATTERING AND ABSORPTION COEFFICIENTS OF ORLON FIBERS

(s and k are given in sq. cm./g.)

Sheet No.	Wavelength, mμ								Basis Wt., g./sq.cm.
	440		500		600		700		
	<u>s</u>	<u>k</u>	<u>s</u>	<u>k</u>	<u>s</u>	<u>k</u>	<u>s</u>	<u>k</u>	
1.5 Denier									
1	--	2.37	299.0	1.78	275.2	1.53	256.0	1.21	0.01221
2	313.1	4.55	299.3	2.45	277.1	2.75	260.1	2.71	0.00502
3	291.9	4.40	276.6	1.93	257.8	1.93	243.5	1.79	0.00951
4	283.8	4.45	271.8	2.11	253.2	2.04	239.7	1.84	0.00772
5	273.4	4.27	259.8	2.24	239.8	2.37	227.4	2.51	0.00562
6	323.8	5.22	306.3	2.73	285.2	2.67	267.9	2.46	0.00674
7	298.4	4.57	289.4	2.57	268.7	2.39	253.2	2.44	0.00702
8	<u>278.5</u>	5.05	<u>270.2</u>	3.20	<u>248.9</u>	3.47	<u>233.2</u>	3.41	0.00411
Average	295		284		263		248		
2.0 Denier									
1	206.4	4.48	202.5	2.06	192.7	1.16	187.9	1.06	0.01535
2	204.6	4.21	199.4	2.06	189.6	1.20	182.7	0.95	0.01275
3	212.7	4.70	206.7	2.52	195.8	1.52	190.6	1.49	0.00891
4	207.0	4.46	199.9	2.20	192.6	1.56	188.2	1.29	0.01210
5	206.3	4.09	197.3	1.79	190.8	1.08	183.8	0.92	0.01402
6	206.4	4.47	198.3	1.99	191.7	1.28	184.4	1.08	0.01406
7	209.2	4.48	202.9	2.09	193.9	1.36	187.9	1.13	0.01230
8	210.8	4.74	199.4	2.05	188.9	1.26	182.2	1.09	0.01259
9	197.3	4.09	191.4	1.79	183.6	1.20	178.2	1.01	0.01403
10	198.1	4.18	193.2	2.19	182.7	1.36	178.2	1.12	0.01155
11	<u>209.9</u>	4.15	<u>205.3</u>	1.88	<u>194.6</u>	0.99	<u>186.0</u>	0.80	0.01767
Average	206		200		191		184		



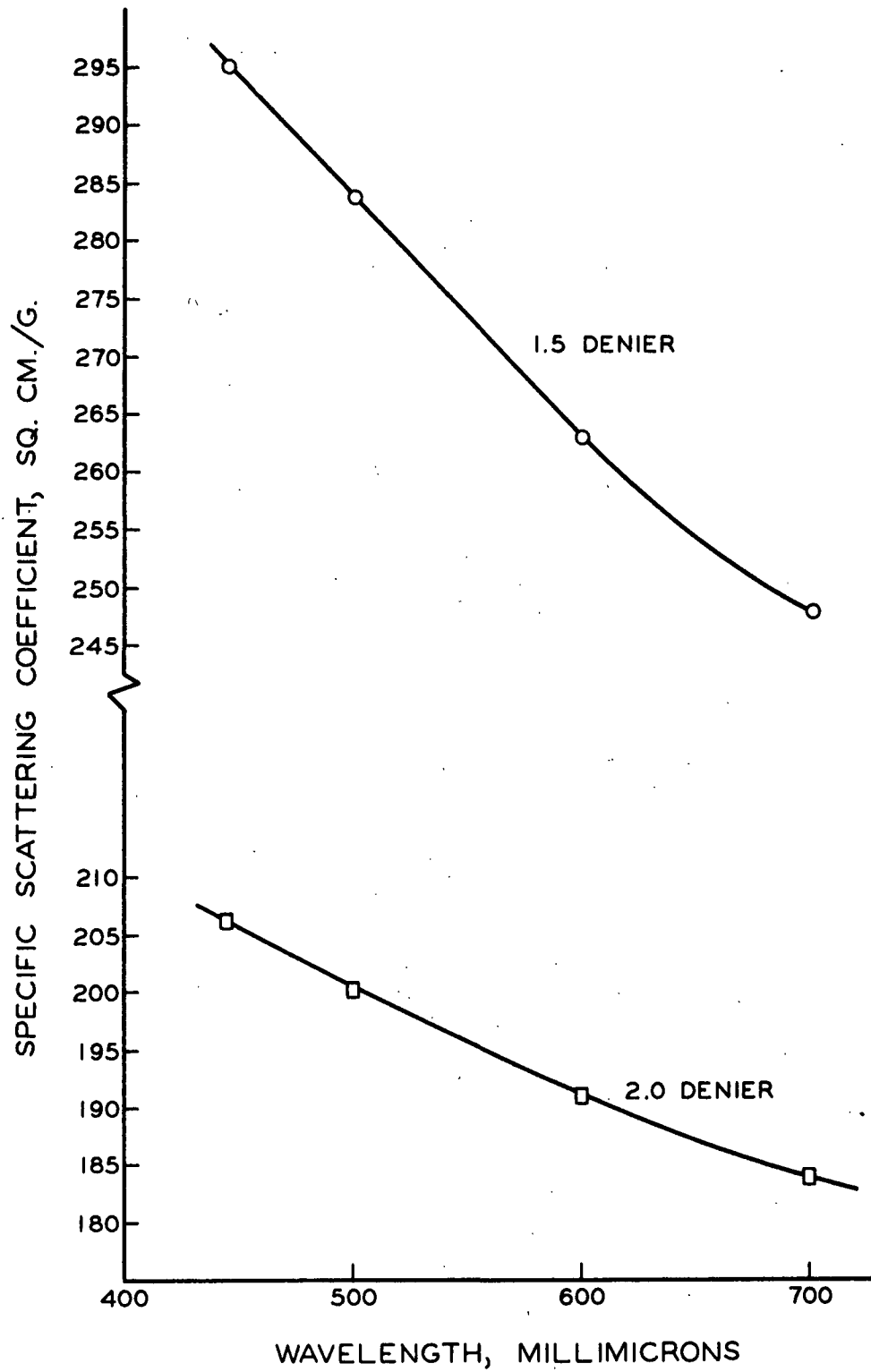


Figure 15. Specific Scattering Coefficient versus Wavelength for the Orlon Fibers

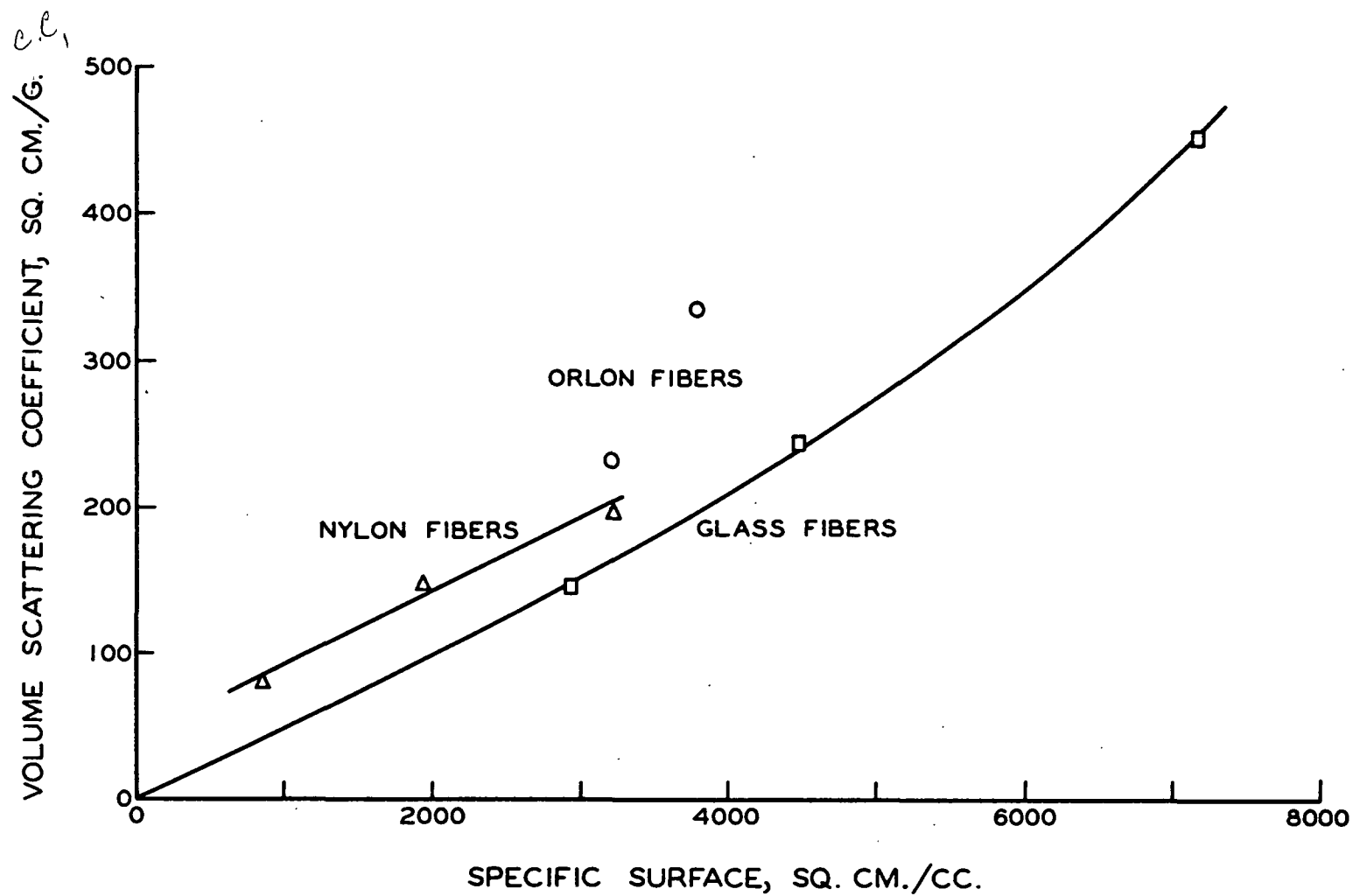


Figure 16. Volume Scattering Coefficient versus Specific Surface  
for Synthetic Fibers at  $440\text{ m}\mu$

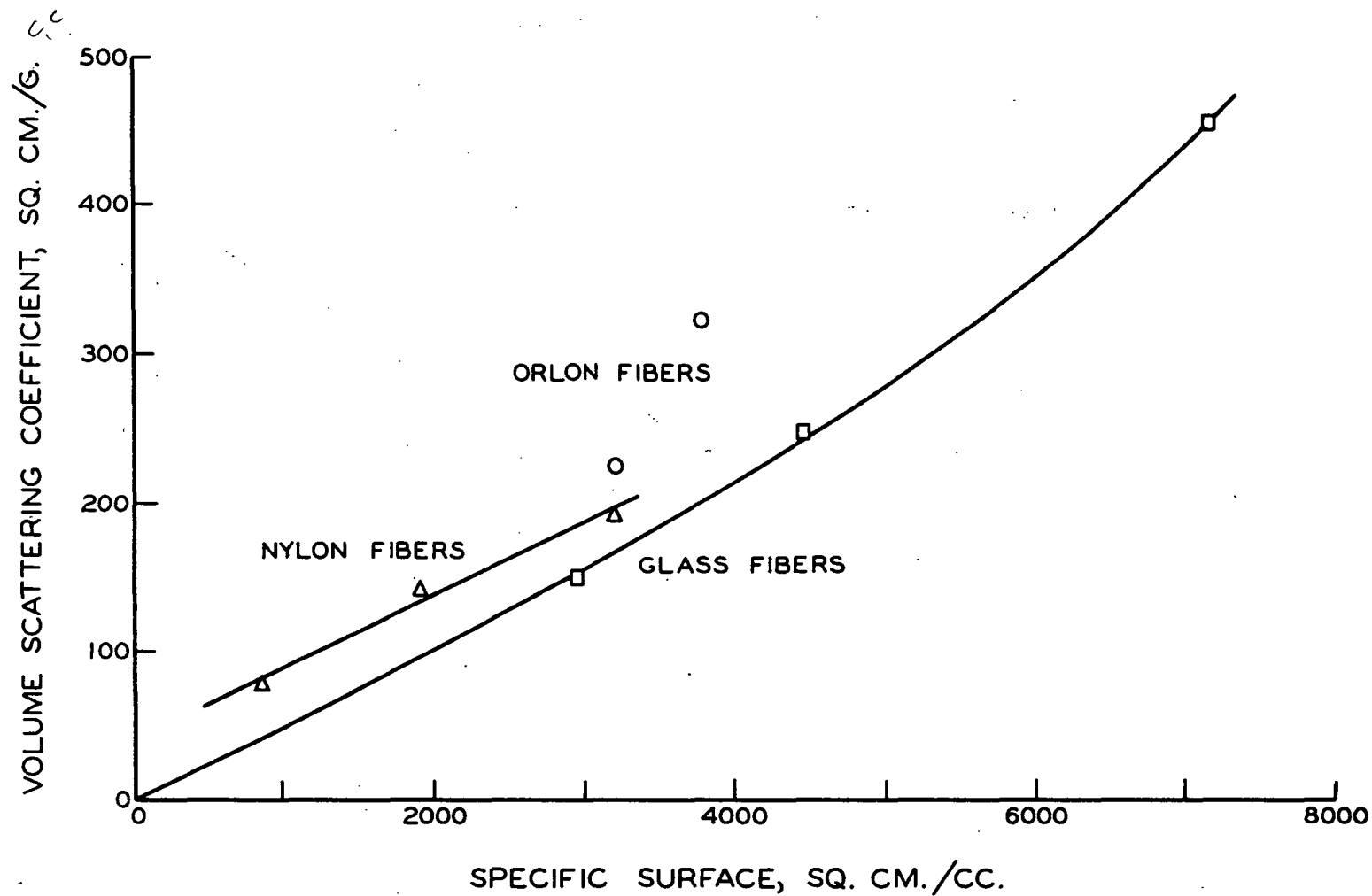


Figure 17. Volume Scattering Coefficient versus Specific Surface for Synthetic Fibers at 500 mμ

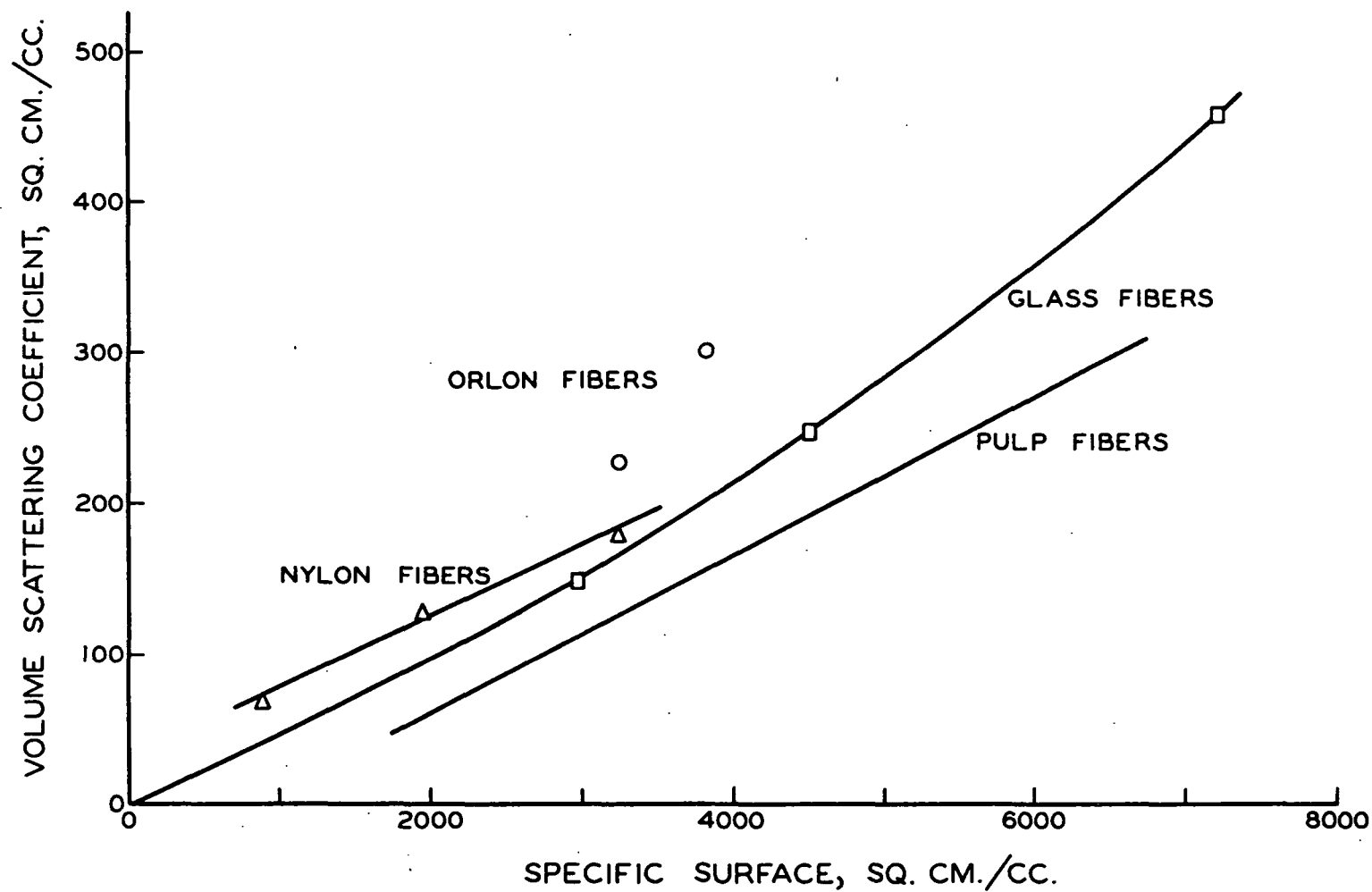


Figure 18. Volume Scattering Coefficient versus Specific Surface  
for Synthetic Fibers at 600 mμ

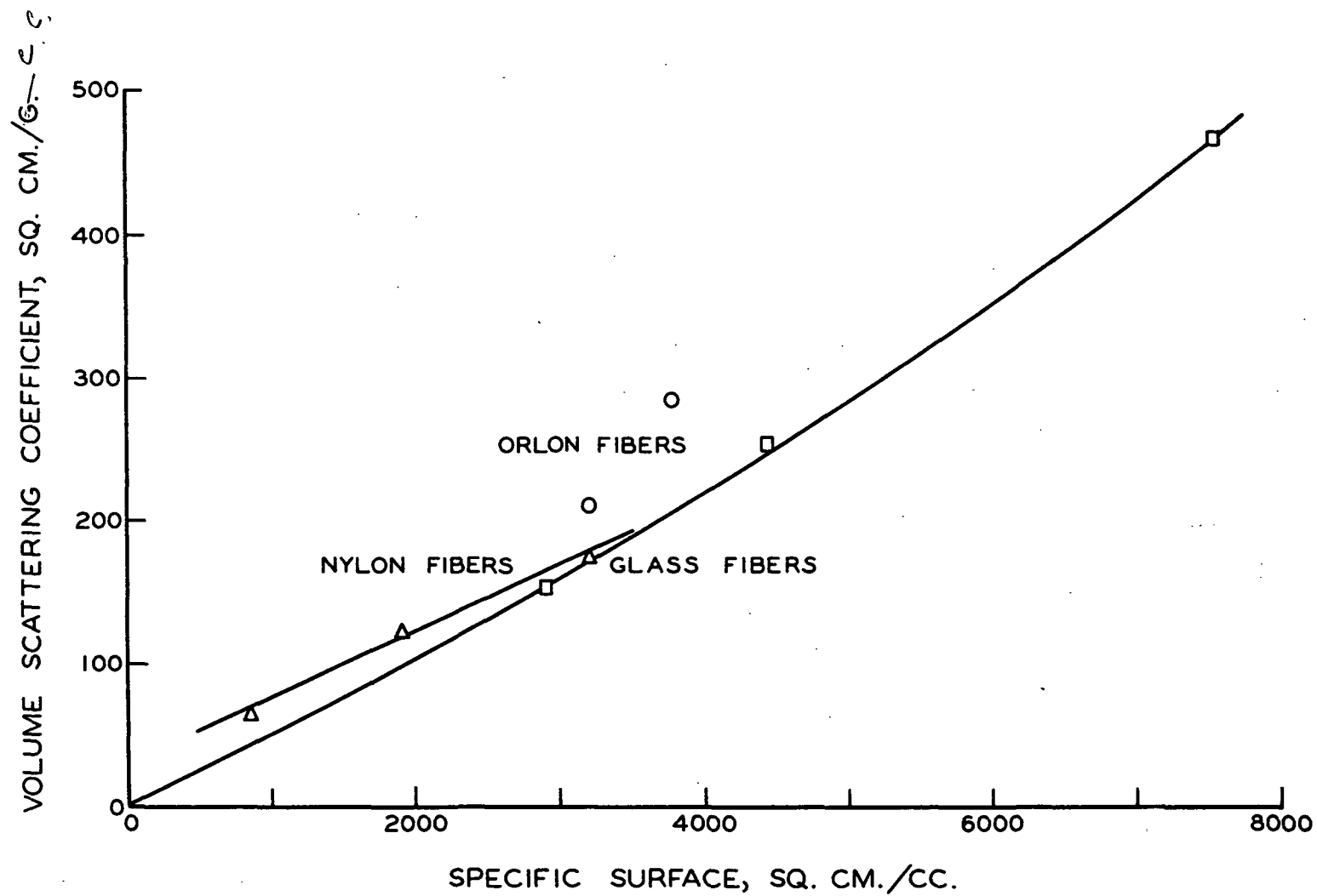


Figure 19. Volume Scattering Coefficient versus Specific Surface  
for Synthetic Fibers at 700 mμ

fibers should go through zero. The curves for glass fibers were forced through zero and fitted with a second-order equation by the method of least squares. The curvature of the curves for glass fibers was significant at above the 99% level. The data for volume scattering coefficients of pulp fibers in Fig. 18 was taken from the work of Haselton (16), using a value of 1.56 g./cc. for the density of cellulose. Haselton determined the specific surface area by the nitrogen adsorption method.

#### COMPARISON OF THE SCATTERING POWER OF PULP SHEETS DETERMINED ON THE NORMAL GERS AND ON THE MODIFIED GERS

It was not known a priori that the scattering power of paper sheets would be the same when the sample was illuminated perpendicular to the surface and the diffuse reflectance measured (normal GERS) as when the sample was illuminated diffusely and the reflectance near the perpendicular was measured (modified GERS). The scattering power is the product of the specific scattering coefficient times the basis weight of the sheet. It was shown on page 41 of this thesis that the reflectance of rather opaque samples was independent of the geometry used. In order to examine this further, other paper samples were compared on the normal and modified GERS's. The papers used were a glassine paper having a transmittance of about 83% and a thin lens tissue of very open structure which had a transmittance of about 79%.

The reflectance of one sheet,  $R_o$ , the transmittance,  $T$ , and the reflectance of an optically infinite pad,  $R_\infty$ , were determined on the normal GERS. Only  $R_o$  and  $R_\infty$  were determined on the modified GERS. Ten samples of the glassine and twenty samples of the lens tissue were run at a wavelength of 600 mμ. The values of the scattering power for the two samples are shown in Table XI.

TABLE XI  
SCATTERING POWER OF GLASSINE AND LENS TISSUE PAPERS  
ON NORMAL GERS COMPARED TO MODIFIED GERS

(Wavelength 600 mμ)

Calculated from	Glassine			Lens Tissue	
	$\frac{R_0 - R_\infty}{T - R_\infty}$	$\frac{T - R_\infty}{T - R_0}$	$\frac{T - R_0}{R_0 - R_\infty}$	$\frac{R_0 - R_\infty}{T - R_\infty}$	$\frac{T - R_\infty}{T - R_0}$
Normal GERS, <u>sW</u>	0.147	0.146	0.147	0.254	0.266
Normal GERS, std. dev. <sup>a</sup>	0.0032			0.0094	
Modified GERS, <u>sW</u>	0.145			0.240	
Modified GERS, std. dev. <sup>a</sup>	0.0035			0.0116	

<sup>a</sup>95% Confidence limits for difference between means =  $\pm 0.004$ .

From Table XI it is evident that, in the case of the glassine paper, the two GERS's gave results which agreed to well within the statistical accuracy of the data. There was, however, a statistical difference between the two GERS's in the case of the lens tissue. There was also a significant difference between the scattering power calculated from  $\frac{T}{R_0}$  and  $\frac{R_\infty}{R_0}$  and the scattering power calculated from  $\frac{R_0}{R_\infty}$  and  $\frac{R_\infty}{R_0}$ .

The sheets of lens tissue were very thin and the formation was poor. The experimental difficulties involved in measuring the reflectances and the transmittances of the thin sheets and the nonuniformity of the sheets may have caused this discrepancy. There is also the possibility that the nonuniformity and open structure of the sheets were sufficient to cause the K-M theory to be incorrect for this case.

## DISCUSSION OF RESULTS

### THEORETICAL RESULTS

The specific scattering coefficient was calculated from Equation (48) for two different fiber diameters, 9.02  $\mu$  and 5.69  $\mu$  at a wavelength of 700 m $\mu$ . The specific scattering coefficient was also calculated at 440 m $\mu$  for the 5.69  $\mu$  fiber. The index of refraction was assumed to be 1.544. The reasons for choosing these points for the calculations were partly practical and partly theoretical in nature. The equation for the scattering diagrams, Equation (37), contains infinite series. In practice, the terms of the series become small after about  $2\pi a/\lambda^\circ$  terms. Thus, for the larger sizes of fibers and for the shorter wavelengths, the number of terms which it would have been necessary to carry would have become much larger and the amount of computer time for the solution of the equation would have become prohibitive. The theoretical reasons were, first that the largest fiber size, 13.7  $\mu$ , was approaching the size where the geometric optics approximations would begin to be valid (20). From the nature of the approximations, various things can be deduced without the necessity of carrying out the entire calculation. The other point was that the small fiber sizes, where the geometric optics approximations were not valid, would give a better test of the equation when compared to the experimental values.

The scattering coefficients of both fibers at 700 m $\mu$  were calculated directly from the appropriate equations. The scattering coefficient of the 5.69  $\mu$  fiber at 440 m $\mu$  was deduced from the following considerations.

The wavelength dependence of the equation for the scattering diagrams, Equation (37), is given by the wavelength and the parameters  $2\pi a/\lambda^\circ$  and  $2\pi am/\lambda^\circ$ . From Equations (7) and (8), it can be seen that the infinite series in Equation



(37) are functions of the last two variables only. The value of  $2\pi a/\lambda^\circ$  for the 9.02  $\mu$  diameter fiber was 40.6 at 700  $m\mu$  and for the 5.69  $\mu$  fiber it was 40.6 at 440  $m\mu$ . Thus, the scattering diagrams for these two points are the same except for the proportionality to wavelength shown in Equation (37). The light intensity back-scattered from a unit length of fiber for the 5.69  $\mu$  fiber at 440  $m\mu$  was readily calculated from the back-scattered light from the 9.02  $\mu$  fiber at 700  $m\mu$ . This, of course, assumed that the refractive indices of the fibers in the two cases were the same, which was not strictly true, since the refractive index of the fibers at 700  $m\mu$  was 1.544 and at 440  $m\mu$  was 1.555. However, the change in refractive index was small; and from the nature of the equations, it would be expected to alter the answer very little. It will be shown for the case of flat glass plates that the back-scattered light at these refractive indices was 15.9 and 16.1%, respectively, for isotropic illumination. The value of the scattering coefficient calculated at a refractive index of 1.544 was probably only a few per cent lower than what would have been calculated at the true refractive index of 1.555.

The scattering coefficients which were calculated are shown in Table XII along with the experimental values. The column labeled  $1 - \sin^{12} \alpha$  was calculated by assuming another type of incident light distribution which will be discussed later, but it is tabulated here for reference.

The disagreement between the experimental and the theoretical values of the scattering coefficients indicates that one or more of the assumptions used in the theoretical development were not valid for the conditions in the glass fiber sheets. The complete electromagnetic equations were used to calculate the scattering diagrams, so the scattering diagrams themselves were correct. The assumptions were:

1. The fibers were identical in size and optical properties.
2. The fibers lay in the plane of the sheet.
3. The fibers were optically smooth and were circular in cross section.
4. The Kubelka-Munk theory was applicable.
5. The fibers were nonabsorbing.
6. The fibers scattered light as if they were infinitely long cylinders and independent from each other.
7. The light illuminating each fiber was isotropic.

TABLE XII

THEORETICAL VALUES OF THE SPECIFIC SCATTERING COEFFICIENT

	Theoretical	Experimental	$\frac{(\text{Theoretical } \underline{s})}{(\text{Experimental } \underline{s})} 100$
Fiber diameter, $\mu$	5.69	5.69	
Wavelength, $m\mu$	700	700	
Refractive index	1.544	1.544	
$\underline{s}$ , sq. cm./g.			
Isotropic	430	183	230%
$1 - \sin^2$	290		160%
	<i>S/A</i>		
	<i>.104</i>		
Fiber diameter, $\mu$	9.02	9.02	
Wavelength, $m\mu$	700	700	
Refractive index	1.544	1.544	
$\underline{s}$ , sq. cm./g.			
Isotropic	240	99	244%
$1 - \sin^2$	160		161%
	<i>.092</i>		
Fiber diameter, $\mu$	5.69	5.69	
Wavelength, $m\mu$	440	440	
Refractive index	1.544	1.555	
$\underline{s}$ , sq. cm./g.			
Isotropic	381	176	215%
$1 - \sin^2$	252		143%
	<i>.090</i>		

from 44  
 surface area for 5.69  $\mu$  fiber  
 9.02  
 2800  $\text{cm}^2/\text{gm}$   
 1740

The fiber diameters were not uniform as was seen in Table I. The effect of this on the theoretical scattering coefficients depends upon the size of the fibers. The geometric optics approximations show that the scattering intensity at any angle is directly proportional to the geometric cross section of the body (20). It can be readily shown, in this case, that the scattering coefficient would be inversely proportional to the fiber diameter. The number average fiber diameter would then be the proper average diameter to use in the calculations. For the sizes of particles in which geometric optics breaks down, the scattering is a complex function of the fiber diameter. No theoretical analysis was carried out to find the correct fiber diameter average to use in this case. The experimental values showed that the scattering coefficient was not strictly inversely proportional to the fiber diameter. The use of the mean fiber diameter in the calculations was, then, not precisely correct, particularly for the smaller fibers. However, this effect was thought to be small, even for the smallest fibers used. Two reasons for this are: first, even the smallest fibers are nearing the region in which geometric optics approximations become valid, and, second, the experimental values of the scattering coefficients deviated only a small amount from the inverse diameter relationship.

The optical clarity of the fibers was found to be very good. The fibers were observed under a microscope with monochromatic light immersed in a fluid of identical refractive index. The fibers disappeared completely from view indicating the uniformity and optical clarity of the fibers. The fibers were imbedded in a methylmethacrylate polymer, and the cross sections were observed. The cross sections were circular in all cases.

Close observation of the sheet indicated that the fibers lay nearly in the plane of the sheet. There was some orientation out of the plane of the sheet,

but it was limited to a few degrees. No fibers were observed to lie in a vertical or nearly vertical direction. It can be seen from the tabulated scattering diagrams, page 95, that the scattering varies slowly with the angle of incidence. Therefore, the effect on the calculated scattering coefficient of the slight orientation of the fibers out of the plane of the sheet was no doubt very small.

The fibers were known to be slightly absorbing. The experimental absorption coefficients were small, but the value of  $R_{\infty}$  for the glass fiber sheets was about 80%. The effect of the absorption would be to decrease the scattering from a single fiber at all angles. The theoretical scattering coefficients were, then, too high. An analysis of the reflectance from an isotropically illuminated plane glass sheet both with and without absorption indicates that the reflectance of the glass slab is almost unaffected by small amounts of absorption (see page 73). Qualitatively, it would no doubt be the same for cylinders; so very little change in the scattering coefficient would be expected due to the presence of absorption.

The applicability of the Kubelka-Munk theory to fibrous structures has been adequately demonstrated in the past as discussed on page 3. The use of the theory in this situation was almost certainly valid.

From an examination of Fig. 7, it is evident that the fibers cannot be considered as an assembly of cylinders which are illuminated and scatter independently. The areas involved in fiber crossings obviously distort both the incident and the scattered fields. There were also fibers which were not actually touching that may have caused a partial shadowing of adjacent fibers and distorted the incident and the scattered fields. These phenomena would probably tend to reduce the total scattered light in the affected regions and would cause a lower scattering coefficient than the one which was calculated.

The experimental observation that the scattering coefficient did not vary with compression of the sheet indicates that this effect was probably small. Compressing the sheet would bring more fibers into contact and into closer proximity to each other. The fact that this did not change the value of  $\underline{s}$  showed that, while the effect was no doubt present, the magnitude of the change was too slight to be noticed.

The light distribution which was assumed incident on each unit length of fiber was isotropic,  $f(\alpha) = 1$ , where  $\alpha$  is the angle between an incident pencil of light and the normal to the sheet.

The light incident on the front surface of the glass sample holder was nearly isotropic. The light transmitted by the glass onto the sample was not isotropic due to the preferential reflectance and absorption as the angle from the perpendicular,  $\alpha$ , increased. Thus, the light illuminating the top layer of the fibers was not isotropic. It would be expected that the fibers in a very thin sheet would each be illuminated by this nonisotropic distribution and would scatter light in accordance with that distribution. A thicker sheet would be illuminated near the top in this fashion, but the light distribution would vary as the light progressed through the sheet due to scattering and absorption in the layers above. In this manner, the light would soon become diffuse and would probably reach an equilibrium distribution which would be constant throughout the remainder of the sheet.

The experimental determinations of  $\underline{s}$  as the basis weight was varied, showed that there was no measurable change in  $\underline{s}$  with basis weight. This indicates that even for the thinnest sheets which were used, the light distribution throughout the majority of the sheet was uniform and similar to that in other sheets of the same material.

It has often been found (32) that sheets which have an appreciable absorption show marked deviations from isotropic reflectance from the front surface. The reflected light normally falls off more rapidly at near grazing angles than would be expected if it were isotropic. The glass fiber sheets had an  $R_{\infty}$  of about 80%, so it is probable that these sheets exhibited this nonisotropic behavior. This would affect the light distribution incident on the fibers in the sheet. In order to find what effect this would have on the calculated scattering coefficients, certain arbitrary light distributions were assumed. The calculations were carried out for the following light distributions:

$$f(\alpha) = 1 - \sin^6 \alpha$$

$$f(\alpha) = 1 - \sin^8 \alpha$$

$$f(\alpha) = 1 - \sin^{12} \alpha$$

Normal Illumination.

The results calculated for the 9.02  $\mu$  diameter fiber at 700 m $\mu$  wavelength are shown in Table XIII.

TABLE XIII.

THEORETICAL VALUES OF  $\underline{s}$  FOR VARIOUS INCIDENT LIGHT DISTRIBUTIONS

Incident Distribution	$\underline{s}$ , sq. cm./g.
$f(\alpha) = 1$	242
$f(\alpha) = 1 - \sin^6 \alpha$	151
$f(\alpha) = 1 - \sin^8 \alpha$	152
$f(\alpha) = 1 - \sin^{12} \alpha$	160
Normal	72
Experimental	99

The light distributions were plotted in Fig. 20 for the light incident on a unit plane area of sheet. The circle is Lambert's Law for isotropic illumination and the others are as indicated.

The distribution  $1 - \sin^2 \alpha$  illuminated a unit plane area of the sheet with only 15% less light than isotropic illumination. This, however, lowered the scattering coefficient by about 35% and brought the theoretical and the experimental values into much closer agreement. One reason for the large decrease in  $s$  was that, at nearly grazing angles of illumination, the large forward scattering due to diffraction was partly contained in the back-scattered part of the light. Cutting out the grazing angles of illumination effectively removed this diffraction portion from the back-scattered light and greatly diminished the calculated value.

The light distribution of the scattering from a single fiber which is illuminated with isotropic illumination was calculated. The results of this calculation are plotted in Fig. 27, page 139. It is evident from the figure that the intense forward scattering of the rays which strike the fiber at angles of  $\alpha$  near  $90^\circ$  causes the scattered intensity to be much higher at these angles than for the angles of  $\alpha$  near  $0^\circ$ . Thus, removing some of the incident light at grazing angles reduces the intense scattering at these angles and lowers the calculated value of the scattering coefficient.

Another reason for the large decrease in the scattering coefficient was that solid objects intercepted more of the light at grazing angles of illumination than a plane surface. Decreasing the amount of light at grazing angles of illumination decreased the light intercepted by the solid object much more than it decreased the amount of light falling on a plane surface. The intensity of

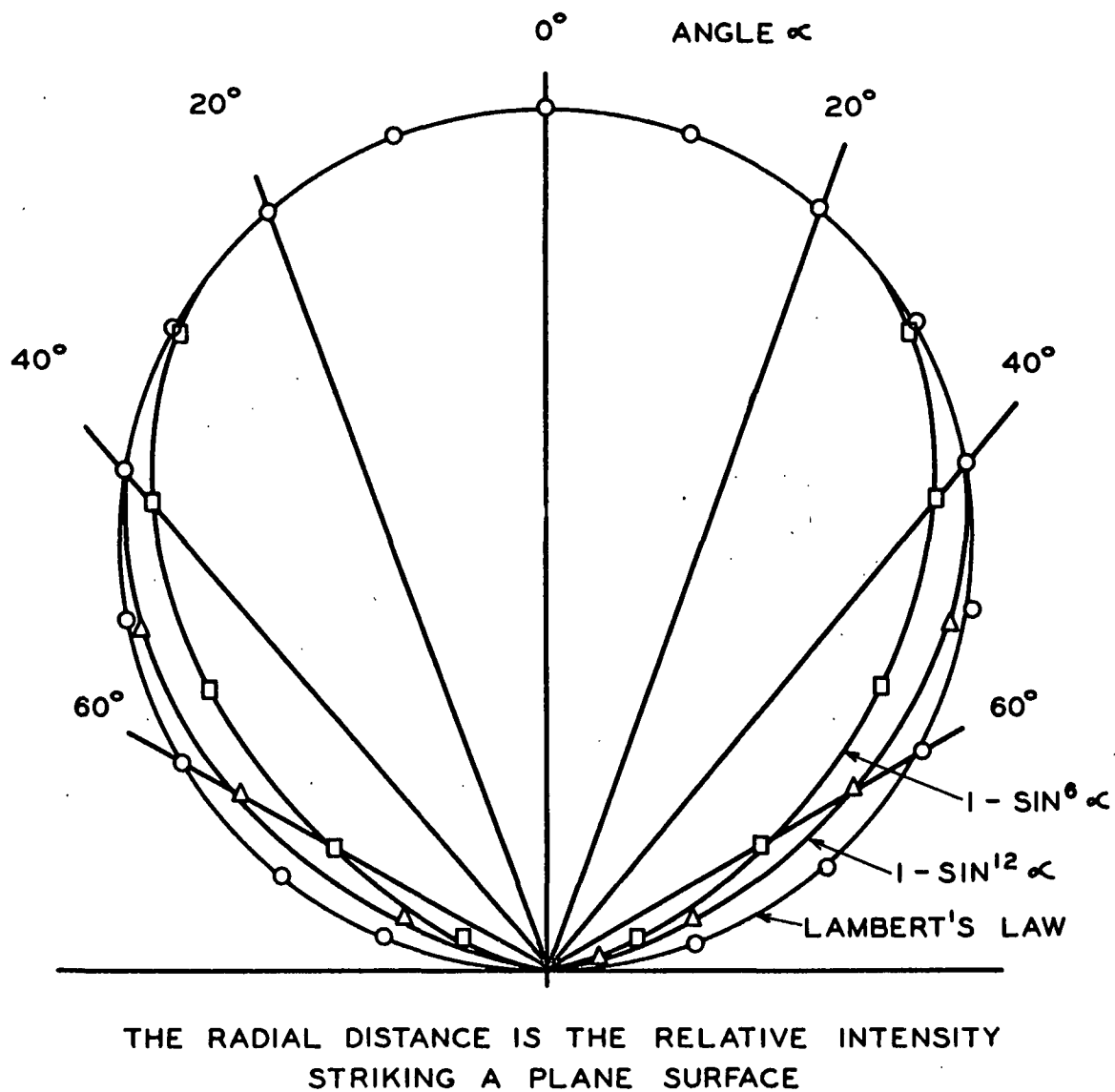


Figure 20. Assumed Light Distributions



the light scattered by a fiber is a function of the amount of light intercepted by the fiber. Thus, an examination of Equation (47) indicates that  $\underline{s}$  would be diminished, since  $\underline{s}$  is proportional to the ratio of the total light back-scattered from a unit length of fiber to the amount of light striking a unit area of a plane surface.

These light distributions were arbitrary. It did point out, however, that the calculated values of  $\underline{s}$  could be varied over wide limits by altering the light distribution; and introducing a light distribution such as is often found for the reflectance of paper sheets gave a calculated value of  $\underline{s}$  which was not far from the experimental value. It may reasonably be concluded that it was the failure of the assumption that there was isotropic light incident on each fiber which caused the majority of the discrepancies between the theoretical and experimental values.

The theoretical equation did predict the way in which the scattering coefficient was found to vary with fiber diameter and with wavelength. If  $1 - \sin^2 \alpha$  is assumed to be a reasonable approximation to the light distribution which was present in the sheet, the theoretical value was shown in Table XII to be 160% of the experimental value for both the 5.69  $\mu$  and the 9.02  $\mu$  fibers at 700 m $\mu$  wavelength and 143% of the experimental value for the 5.69  $\mu$  fiber at 440 m $\mu$ . It should be remembered that the last point was calculated assuming a refractive index of 1.544 whereas the experimentally determined value was 1.555. The calculated value was somewhat low because of this.

It may be concluded that the methods used in the derivation of the theoretical equation are suitable for predicting qualitatively the optical behavior of sheets composed of cylindrical, transparent fibers of varying diameters and at various wavelengths.

This is a useful contribution, since it is now possible to examine certain aspects of the empirical approximation,  $\underline{s} = \underline{KA}$ , which has been used in the past. The present theory predicts that the scattering coefficient would be a linear function of the specific surface area for fiber sizes in the region where geometric optics approximations are valid and where the fiber shapes are uniform. In this region of fiber properties, the approximation  $\underline{s} = \underline{KA}$  would be accurate, simple, and useful. However, the theory also predicts that for smaller fiber sizes the scattering coefficient would be a complicated, oscillating function of the fiber size (see page 20). In this region, which ranges from zero to at least  $10 \mu$  fiber diameter, the approximation  $\underline{s} = \underline{KA}$  would not be true and no simple relationship exists. The usefulness of this approximation, or any other linear approximation, is limited to large, uniform fibers. For smaller fibers, it would be possible to have two or more fiber diameters that would give the same scattering coefficient, since the scattering from small fibers is an oscillating function of size. This is a severe limitation on the usefulness of the scattering coefficient as a measure of individual fiber properties.

Whole pulp fibers are normally larger than  $10 \mu$ , so it might be thought that such a system would obey the geometric optics approximations. However, fibers are seldom whole in a sheet of paper, particularly after refining. There would be many fiber elements which would be below the minimum size that would obey the laws of geometric optics. Certain parts of the pulp fiber system would scatter as large scatterers and other parts would scatter in the complex manner described by the electromagnetic equations. In this situation, the relationship  $\underline{s} = \underline{KA}$  would not be a useful or accurate description of the scattering process. If the relationship is found experimentally to be valid, it can only be that, due to a fortuitous combination of the various types of scattering, the relation appears to hold or that the number of small elements is so small that the effect is unobservable.

Nylon fibers, which contained small pigment particles, were used in order to demonstrate the effect these small particles might have on the scattering behavior of the sheet. This work will be discussed beginning on page 73.

Only minor improvements in the theoretical equations would be possible without changing the basic technique used in the derivation. The technique was to assume that each unit length of fiber was illuminated identically and scattered independently. Minor modifications might include: (a) incorporating a complex index of refraction in the scattering equations to account for the absorption of light in the fibers, (b) using a different light distribution incident on each unit length of fiber which would be less arbitrary than the one used, (c) finding the correct fiber diameter average to be used, (d) determining the amount of fiber length which does not scatter appreciably because of fiber crossings, (e) accounting for the slight orientation of the fibers out of the plane of the sheet. Any major improvement would have to be made by dropping the assumption that each unit length of fiber behaves independently. This would involve solving the problem of multiple scattering where each point on the fiber is illuminated by the incident light and also by the light scattered by all of the other fibers. This has been done (33) for small particles where the scattering diagrams are axially symmetrical and are simple in form, such as Rayleigh's law, and where the particles are far removed from each other. In the case of a sheet of fibers of the size of interest in papermaking, the scattering diagrams are very complex and are not axially symmetrical, nor are the fibers widely separated. The problem would be inherently much more complex than the ones which have been solved.

Lathrop (34) has calculated the light back-scattered from an infinitely extended plane slab of glass for both the nonabsorbing and the absorbing cases. This can be used to calculate the scattering and absorption coefficients of a

sheet composed of flat ribbons of glass arranged so that the major axis and the largest minor axis of the ribbons are in the plane of the sheet. The assumptions are the same as those discussed for the cylindrical fibers with the added assumptions that the geometric optics approximations are valid and that the edges of the ribbons do not affect the scattering. Let the dimensions of the ribbon be as shown in Fig. 21.

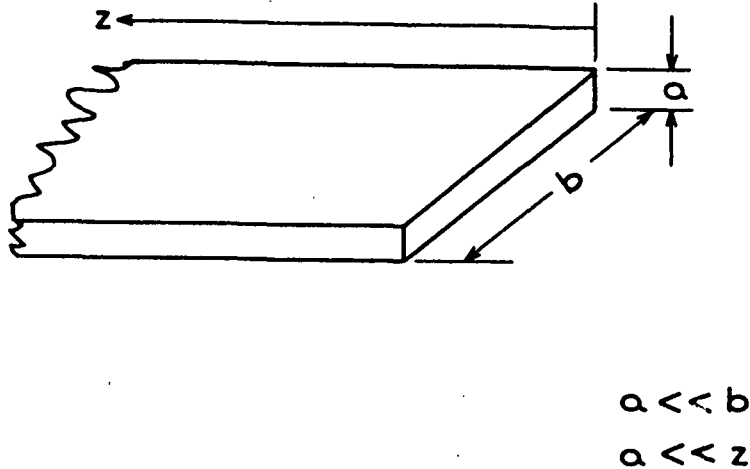


Figure 21. Assumed Dimensions of a Ribbonlike Fiber

Let the fraction scattered backwards from the ribbon for isotropic illumination be REFL and the fraction absorbed be ABS. The specific scattering and absorption coefficients can be shown to be:

$$s = \text{REFL} / a\rho_f \quad (59)$$

$$k = \text{ABS} / a\rho_f \quad (60).$$

The value of REFL at an index of refraction of 1.555 was calculated to be 0.161 and for a refractive index of 1.544 it was 0.159 for the case of no absorption. For an absorption, ABS, of 0.011, the values of REFL dropped to 0.160 and 0.158, respectively. The case where there was no absorption, assuming a ribbon 5  $\mu$  thick, gave an  $\underline{s}$  of:

$\underline{s} = 125$  sq. cm./g., refractive index equalled 1.544

$\underline{s} = 127$  sq. cm./g., refractive index equalled 1.555.

The values of  $\underline{s}$  and  $\underline{k}$  for the absorbing case were found to be:

$\underline{s} = 124$  sq. cm./g., refractive index equalled 1.544

$\underline{k} = 8.6$  sq. cm./g.

$\underline{s} = 126$  sq. cm./g., refractive index equalled 1.555

$\underline{k} = 8.6$  sq. cm./g.

This shows that varying the refractive index by varying the wavelength and introducing absorption into the ribbons caused very little change in the calculated values of  $\underline{s}$ . This supports what has commonly been found in practice, that  $\underline{s}$  is not a noticeable function of  $\underline{k}$ . Cylindrical fibers and fibers of other shapes would no doubt exhibit variations of a similar order of magnitude.

It would not be useful to try to fit this model to an actual sheet of paper. The pulp fibers often collapse into ribbons during drying; however, the thickness of the collapsed fibers varies widely. The cross-sectional shape of the fibers would not be rectangular as assumed here, nor would the edges affect the scattering a negligible amount.

#### DISCUSSION OF THE EXPERIMENTAL RESULTS FOR NYLON AND ORLON SHEETS

Sheets made from pulp fibers exhibit both an increasing and a decreasing functional relationship of  $\underline{s}$  with wavelength. It was thought that the effect of small scattering centers in the pulp sheets might account for the observed variations. These effects would be particularly noticeable if the size of the small particles was of the order of a wavelength of light, since particles of this size scatter strongly, and the scattering is a rapid function of wavelength.

The wavelength dependence of small particles of a size less than the wavelength of light can be approximated by Rayleigh's law. Rayleigh's law states that the scattering should be proportional to the reciprocal of the wavelength to the fourth power. Thus, it would be expected that any sheet which contained particles in this small size range would show a decreasing scattering coefficient as the wavelength was increased.

In order to test this hypothesis, sheets were prepared from nylon fibers which contained a titanium dioxide pigment. The diffraction patterns of the particles in the nylon were clearly visible under the light microscope, but the outlines of the particles could not be distinguished. This indicates that the particles were of the order of a wavelength of light in size. The scattering coefficients were found to decrease with increasing wavelength as shown in Fig. 13. This agrees with the hypothesis outlined above.

The indices of refraction of the nylon and the glass fibers were nearly identical. Since the variation in  $\underline{s}$  with the index of refraction is small, the volume scattering coefficients of the two fibers can be compared directly. It can be found from Fig. 16 through 19 that the presence of the titanium dioxide particles in the nylon gave a larger volume scattering coefficient. At 3200 sq. cm./cc. specific surface, the per cent which  $\underline{s}_v$  was larger for the nylon than for the glass is shown in Fig. 22.

The percentage increase in the volume scattering coefficient was greatest for the short wavelengths and dropped off to about 4% at 700 m $\mu$ . This is in qualitative agreement with Rayleigh's law which indicates that the scattering of small particles should be about 6.5 times as intense at 440 as at 700 m $\mu$ .

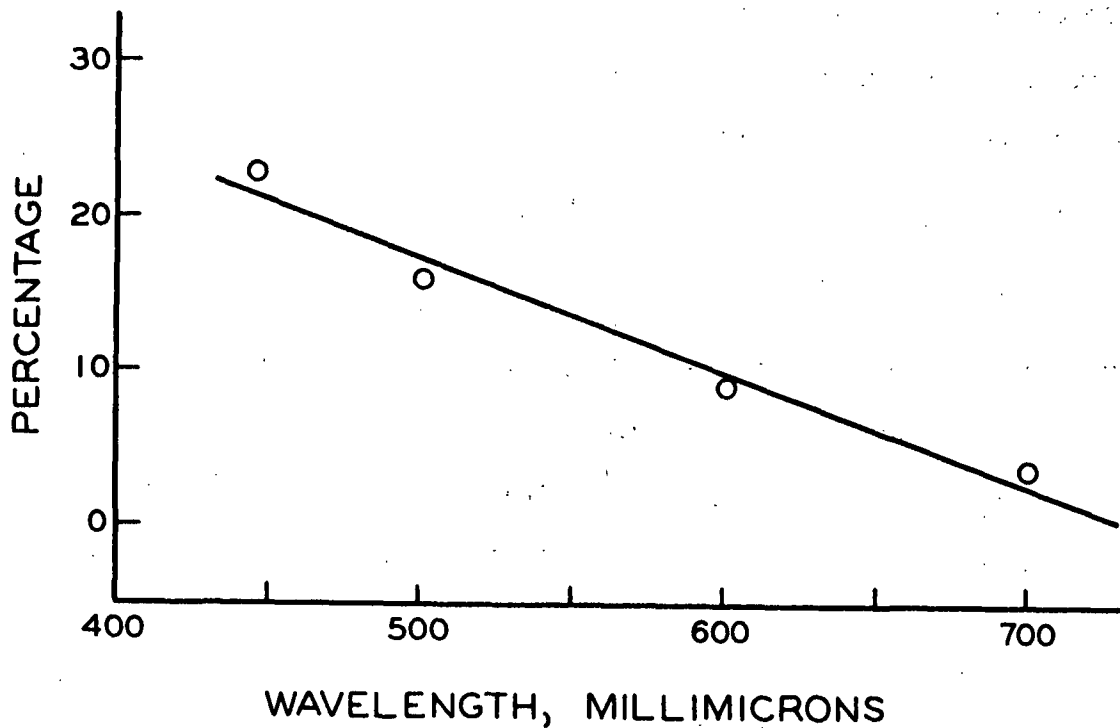


Figure 22. The Percentage by which  $\underline{s}_v$  is Greater  
for Nylon Fibers than for Glass Fibers

The weight concentration of the titanium dioxide was only 0.33% which corresponds to a volume concentration of only about 0.08%. It is evident that a relatively small number of scattering centers can alter the magnitude of the scattering coefficient a rather large amount. The small amount of pigment was also sufficient to change the wavelength variation of the scattering coefficient from a positive to a negative function of wavelength.

This is experimental evidence confirming the phenomena postulated previously from the theoretical equations that the introduction of small elements into the sheet greatly altered the dependence of  $\underline{s}$  on fiber diameter and also altered the  $\underline{s}$ -versus-wavelength relationship.

This has also been verified in work with titanium dioxide pigment suspensions. It has been shown experimentally (35), and can be shown theoretically from the

electromagnetic equations, that the particles exhibited a maximum scattering per unit particle volume at a diameter of about one wavelength of light in the slurry. For smaller particles, or longer wavelengths, the intensity decreased rapidly and for larger particles the intensity decreased to about half the maximum value.

This is no doubt the reason for the apparently anomalous variation of  $\underline{s}$  with wavelength that has been observed with pulp fibers. With some types of pulp fibers which contain few small scattering centers,  $\underline{s}$  was found to increase as the wavelength was increased. Other types of pulp fibers, which contained small particles that tended to scatter more nearly as Rayleigh scatters, produced a decreasing function of  $\underline{s}$  with wavelength.

This phenomenon is observable in the data of Ingmanson and Thode (17). They reported the scattering coefficients for ordinary pulp handsheets, pressed and water dried, and also for sheets made from the same pulp which had been solvent exchanged and dried from butanol. Their data are reported at various refining intervals and for classified and unclassified pulps. The data for three beating intervals are shown in Table XIV.

In each case, the percentage drop in  $\underline{s}$  as the wavelength increased from 450 to 650 m $\mu$  was greater in the case of the butanol-dried sheets than in the case of the handsheets. Drying sheets from butanol allows the cellulose to retain an expanded configuration without the high surface tension forces which would compact the sheet and draw the fiber elements together into a dense, hydrogen-bonded structure as happens when the sheets are water dried. Thus, there are more small elements which are unbonded and can cause light scattering in the butanol-dried sheets than in the water-dried sheets. This is indicated by the higher scattering coefficient for the butanol-dried sheets. It can also be seen in the electron



photomicrographs of water-dried and butanol-dried fibers in the work of Haselton (16). The larger number of small elements which scattered light in the butanol-dried sheets caused the scattering coefficient to drop more rapidly with increasing wavelength than for the water-dried sheets because the small scattering centers behaved more nearly as Rayleigh scatters.

TABLE XIV

VARIATION OF THE SPECIFIC SCATTERING COEFFICIENT  
WITH WAVELENGTH FOR PULP SHEETS

	Refining Time, min.	Unclassified		Drop in $\frac{s}{\mu}$ Between 450 and 650 $\mu$ , %	Classified		Drop in $\frac{s}{\mu}$ Between 450 and 650 $\mu$ , %
		650 $\mu$	450 $\mu$		650 $\mu$	450 $\mu$	
Butanol	0	429	495	13	400	456	12
Handsheets	0	242	267	9.4	239	265	9.8
Butanol	50	539	608	11	466	540	14
Handsheets	50	162	179	9.5	172	191	9.9
Butanol	200	761	896	15	556	663	16
Handsheets	200	56	64	12	91	101	9.9

The large scattering coefficient of the butanol-dried sheets can be attributed to two causes: (a) the unbonded fibrils and fiber elements create more air-solid boundaries for scattering than the water-dried sheets, and (b) the small fibrils and fiber elements exhibit an increased scattering per unit volume in a manner completely analogous to that described previously in the case of the titanium dioxide particles.

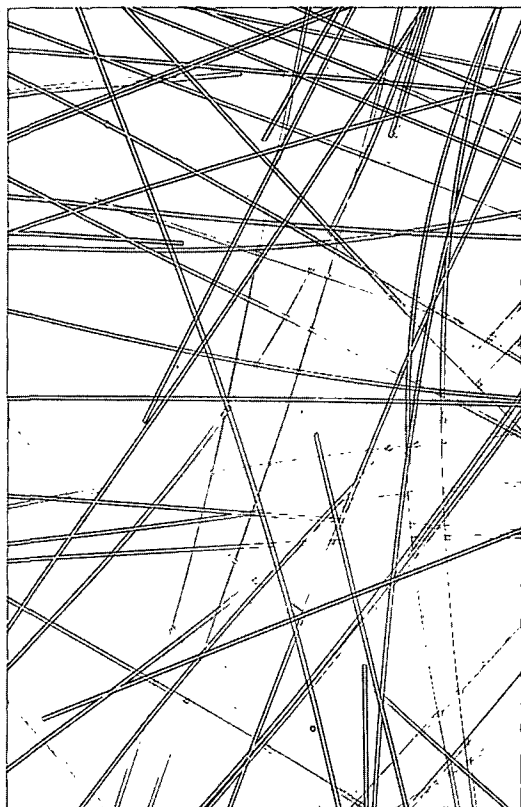
The scattering coefficients of the orlon fibers were determined in order to gain some insight into the effect of the shape of the fibers on the scattering coefficient. The cross sections of the orlon fibers were shown in Fig. 10 and are dog-boned in shape.

The fibers were formed into sheets in such a manner that the major axes of the fibers were randomly oriented in the plane of the sheet. However, there was no significant orientation of the flattened sides of the fibers in any particular plane. The sheets differed in this respect from pulp sheets which commonly are formed so that the fibers collapse primarily in the plane of the sheet.

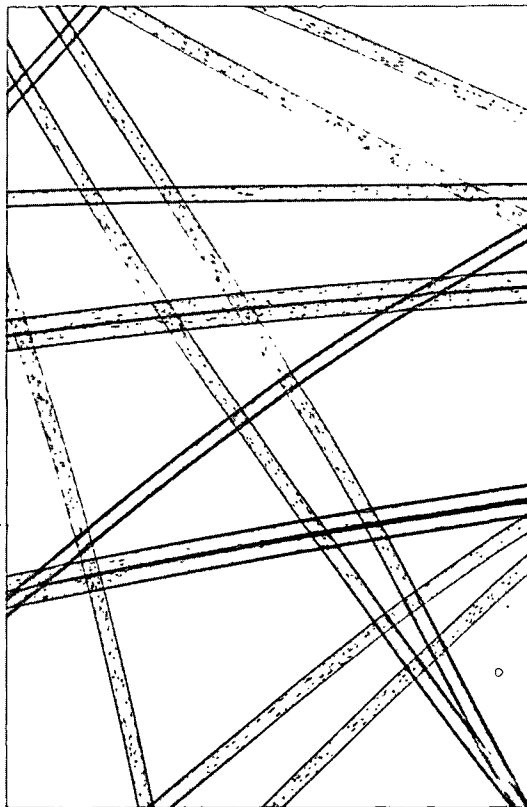
The results of the specific scattering coefficient determinations were tabulated in Table X, and the volume scattering coefficients of the orlon fibers are shown in Fig. 16 through 19 in comparison to the data for the other synthetic fibers. It can be seen from the figures that the orlon fibers exhibited a much larger scattering coefficient than the nylon or glass fibers. The orlon fibers both contained inorganic materials; the 2.0-denier fibers contained 0.20% and the 1.5-denier contained 0.55% by weight of inorganic materials. In comparison, the nylon contained 0.33% filler.

The three types of fibers used in this thesis are shown in Fig. 23.

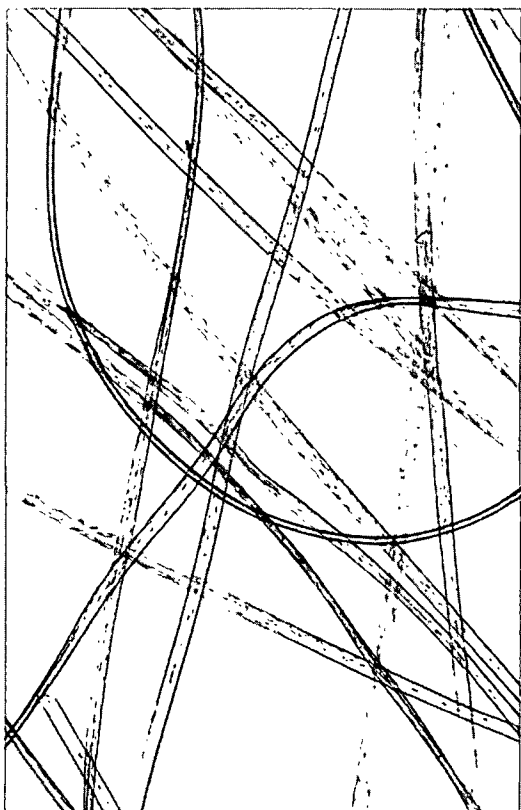
The filler can be seen easily in the nylon fibers and in the 1.5-denier orlon fibers. The 2.0-denier orlon fibers appear to contain no filler except for an occasional fiber. From these pictures, it would be expected that the increase in the volume scattering coefficient due to the filler alone would be much less in the case of the orlon than for the nylon. The index of refraction of the orlon was slightly lower than the glass or the nylon, but the change in  $\underline{s}$  with changing refractive index is small. From the smaller amount of filler in the 2.0-denier orlon and from the small contribution due to the lower refractive index, one would expect the volume scattering coefficient of the orlon to be lower than  $\underline{s}_v$  for the nylon, unless the fiber shape was an important factor. Thus, the difference between the  $\underline{s}_v$  for the orlon and the nylon fibers must be attributed



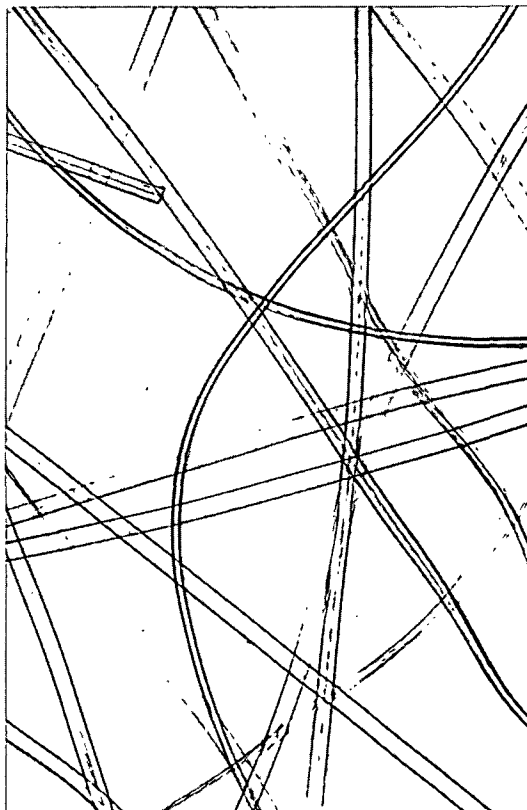
Glass Fibers



Nylon Fibers



1.5-Denier Orlon Fibers



2.0-Denier Orlon Fibers

Figure 23. Pictures of Nylon, Glass, and Orlon Fibers

primarily to the dog-boned cross-sectional shape of the orlon fibers. The difference might be even greater if the materials from which the fibers were made were identical and only the shapes were different. The percentage increase in the volume scattering coefficient of the 2.0-denier orlon over the  $\underline{s}_v$  of the nylon at a specific surface of 3200 sq. cm./cc. is shown in Fig. 24 as a function of the wavelength of light.

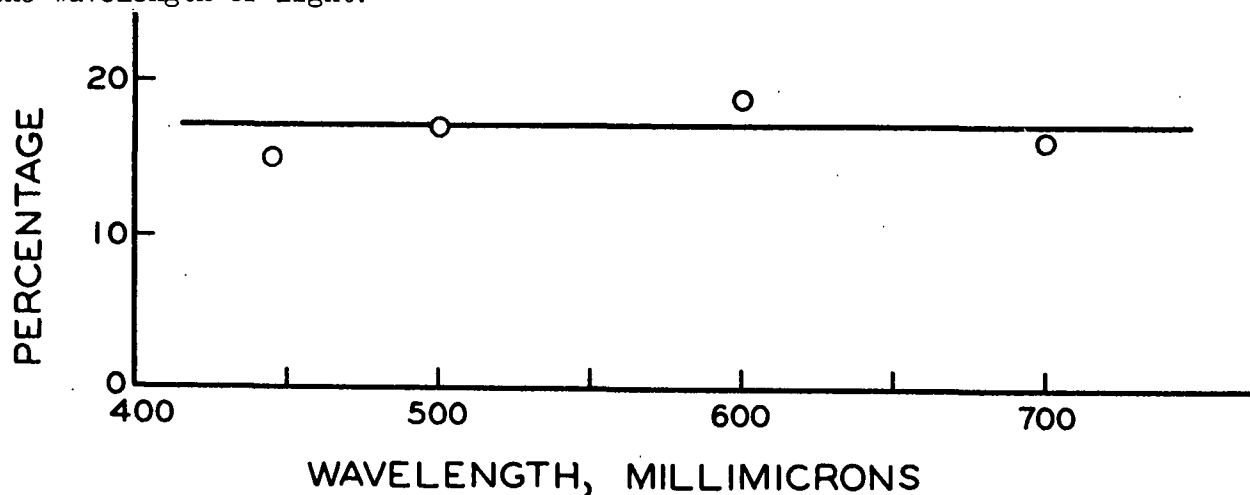


Figure 24. The Percentage by Which  $\underline{s}_v$  was Greater for Orlon Fibers Than for Nylon Fibers

These results help explain the family of curves which Swanson and Steber obtained, Fig. 3. The pulps refined to different extents had different sized and shaped particles. This caused the  $\underline{s}$  versus surface area relationship to be different for the different refining intervals which resulted in the family of curves.

#### DISCUSSION OF THE OPTICAL TECHNIQUES USED TO DETERMINE INDIVIDUAL FIBER PROPERTIES

The validity of using optical techniques to determine individual fiber properties can now be examined critically in the light of these experimental and theoretical results.

It was shown that the scattering in a sheet of paper is an inherently more complex problem than it was possible to solve in the derivation of the theoretical equation. The equation derived was shown to predict qualitatively the scattering behavior of glass fiber sheets as the wavelength of the light and the diameter of the fibers were varied. The equation correctly predicted the experimentally verified fact that the scattering coefficient was not a linear function of the reciprocal of the diameter or of the surface area for fibers of this size range (5.69 to 13.7  $\mu$ ). The scattering coefficient of the small fibers was higher than would be predicted from the approximation  $s = KA$ . It was also experimentally shown that the inclusion of small particles whose size was of the order of a wavelength of light increased the scattering coefficient. The experimental data showed that small fibers and fibers containing small particles exhibited a different  $s$  versus wavelength relationship from that found from the large fibers. Finally, it was shown that changing the shape of the particles altered the  $s$  versus specific surface relationship.

A sheet of pulp fibers is a heterogeneous system which contains many particles of different sizes and shapes. The springwood fibers of many wood species collapse in a sheet into a ribbonlike configuration while the summerwood fibers often retain a circular or roughly rectangular shape. The size of the fibers varies widely; and, if the fibers have been beaten, there are fiber elements and fibrils which can scatter light. In a pulp fiber sheet, it would be expected that there would be particles scattering light whose size would range from fibrils of the order of 10 A. to whole pulp fibers whose size might be nearly 85  $\mu$  in diameter. The shape would be highly variable and probably would include particles that were cylindrical, spherical, rectangular, ribbonlike, as well as others of a highly irregular shape.

From the experimental and theoretical considerations, it was shown that the particles whose size was less than a wavelength of light would tend to scatter as Rayleigh scatters, the particles whose size was of the order of a wavelength of light would scatter very strongly, and the large particles would tend to scatter more nearly as described by the laws of geometric optics. The total scattering in the sheet is made up of a combination of all of these types of scattering.

For this reason, the scattering coefficient is not a unique, relative measure of the total unbonded surface area of the fibers. Anything which would change the relative amounts of small and large particles, the size of the particles, the shape of the particles, and the optical properties of the particles would be expected to change the scattering coefficient-surface area relationship. Pulp treatments such as refining, wet pressing, chemical treatments, etc., can alter one or more of these fiber properties.

In any particular situation, it might be found experimentally that  $\underline{s}$  versus  $\underline{A}$  is the same for pulp fibers treated in various manners. This could result from a fortuitous combination of the various effects or from the fact that the changes were too slight to alter the individual fiber properties significantly. If the wavelength variation of  $\underline{s}$  is found to be different for the various pulp treatments, this is good evidence that the  $\underline{s}$  versus  $\underline{A}$  relationship would probably also be different. However, the converse is not true; so the fact that the different pulp treatments do not alter the  $\underline{s}$  versus wavelength relation does not necessarily mean that the  $\underline{s}$  versus  $\underline{A}$  relationship is unchanged.

The term "surface area" as applied to pulp fibers is ambiguous. The surface area is usually defined by the type of experiment used to determine the surface

area. Various methods are available for determining the surface area, such as the gas adsorption method, the permeability method, the dye adsorption method, the silvering method, and the microscopic method. Each of these methods, in general, gives a different surface area for a particular pulp sample. Haselton (16) and others have used the nitrogen adsorption method to determine the surface area of pulps and have compared it to the specific scattering coefficient. The data of Haselton have been plotted in Fig. 18 in comparison with the data from the present study for synthetic fibers. It can be seen that the data for the pulp fall well below the data for the synthetic fibers. This indicates that the nitrogen adsorption surface area determination probably measures the total microscopic area, including areas which are in such close proximity to adjacent areas that negligible light is scattered from these areas.

## SUMMARY AND CONCLUSIONS

In the past, many workers have attempted to determine certain individual fiber properties from the optical behavior of pulp fiber sheets. These attempts have been hindered by a lack of knowledge of the fundamental scattering processes within the sheet and the relationship of these processes to the optical behavior of the sheet. The present work was undertaken to formulate a relationship between the scattering from individual fibers and the optical behavior of the sheet for a model sheet composed of cylindrical fibers arranged randomly in the plane of the sheet. The scattering from the individual fibers was calculated from Wait's solution of the Maxwell equations for a fiber of this shape.

The equation derived was found to account qualitatively for the scattering behavior of sheets of glass fibers for different fiber diameters and at different wavelengths. The magnitude of the calculated scattering coefficients were considerably higher than the experimental values; but the calculations did predict the nonlinear variation of  $s$  with the reciprocal of the fiber diameter, and also it predicted the large increase in  $s$  with increasing wavelength which was found experimentally for the  $5.69 \mu$  diameter fibers.

It was felt that significant improvements in the theoretical equation could only be accomplished by abandoning the assumption that each unit length of fiber scattered independently. This would require the solution of the multiple scattering problem of spherically nonsymmetrical particles in close proximity to each other. The solution of such a problem would be very difficult.

The experimental data showed that the scattering coefficient can vary in a nonlinear manner with the reciprocal of the diameter. It was found that the presence of small amounts of particles in the fibers whose size was of the order



of a wavelength of light increased the scattering coefficient significantly and altered the  $\underline{s}$  versus wavelength relationship. Also, fibers whose cross-sectional shapes were dog boned gave much higher scattering coefficients than either the pigmented or the clear circularly cylindrical fibers. These effects were also noted in some data from the literature on the scattering in pulp fiber sheets.

In the light of these theoretical and experimental results, it has been pointed out that great care must be exercised in comparing individual fiber properties of pulp sheets by means of the scattering coefficients of the sheet. In particular, it is unlikely that pulp fibers which have different shapes and/or sizes would exhibit the same scattering coefficient-surface area relationship.

The validity of the Kubelka-Munk theory of light scattering in a fibrous sheet has been further confirmed in this work. It was shown that the agreement between  $\underline{R}_0$ ,  $\underline{T}$ , and  $\underline{R}_\infty$  calculated from the K-M theory and experimentally determined for sheets of a glassine as well as for more opaque types of papers agreed well within the instrumental accuracy of the GERS. It was demonstrated that the normal GERS and the modified GERS gave reflectance values in complete agreement for glassine, newsprint, and bond papers.

There was found to be no change in the reflectances nor in the calculated values of  $\underline{s}$  for the synthetic fiber sheets as they were compressed from a solid fraction of 0.033 to about 0.15. It was also shown that varying the basis weight had no influence on  $\underline{s}$ . This is further evidence that the K-M theory was valid for this situation.

#### ACKNOWLEDGMENTS

The author wishes to acknowledge the help and encouragement which he received from Dr. Lathrop and Dr. Nelson who served on his thesis advisory committee. He is particularly grateful to Dr. Lathrop for permission to use his computer programs for calculating the light reflected from a glass slab.

Mr. Dearth and Mr. Shillcox were especially helpful in setting up the GERS's for the scattering coefficient determinations and for their useful criticism of the various experimental techniques and results in this thesis.

The author wishes to thank Mr. Robert Jones for his help in perfecting the techniques which were used in the fiber preparation and sheet-forming processes.

# NOMENCLATURE

$\underline{A}$	= surface area, sq. cm./g.
$\underline{A_v}$	= specific surface area, sq. cm./cc.
$\underline{A_n}, \underline{B_n}, \underline{C_n}, \underline{D_n}$	= coefficients defined by Equations (11) and (12)
$\underline{a}$	= radius of a cylinder, microns
$\underline{a}$	= $(1/\underline{R_\infty} + \underline{R_\infty})/2$
$\underline{a_n}, \underline{b_n}, \underline{c_n}, \underline{d_n}$	= coefficients in Equations (3) through (6)
$\underline{a'}, \underline{b'}, \underline{c'}, \underline{d'}$	= real components of the coefficients $\underline{A_n}, \underline{B_n}, \underline{C_n}, \underline{D_n}$
$\underline{a''}, \underline{b''}, \underline{c''}, \underline{d''}$	= imaginary components of the coefficients $\underline{A_n}, \underline{B_n}, \underline{C_n}, \underline{D_n}$
$\mathcal{E}$	= electric amplitude vector component
$\mathcal{H}$	= magnetic amplitude vector component
$\underline{H_n}^{(2)}(\underline{Z})$	= Hankel's function of the second kind of order $\underline{n}$ and argument $\underline{Z}$
$\underline{I_o}$	= incident intensity defined on page 24, joules/sq.cm./steradian
$\underline{I_B}$	= total back-scattered light from a unit length of fiber, joules/cm.
$\underline{I}(\theta, \phi)$	= light scattered into an angle increment $d\phi$ at a distance $\rho$ from the $\underline{z}$ -axis when illuminated at an angle $\theta$ , joules/sq. cm.
$\underline{i_R}$	= light moving downward onto a differential layer in the interior of a sheet, joules/sq. cm.
$\underline{i_T}$	= light moving upward from a differential layer in the interior of a sheet, joules/sq. cm.
$\underline{J_n}(\underline{Z})$	= Bessel's function of the first kind of order $\underline{n}$ and argument $\underline{Z}$
$\underline{K}$	= proportionality constant in the equation $\underline{s} = \underline{KA}$
$\underline{k}$	= specific absorption coefficient, sq. cm./g.
$\underline{k}$	= $2\pi/\lambda^\circ$
$\underline{L}$	= length per gram of fiber, cm./g.
$\underline{m}$	= refractive index
$\underline{n}$	= order of a series or Bessel's function
$\underline{P_a}, \underline{P_b}, \underline{P_c}, \underline{P_d}$	= real part of the series in Equations (13) and (14)

$\underline{Q}_a, \underline{Q}_b, \underline{Q}_c, \underline{Q}_d$	= imaginary part of the series in Equations (13) and (14)
$\underline{Q}$	= efficiency factor
$\underline{R}_o$	= absolute reflectance of one sheet backed by a black body
$\underline{R}_\infty$	= absolute reflectance of an infinite pad of the material
$\underline{R}_g$	= absolute reflectance of the backing material
$\underline{R}_{R_g}$	= absolute reflectance of one sheet backed by a backing of reflectance $\underline{R}_g$
$\underline{s}$	= specific scattering coefficient, sq. cm./g.
$\underline{s}_v$	= volume scattering coefficient, sq. cm./cc.
$\underline{W}$	= basis weight, g./sq. cm.
$\underline{x}$	= $2\pi a/\lambda^\circ$
$\underline{Y}_n(\underline{Z})$	= Bessel's function of the second kind of order $\underline{n}$ and argument $\underline{Z}$
$\underline{y}$	= $\underline{mx}$
$\underline{x}, \underline{y}, \underline{z}$	= rectangular co-ordinates
$\alpha$	= angle between the perpendicular to a sheet and an incident pencil of light, radians
$\beta_1$	= $2\pi m/\lambda^\circ$
$\beta_2$	= $2\pi/\lambda^\circ$
$\epsilon, \mu$	= inductive capacities
$\lambda^\circ$	= wavelength of light in vacuum, microns
$\mu$	= microns
$(\rho, \phi, \underline{z})$	= cylindrical co-ordinates defining point at which scattered field is calculated
$\rho_f$	= density of the fibers, g./cc.
$\Phi$	= angle defined in Fig. 8
$\theta$	= angle between fiber axis and the incident direction

LITERATURE CITED

1. Kubelka, P., and Munk, F., Z. tech. Physik 12, no. 11a:593-601(Nov., 1931).
2. Steele, F. A., Paper Trade J. 100, no. 12:37-42(1935).
3. Van den Akker, J. A., Tappi 32, no. 11:498(1949).
4. Kubelka, P., J. Opt. Soc. Am. 38:448-57(1948).
5. Judd, D. B., J. Research Natl. Bur. Standards 19:287-317(Sept., 1937).
6. Judd, D. B., Paper Trade J. 106, no. 1:39-46(Jan. 6, 1938).
7. Stenius, A. S:son, J. Opt. Soc. Am. 45, no. 9:727(1955).
8. Stenius, A. S:son, J. Opt. Soc. Am. 44:804-5(1954).
9. Stenius, A. S:son, Svensk Papperstidn. 54, no. 19:663-70(1951).
10. Stenius, A. S:son, Svensk Papperstidn. 54, no. 20:701-7(1951).
11. Stenius, A. S:son, Svensk Papperstidn. 56, no. 16:607-14(1953).
12. Davis, M. N., Paper Trade J. 111, no. 14:40-4(Oct. 3, 1940).
13. Parsons, S. R., Tech. Assoc. Papers 25:360(1942).
14. Ratliff, F. T., Tappi 32, no. 8:357(1949).
15. Leech, H. J., Tappi 37, no. 8:343(1954).
16. Haselton, W. R. An investigation of the adsorption of gases by wood and its components and of gas adsorption techniques as a means of studying the area and structure of pulp and paper. Doctor's Dissertation. Appleton, Wis., The Institute of Paper Chemistry, 1953. 172 p.
17. Ingmanson, W. L., and Thode, E. F., Tappi 42, no. 1:83(1959).
18. Swanson, J. W., and Steber, A. J., Tappi 42, no. 12:986(1959).
19. Bouwkamp, C. J., Rep. Progr. Phys. 17:35-100(1954).
20. Van de Hulst, H. C. Light scattering by small particles. New York, Wiley, 1957.
21. Wait, J. R., Can. J. Phys. 33, no. 5:189-95(May, 1955).
22. Burberg, R., Z. Naturforsch. 11a, no. 10:800(1956); 11a, no. 10:807(1956).

23. Wilhelmsson, H., Trans. Chalmers Univ. of Technol., no. 155, Report no. 32, Res. Lab. of Electronics 1954; no. 168, Report no. 35, Res. Lab. of Electronics, 1955; no. 198, Report no. 45, Res. Lab. of Electronics.
24. Stratton, J. A. Electromagnetic theory. New York, McGraw-Hill, 1941. 615 p.
25. Viles, F. J., and Silverman, L., Anal. Chem. 21, no. 8:950(1949).
26. Jones, R. L. An investigation of the effect of fiber structural properties on the compression response of fibrous beds. Doctor's Dissertation. Appleton, Wis., The Institute of Paper Chemistry, 1962.
27. Johnson, R. C. Personal communication, 1962.
28. Du Pont. Technical Information Bulletin X-12. Wilmington, Del., E. I. du Pont de Nemours & Co., Inc., Jan., 1956.
29. Harris, M. Handbook of textile fibers. Washington, D. C., Harris Research Laboratories, Inc., 1954. 356 p.
30. Judd, D. B. Color in business, science and industry. p. 83. New York, Wiley, 1952.
31. Van den Akker, J. A., J. Opt. Soc. Am. 33, no. 5:257-9(May, 1943).
32. Harrison, V. G. W. Definition and measurement of gloss. Leatherhead, Surrey, England, Printing and Allied Trades Research Association, 1945.
33. Chandrasekhar, S. Radiative transfer. New York, Dover Publ., 1960.
34. Lathrop, A. L. Personal communication, 1962.
35. Clewell, D. H., J. Opt. Soc. Am. 31, no. 8:521-7(1941).
36. Royal Society. British Association Mathematical Tables, Vol. VI, Part I, and Vol. X, Part II, Bessel's functions. Cambridge, Eng., British Association for the Advancement of Science, 1958, 1960.
37. Hildebrand, F. B. Introduction to numerical analysis. New York, McGraw-Hill, 1956. 511 p.

# APPENDIX I

## DETAILS OF THE NUMERICAL INTEGRATION PROCEDURE

The equation for the total back-scattered light per unit incident light was given previously [Equation (50)]:

$$\frac{I_B}{I_0} = 4 \int_0^{\pi/2} \int_0^{\pi/2} \int_{\phi=\phi-\pi/2}^{\phi=\phi+\pi/2} \left( \frac{I(\phi, \theta)}{I_0} \right) f(\alpha) \sin \theta d\phi d\theta d\phi \quad (50).$$

The computations were carried out on an IBM 1620 computer. The first step was to calculate the quantity  $[I(\phi, \theta)/I_0]_\rho$  from Wait's solution, Equation (37), by the following procedure:

1. The values of  $\underline{u}$  and  $\underline{v}$  were calculated from equations given on page 14.
2. Bessel's functions of order zero and one of the first kind,  $\underline{J}_n(\rho)$ , and the second kind,  $\underline{Y}_n(\rho)$ , were taken from tables (36).
3. The recurrence relation was then used to compute the Bessel's function of higher orders. The recurrence relation used was:

$$\underline{Z}_{n+1}(\rho) = \frac{2n}{\rho} \underline{Z}_n(\rho) - \underline{Z}_{n-1}(\rho)$$

where  $\underline{Z}$  is either Bessel's function and  $\rho$  is the argument. The first type of Bessel's function becomes small as  $\underline{n}$  gets larger than the argument. The nature of the recurrence relation is such that the accuracy gets poor as the size function becomes of the same order as the number of digits carried in the calculation. Eight digits were carried, so the calculated Bessel's functions could only be used up to orders where the function was above about  $10^{-5}$ . Fortunately, the coefficients  $\underline{A}_n$ ,  $\underline{B}_n$ , etc., became small,  $<10^{-6}$ , before the accuracy of the Bessel's functions became poor. Calculated Bessel's functions were checked against tabulated values (36) for the high orders and were found to agree quite well.

4. The Bessel's functions were then used to calculate  $\underline{A}_n$ ,  $\underline{B}_n$ , etc., from Equations (8) and (9). The complex numbers in the equations

were handled without rectification by suitable programming techniques on the computer.

5. The series in Equation (22) were then summed for each point at which the scattering was to be calculated.

The equations by Van de Hulst, Equations (38) and (39), were programmed on the IBM 1620 computer. The program was checked by comparing the calculated scattering diagram to some data published by Van de Hulst for cylinders of a size where  $2\pi a/\lambda^\circ \leq 6.0$ . The results compared very well considering the fact that Van de Hulst used a graphical interpolation method for calculating the terms in the series. Also, one term was hand calculated and found to be correct.

This program was then used to calculate the scattering diagram corresponding to a fiber diameter of  $9.02 \mu$ , an index of refraction of 1.544, and a wavelength of  $700 \mu$ . The results were found to agree with the results calculated from Wait's equation to about four significant figures.

The number of equally spaced points which were calculated for each curve was 337 between the angles of  $\phi = 0$  and  $\phi = \pi$ . Twenty-one curves were calculated for angles of  $\theta$  ranging from 0 to  $\pi/2$ . An examination of the plots of the scattering diagrams, Fig. 24 and 25, showed that each maximum and minimum was adequately defined by this number of points. The accuracy of the subsequent numerical integration would, no doubt, be improved by using more points. However, it was felt that the added computer time required to calculate the extra points would not be justified by the slight increase in accuracy. It is also believed that calculation of 20 intervals of  $\theta$  gave sufficient accuracy, since the scattering diagrams are not a rapid function of  $\theta$ . Using this number of points required about 100 hours of computer time, so increasing the number of points in the integration would have required a prohibitive amount of computer time.



The integration was carried out in two steps. First, the Newton-Cotes (37) seven-point integration formula was used to form the integral of  $[I(\phi, \theta)/I_0]_0$  over the angles  $\phi$ . This was integrated in such a manner that the integral was obtained over the first six intervals, then the first twelve, etc., until the total integral over the 336 intervals was obtained. From these partial integrals, the integral of  $[I(\phi, \theta)/I_0]_0$  from, say,  $\phi = -\pi/2$  to  $\phi = +\pi/2$  could be found by simply adding the partial integral at  $-\pi/2$  to the partial integral at  $+\pi/2$ .

The final integrations were then carried out using the Newton-Cotes five-point integration formula as follows:

1. Initial values of  $\theta$  and  $\phi$  were chosen.
2. The value of  $\int_{\phi=-\pi/2}^{\phi=+\pi/2} (I/I_0)_0 d\phi$  was found by simple addition of the proper partial integrals as described above.
3. The angle  $\alpha$  was calculated from  $\theta$  and  $\phi$  and the integral found in (2) was multiplied by the calculated values of  $f(\alpha)$  and  $\sin \theta$ .
4. This point was stored in the computer,  $\phi$  was incremented, and the procedure was repeated until all values of  $\phi$  had been calculated, 29 points for  $0 \leq \phi \leq \pi/2$ . The Newton-Cotes five-point integration formula was used to perform the integration over  $\phi$ . This was then stored in the computer.
5. The value of  $\phi$  was brought back into its initial value,  $\theta$  was incremented, and a new value of the integral of  $\phi$  was calculated.
6. When  $\theta$  had been varied from 0 to  $\pi/2$  (20 intervals), the final integration was performed over  $\theta$  by use of the Newton-Cotes five-point formula to give a value of  $I_B$ .

## APPENDIX II

### SCATTERING DIAGRAMS

The scattering diagrams were calculated as described previously at 20 equally spaced intervals of  $\theta$ . The angle  $\theta$  is the angle between the incident plane wave and the fiber axis. The fibers were assumed to be absorptionless, circular in cross section, and infinitely long. The index of refraction of the fiber was 1.544. The angle  $\phi$ , in radians, is the angle in the plane perpendicular to the fiber axis, where  $\phi = 0$  indicates direct back scattering and  $\phi = \pi$  indicates straightforward scattering. The scattered intensity is tabulated at equal increments of  $\phi$ ; the increment was 0.0093499779 radians which gives 337 points between  $\phi = 0$  and  $\phi = \pi$ . The quantity tabulated is  $\frac{I(\theta, \phi)\rho}{I_0(\sin \theta)}$  where  $\rho$  is given in microns and the intensities can be any convenient units. The quantities were calculated assuming unpolarized light of 700 m $\mu$  wavelength incident on the fiber. The intensities of the two states of polarization of the scattered light were added together to give the total scattered intensity at each angle  $\phi$ . The E-notation was used in the tables to position the decimal point for numbers less than 0.1. As an example, the meaning of 1.964E-3 is  $1.964 \times 10^{-3}$  or 0.001964. The scattering diagrams for certain values of  $\theta$  were plotted as a function of  $\phi$  in Fig. 25 and 26.

*see table 19-7*

TABLE XV

SCATTERING DIAGRAMS FOR 9.02  $\mu$  DIAMETER FIBERS  
 $\theta = 1.57079640$

$\theta=0$	$\theta=0.38335$	$\theta=0.77605$	$\theta=1.1678$	$\theta=1.5614$	$\theta=1.9541$	$\theta=2.3468$	$\theta=2.7395$
1.4116	.4942 <sup>20°</sup>	.2121 <sup>45°</sup>	.3101 <sup>67°</sup>	.1599 <sup>90°</sup>	1.1921 <sup>121°</sup>	1.2171 <sup>135°</sup>	2.2461 <sup>157°</sup>
1.325	.4026	.2348	.2629	.2039	1.463	1.323	3.206
1.117	.2816	.2172	.1869	.2951	1.492	1.739	4.466
.9057	.1712	.1640	.1154	.3759	1.266	2.306	5.749
.8130	.1015	.1020	7.357E-27 <sup>86°</sup>	.3977	.9121	2.804	6.759
.8924	8.087E-2	6.774E-2	6.801E-2	.3503	.6333	3.041	7.248
1.098	9.731E-2	8.786E-2	8.794E-2	.2670	.6014	2.934	7.091
1.311	.1292	.1634	.1152	.2030	.8606	2.543	6.347
1.404	.1576	.2668	.1365	.2006	1.298	2.054	5.277
1.316	.1726	.3541 <sup>53°</sup>	.1486	.2629	1.700	1.707	4.287
1.082	.1731	.3868	.1560	.3518	1.860	1.700	3.808
.8169	.1626	.3507	.1631	.4134 <sup>121°</sup>	1.694	2.109	4.131
.6470	.1448	.2621	.1678	.4129 <sup>121°</sup>	1.284	2.849	5.277
.6454	.1239	.1584	.1627	.3590 <sup>at 95°</sup>	.8479	3.697	6.951
.7922	.1048	7.890E-2	.1426	.2993	.6266	4.376	8.624
.9913	9.431E-2	4.551E-2	.1127	.2905	.7635	4.655	9.721
1.128	9.783E-2	5.573E-2	9.016E-2	.3600	1.225	4.442	9.835
1.139	.1155	8.838E-2	9.610E-2	.4841	1.814	3.830	8.886
1.040	.1395	.1186	.1420	.5988	2.260	3.065	7.134
.9204	.1565	.1320	.2186	.6376	2.351	2.465	5.054
.8791	.1549	.1300	.2966	.5755	2.041	2.293	3.137
.9670	.1333	.1239	.3399	.4504	1.471	2.662	1.719
1.150	.1044	.1232	.3270	.3468	.9099	3.480	.9289
1.324	9.017E-2	.1275	.2658	.3482	.6259	4.480	.7773
1.372	.1105	.1264	.1929	.4845	.7662	5.320	1.308
1.231	.1704	.1090	.1562	.7075	1.286	5.707	2.697
.9307	.2543	7.487E-2	.1873	.9108	1.974	5.516	5.195
.5832	.3309	3.924E-2	.2821	.9877	2.540	4.837	8.896
.3305	.3677	2.717E-2	.3993	.8938	2.751	3.939	13.45
.2741	.3472	5.892E-2	.4811	.6789	2.525	3.173	17.92
.4268	.2756	.1354	.4845	.4666	1.970	2.830	20.92
.7092	.1801	.2334	.4071	.3890	1.324	3.033	2.108
.9912	9.457E-2	.3143	.2895	.5113	.8615	3.692	17.79
1.154	4.291E-2	.3432	.1950	.7907	.7685	4.543	11.76
1.145	2.966E-2	.3081	.1745	1.092	1.076	5.251	5.208
.9912	4.143E-2	.2275	.2379	1.263	1.651	5.536	1.377
.7742	5.856E-2	.1419	.3482	1.211	2.258	5.272	3.515
.5874	6.872E-2	9.377E-2	.4419	.9673	2.658	4.523	13.57
.4879	7.387E-2	.1055	.4653	.6677	2.709	3.513	31.18
.4767	8.635E-2	.1686	.4048	.4874	2.414	2.545	53.36
.5097	.1172	.2490	.2941	.5422	1.921	1.904	75.16
.5287	.1648	.3052	.1948	.8222	1.453	1.784	91.11
							96.98-180°

42  
336

336 nos.  $\rightarrow$  180°

42 numbers  
each column

TABLE XV (Continued)

SCATTERING DIAGRAMS FOR 9.02  $\mu$  DIAMETER FIBERS  
 $\theta = 1.49225658$

$\phi=0$	$\phi=0.38335$	$\phi=0.77605$	$\phi=1.1678$	$\phi=1.5614$	$\phi=1.9541$	$\phi=2.3468$	$\phi=2.7395$
1.545	.3195	7.145E-2	.2292	.1886	.8436	1.287	2.245
1.459	.2697	6.759E-2	.1862	.2538	.9962	1.377	3.297
1.242	.2031	6.501E-2	.1356	.3627	1.054	1.910	4.717
.9949	.1304	6.186E-2	.1027	.4595	.9846	2.693	6.190
.8227	7.091E-2	6.355E-2	.1043	.4920	.8289	3.416	7.348
.7850	4.264E-2	7.897E-2	.1395	.4407	.6850	3.784	7.876
.8643	5.519E-2	.1132	.1910	.3311	.6563	3.648	7.627
.9823	.1057	.1617	.2338	.2213	.7909	3.078	6.700
1.046	.1799	.2096	.2484	.1715	1.048	2.338	5.433
1.004	.2566	.2382	.2299	.2106	1.313	1.786	4.312
.8728	.3141	.2346	.1895	.3204	1.451	1.724	3.795
.7270	.3365	.1999	.1473	.4445	1.383	2.260	4.136
.6573	.3189	.1504	.1216	.5197	1.135	3.256	5.270
.7164	.2683	.1100	.1201	.5102	.8322	4.376	6.830
.8877	.2012	9.915E-2	.1381	.4272	.6458	5.211	8.273
1.091	.1370	.1240	.1629	.3225	.7058	5.451	9.091
1.228	9.131E-2	.1734	.1822	.2580	1.030	5.012	8.998
1.228	6.980E-2	.2242	.1901	.2717	1.504	4.075	8.022
1.090	6.818E-2	.2526	.1881	.3564	1.927	3.021	6.456
.8786	7.590E-2	.2458	.1816	.4653	2.106	2.275	4.710
.6889	8.322E-2	.2071	.1755	.5404	1.948	2.139	3.139
.5983	8.704E-2	.1528	.1715	.5464	1.514	2.670	1.945
.6254	9.232E-2	.1034	.1692	.4910	.9999	3.662	1.200
.7245	.1081	7.330E-2	.1697	.4193	.6519	4.727	.9632
.8132	.1406	6.546E-2	.1774	.3855	.6556	5.458	1.406
.8187	.1866	7.293E-2	.1979	.4199	1.047	5.585	2.835
.7172	.2331	8.513E-2	.2330	.5101	1.690	5.074	5.548
.5467	.2621	9.487E-2	.2758	.6082	2.331	4.135	9.569
.3870	.2601	.1014	.3111	.6605	2.706	3.127	14.39
.3191	.2258	.1087	.3218	.6408	2.660	2.415	18.94
.3851	.1725	.1197	.2995	.5679	2.214	2.237	21.73
.5684	.1222	.1324	.2527	.4956	1.562	2.621	21.50
.8026	9.589E-2	.1399	.2056	.4805	.9897	3.399	17.79
1.002	.1027	.1351	.1880	.5465	.7521	4.276	11.45
1.102	.1364	.1168	.2183	.6687	.9647	4.945	4.740
1.077	.1782	9.323E-2	.2910	.7857	1.552	5.185	.7274
.9510	.2071	7.892E-2	.3758	.8353	2.281	4.922	2.373
.7756	.2096	8.748E-2	.4314	.7934	2.857	4.234	11.35
.6065	.1858	.1226	.4275	.6906	3.052	3.319	27.20
.4796	.1472	.1742	.3628	.5978	2.804	2.436	47.14
.4019	.1094	.2215	.2693	.5850	2.243	1.845	66.69
.3571	8.352E-2	.2432	.1971	.6791	1.639	1.748	80.96
							86.20

TABLE XV (Continued)

SCATTERING DIAGRAMS FOR 9.02  $\mu$  DIAMETER FIBERS  
 $\theta = 1.41371676$

$\phi=0$	$\phi=0.38335$	$\phi=0.77605$	$\phi=1.1678$	$\phi=1.5614$	$\phi=1.9541$	$\phi=2.3468$	$\phi=2.7395$
1.142	.1232	9.627E-2	.1267	.2610	.7820	1.528	2.147
1.091	.1189	.1202	.1083	.3134	.6839	1.588	3.140
.9596	.1192	.1401	9.252E-2	.3829	.6161	2.069	4.684
.8006	.1240	.1482	8.854E-2	.4368	.6115	2.806	6.393
.6746	.1400	.1421	.1001	.4474	.6805	3.506	7.791
.6195	.1724	.1261	.1226	.4068	.8092	3.873	8.463
.6349	.2186	.1086	.1450	.3335	.9653	3.741	8.203
.6861	.2672	9.747E-2	.1562	.2652	1.107	3.152	7.100
.7251	.3026	9.616E-2	.1507	.2403	1.197	2.353	5.528
.7181	.3122	.1025	.1324	.2780	1.209	1.695	4.024
.6628	.2918	.1108	.1119	.3669	1.142	1.495	3.100
.5894	.2471	.1159	.1008	.4681	1.019	1.895	3.061
.5418	.1909	.1163	.1054	.5339	.8908	2.797	3.892
.5523	.1381	.1145	.1234	.5309	.8162	3.891	5.280
.6220	9.982E-2	.1149	.1457	.4585	.8487	4.779	6.739
.7177	8.144E-2	.1200	.1620	.3505	1.010	5.126	7.803
.7882	8.223E-2	.1277	.1667	.2608	1.277	4.803	8.190
.7907	9.718E-2	.1327	.1614	.2369	1.575	3.935	7.863
.7131	.1192	.1294	.1537	.2966	1.807	2.859	6.994
.5819	.1410	.1165	.1520	.4179	1.882	1.989	5.835
.4499	.1564	9.839E-2	.1604	.5485	1.764	1.655	4.604
.3714	.1612	8.363E-2	.1773	.6303	1.491	1.977	3.433
.3761	.1544	8.047E-2	.1966	.6270	1.174	2.822	2.426
.4569	.1383	9.200E-2	.2122	.5424	.9596	3.859	1.760
.5752	.1184	.1141	.2216	.4187	.9677	4.692	1.765
.6825	.1015	.1375	.2266	.3175	1.238	5.010	2.883
.7454	9.337E-2	.1529	.2308	.2905	1.701	4.702	5.473
.7610	9.618E-2	.1553	.2364	.3553	2.199	3.893	9.535
.7564	.1082	.1472	.2422	.4874	2.541	2.887	14.48
.7716	.1250	.1357	.2445	.6314	2.590	2.051	19.14
.8354	.1411	.1284	.2411	.7274	2.326	1.690	21.99
.9480	.1530	.1286	.2347	.7380	1.862	1.937	21.78
1.077	.1594	.1341	.2328	.6650	1.404	2.725	18.07
1.173	.1609	.1390	.2442	.5481	1.167	3.815	11.72
1.190	.1580	.1383	.2728	.4456	1.279	4.879	4.896
1.105	.1503	.1314	.3126	.4085	1.718	5.600	.5127
.9322	.1371	.1227	.3490	.4580	2.316	5.770	1.336
.7107	.1185	.1182	.3652	.5780	2.831	5.338	8.917
.4916	9.754E-2	.1215	.3517	.7236	3.046	4.431	22.83
.3156	7.988E-2	.1304	.3135	.8412	2.875	3.324	40.54
.2014	7.203E-2	.1384	.2699	.8918	2.405	2.368	57.99
.1438	7.793E-2	.1381	.2464	.8652	1.866	1.900	70.75
							75.44

TABLE XV (Continued)

SCATTERING DIAGRAMS FOR 9.02  $\mu$  DIAMETER FIBERS  
 $\theta = 1.33517694$

$\phi=0$	$\phi=0.38335$	$\phi=0.77605$	$\phi=1.1678$	$\phi=1.5614$	$\phi=1.9541$	$\phi=2.3468$	$\phi=2.7395$
.5910	.2120	9.127E-2	.1558	.4565	1.260	1.412	2.956
.5715	.2467	.1019	.1838	.5265	.9628	2.052	3.849
.5179	.2743	.1361	.1955	.5283	.6561	2.793	5.128
.4439	.2843	.1723	.1841	.4698	.4833	3.385	6.470
.3663	.2697	.1906	.1574	.3877	.5376	3.628	7.498
.3000	.2315	.1828	.1339	.3300	.8162	3.450	7.903
.2543	.1803	.1552	.1320	.3317	1.214	2.937	7.547
.2317	.1329	.1235	.1586	.3989	1.567	2.298	6.528
.2295	.1064	.1028	.2041	.5066	1.720	1.785	5.154
.2430	.1100	9.903E-2	.2476	.6126	1.602	1.604	3.845
.2669	.1401	.1063	.2677	.6773	1.257	1.838	2.992
.2968	.1811	.1124	.2558	.6824	.8333	2.418	2.817
.3283	.2123	.1075	.2210	.6371	.5185	3.149	3.308
.3574	.2179	9.206E-2	.1856	.5714	.4580	3.785	4.235
.3817	.1946	7.690E-2	.1728	.5211	.6886	4.118	5.253
.4028	.1538	7.752E-2	.1929	.5118	1.119	4.052	6.042
.4282	.1158	.1035	.2370	.5497	1.570	3.639	6.414
.4708	9.980E-2	.1512	.2813	.6228	1.852	3.051	6.347
.5456	.1141	.2034	.3001	.7080	1.845	2.523	5.945
.6637	.1520	.2373	.2812	.7818	1.561	2.261	5.341
.8259	.1951	.2369	.2330	.8274	1.130	2.372	4.627
1.019	.2229	.2020	.1809	.8370	.7515	2.821	3.843
1.220	.2232	.1500	.1535	.8121	.5985	3.450	3.054
1.398	.1974	.1073	.1664	.7614	.7470	4.028	2.448
1.525	.1588	9.593E-2	.2125	.7011	1.139	4.341	2.391
1.584	.1246	.1218	.2659	.6531	1.609	4.261	3.364
1.572	.1062	.1718	.2952	.6418	1.956	3.794	5.753
1.498	.1037	.2200	.2820	.6851	2.037	3.079	9.578
1.379	.1073	.2417	.2322	.7849	1.824	2.342	14.27
1.232	.1046	.2259	.1733	.9189	1.425	1.823	18.71
1.071	9.003E-2	.1807	.1410	1.043	1.033	1.698	21.42
.9080	6.927E-2	.1286	.1582	1.107	.8433	2.029	38.45
.7483	5.735E-2	9.400E-2	.2224	1.075	.9674	2.741	17.65
.5982	6.974E-2	9.037E-2	.3048	.9487	1.382	3.650	11.58
.4635	.1123	.1140	.3652	.7722	1.936	4.512	5.040
.3501	.1758	.1476	.3729	.6239	2.415	5.098	.8113
.2621	.2383	.1704	.3244	.5820	2.626	5.255	1.514
.2010	.2752	.1707	.2467	.6873	2.488	4.953	8.619
.1654	.2715	.1514	.1841	.9179	2.063	4.297	21.72
.1525	.2296	.1278	.1759	1.190	1.537	3.509	38.43
.1587	.1686	.1172	.2359	1.390	1.146	2.866	54.90
.1801	.1154	.1283	.3441	1.422	1.082	2.628	66.95
							71.38

TABLE XV (Continued)

SCATTERING DIAGRAMS FOR 9.02  $\mu$  DIAMETER FIBERS  
 $\theta = 1.25663712$

$\phi=0$	$\phi=0.38335$	$\phi=0.77605$	$\phi=1.1678$	$\phi=1.5614$	$\phi=1.9541$	$\phi=2.3468$	$\phi=2.7395$
1.027	.3727	.1132	.2009	.4402	.6834	1.666	2.959
.9933	.3147	9.558E-2	.2019	.3847	.6508	2.321	3.957
.9051	.2356	8.077E-2	.1819	.3013	.7019	2.971	5.300
.7953	.1549	7.450E-2	.1515	.2312	.8348	3.389	6.649
.7013	9.667E-2	7.989E-2	.1271	.2134	1.012	3.434	7.627
.6478	7.729E-2	9.598E-2	.1228	.2653	1.174	3.109	7.944
.6380	9.814E-2	.1178	.1433	.3720	1.256	2.557	7.490
.6567	.1451	.1386	.1805	.4910	1.222	2.012	6.378
.6833	.1964	.1518	.2173	.5709	1.083	1.710	4.906
.7067	.2322	.1541	.2359	.5756	.8978	1.793	3.459
.7340	.2437	.1461	.2270	.5017	.7531	2.260	2.380
.7873	.2344	.1317	.1947	.3815	.7297	2.958	1.871
.8900	.2158	.1171	.1548	.2699	.8636	3.638	1.955
1.050	.1990	.1080	.1273	.2189	1.124	4.048	2.503
1.251	.1891	.1077	.1258	.2548	1.421	4.030	3.316
1.451	.1826	.1163	.1513	.3658	1.637	3.583	4.211
1.604	.1720	.1306	.1918	.5073	1.680	2.863	5.065
1.674	.1516	.1456	.2287	.6219	1.524	2.136	5.810
1.652	.1224	.1563	.2467	.6650	1.229	1.674	6.386
1.562	9.295E-2	.1596	.2411	.6233	.9226	1.662	6.702
1.445	7.499E-2	.1554	.2195	.5200	.7506	2.128	6.630
1.340	7.708E-2	.1462	.1964	.4034	.8142	2.932	6.080
1.265	9.954E-2	.1358	.1853	.3253	1.123	3.819	5.098
1.211	.1337	.1275	.1910	.3197	1.583	4.502	3.950
1.147	.1658	.1226	.2082	.3899	2.031	4.768	3.124
1.039	.1835	.1203	.2258	.5091	2.294	4.536	3.189
.8733	.1816	.1187	.2343	.6339	2.266	3.888	4.568
.6639	.1638	.1164	.2325	.7218	1.953	3.029	7.284
.4518	.1403	.1139	.2277	.7478	1.478	2.221	10.81
.2866	.1224	.1133	.2306	.7115	1.036	1.702	14.13
.2055	.1171	.1164	.2480	.6351	.8220	1.617	16.06
.2169	.1244	.1237	.2765	.5532	.9480	1.986	
.2978	.1388	.1323	.3035	.5003	1.399	2.702	12.91
.4046	.1524	.1373	.3141	.4995	2.034	3.571	8.576
.4932	.1599	.1344	.3005	.5564	2.635	4.361	4.525
.5362	.1598	.1227	.2692	.6582	2.990	4.863	3.054
.5312	.1550	.1066	.2391	.7777	2.978	4.949	6.163
.4966	.1495	9.481E-2	.2329	.8813	2.611	4.606	14.78
.4574	.1456	9.590E-2	.2640	.9386	2.038	3.950	28.27
.4307	.1428	.1140	.3271	.9328	1.484	3.203	44.36
.4173	.1380	.1454	.3979	.8680	1.172	2.640	59.68
.4038	.1284	.1789	.4439	.7707	1.235	2.511	70.69
							74.70

TABLE XV (Continued)

SCATTERING DIAGRAMS FOR 9.02  $\mu$  DIAMETER FIBERS  
 $\theta = 1.17809730$

$\phi=0$	$\phi=0.38335$	$\phi=0.77605$	$\phi=1.1678$	$\phi=1.5614$	$\phi=1.9541$	$\phi=2.3468$	$\phi=2.7395$
.3996	8.356E-2	.1018	.1222	.1479	.8461	2.060	2.022
.4494	9.931E-2	.1072	.1315	.1777	.9969	2.573	2.465
.5834	.1168	.1101	.1410	.2708	1.125	2.967	3.395
.7612	.1342	.1120	.1482	.3436	1.200	3.087	4.524
.9328	.1509	.1151	.1516	.4249	1.204	2.877	5.516
1.057	.1658	.1207	.1508	.4624	1.142	2.401	6.094
1.115	.1767	.1285	.1466	.4168	1.037	1.826	6.113
1.115	.1811	.1362	.1405	.3671	.9260	1.362	5.586
1.086	.1770	.1409	.1341	.2731	.8493	1.189	4.661
1.061	.1643	.1403	.1293	.2012	.8419	1.389	3.556
1.062	.1455	.1344	.1275	.1886	.9215	1.918	2.497
1.093	.1246	.1250	.1299	.2508	1.080	2.618	1.675
1.134	.1064	.1157	.1365	.3733	1.284	3.268	1.229
1.155	9.418E-2	.1094	.1460	.5153	1.479	3.658	1.255
1.128	8.911E-2	.1078	.1561	.6250	1.605	3.660	1.820
1.041	9.028E-2	.1099	.1637	.6611	1.620	3.139	2.946
.9023	9.549E-2	.1127	.1659	.6105	1.513	2.598	4.581
.7414	.1026	.1131	.1612	.4955	1.318	1.858	6.557
.5959	.1106	.1089	.1504	.3664	1.109	1.275	8.566
.4986	.1195	.1007	.1370	.2814	.9714	1.033	10.19
.4659	.1296	9.107E-2	.1262	.2831	.9756	1.214	11.03
.4933	.1409	8.366E-2	.1234	.3799	1.147	1.776	10.78
.5587	.1518	8.149E-2	.1321	.5421	1.451	2.566	9.426
.6327	.1596	8.536E-2	.1527	.7127	1.798	3.362	7.268
.6894	.1614	9.354E-2	.1810	.8304	2.074	3.939	4.891
.7149	.1556	.1025	.2097	.8546	2.183	4.138	2.979
.7103	.1429	.1088	.2299	.7818	2.085	3.911	2.081
.6872	.1266	.1106	.2346	.6469	1.819	3.341	2.386
.6607	.1113	.1084	.2212	.5093	1.489	2.625	3.629
.6414	.1012	.1050	.1931	.4287	1.231	2.020	5.181
.6310	9.849E-2	.1040	.1598	.4419	1.161	1.765	6.321
.6217	.1021	.1077	.1344	.5485	1.326	2.009	6.607
.6016	.1086	.1165	.1286	.7126	1.684	2.755	6.208
.5598	.1137	.1281	.1491	.8778	2.114	3.847	6.037
.4926	.1137	.1387	.1931	.9891	2.463	5.009	7.598
.4046	.1080	.1447	.2488	1.014	2.604	5.921	12.54
.3081	9.839E-2	.1442	.2982	.9539	2.485	6.317	22.08
.2175	8.856E-2	.1378	.3235	.8395	2.158	6.076	36.41
.1454	8.232E-2	.1284	.3142	.7201	1.760	5.263	54.35
9.832E-2	8.176E-2	.1197	.2726	.6435	1.459	4.119	73.49
7.615E-2	8.652E-2	.1150	.2145	.6403	1.395	2.988	90.61
7.367E-2	9.421E-2	.1160	.1648	.7148	1.616	2.212	102.4
							106.7



TABLE XV (Continued)

SCATTERING DIAGRAMS FOR 9.02  $\mu$  DIAMETER FIBERS

$\theta = 1.09955748$

$\phi=0$	$\phi=0.38335$	$\phi=0.77605$	$\phi=1.1678$	$\phi=1.5614$	$\phi=1.9541$	$\phi=2.3468$	$\phi=2.7395$
.1063	.1681	8.214E-2	.1137	.3604	.8478	2.931	1.562
.1659	.1672	9.637E-2	.1113	.3246	.9686	3.362	1.944
.3299	.1593	.1116	.1125	.2668	1.019	3.397	2.706
.5586	.1435	.1230	.1149	.2086	.9801	3.030	3.654
.8008	.1241	.1280	.1160	.1716	.8631	2.391	4.569
1.010	.1080	.1271	.1150	.1699	.7130	1.697	5.263
1.158	.1011	.1234	.1135	.2055	.5935	1.184	5.610
1.244	.1053	.1202	.1143	.2678	.5654	1.021	5.560
1.287	.1176	.1194	.1194	.3377	.6619	1.261	5.131
1.319	.1311	.1202	.1286	.3942	.8723	1.826	4.399
1.370	.1389	.1200	.1385	.4215	1.140	2.529	3.489
1.452	.1368	.1157	.1437	.4138	1.380	3.144	2.565
1.558	.1255	.1061	.1397	.3771	1.509	3.474	1.827
1.662	.1100	9.294E-2	.1254	.3263	1.476	3.414	1.481
1.731	9.722E-2	8.013E-2	.1053	.2799	1.290	2.985	1.705
1.736	9.236E-2	7.237E-2	8.754E-2	.2544	1.019	2.323	2.587
1.664	9.709E-2	7.246E-2	8.160E-2	.2589	.7732	1.640	4.075
1.523	.1087	7.972E-2	9.361E-2	.2931	.6631	1.160	5.948
1.341	.1218	9.006E-2	.1229	.3478	.7598	1.049	7.838
1.152	.1312	9.774E-2	.1616	.4086	1.061	1.373	9.304
.9882	.1340	9.815E-2	.1966	.4605	1.486	2.070	25.75
.8649	.1310	9.015E-2	.2148	.4916	1.901	2.971	9.572
.7810	.1257	7.695E-2	.2089	.4967	2.161	3.845	8.195
.7193	.1221	6.478E-2	.1811	.4774	2.170	4.458	6.134
.6563	.1223	6.016E-2	.1426	.4420	1.918	4.645	3.875
.5728	.1253	6.681E-2	.1102	.4027	1.492	4.352	1.937
.4625	.1276	8.380E-2	9.939E-2	.3728	1.053	3.658	.6872
.3346	.1251	.1058	.1179	.3640	.7775	2.759	.2291
.2098	.1157	.1254	.1624	.3831	.7936	1.915	.3877
.1125	.1004	.1363	.2188	.4307	1.131	1.380	.8285
6.049E-2	8.378E-2	.1359	.2675	.4998	1.706	1.328	1.275
5.862E-2	7.135E-2	.1266	.2908	.5763	2.339	1.806	1.749
9.722E-2	6.748E-2	.1141	.2802	.6421	2.822	2.707	2.732
.1561	7.301E-2	.1051	.2399	.6795	2.990	3.803	5.162
.2123	8.478E-2	.1038	.1858	.6774	2.780	4.807	10.23
.2484	9.700E-2	.1107	.1394	.6357	2.262	5.451	19.02
.2570	.1039	.1222	.1201	.5684	1.617	5.564	32.07
.2423	.1025	.1329	.1379	.5011	1.073	5.125	49.00
.2157	9.393E-2	.1383	.1891	.4641	.8327	4.261	68.38
.1899	8.258E-2	.1365	.2579	.4823	.9933	3.216	87.87
.1734	7.442E-2	.1293	.3218	.5647	1.517	2.272	104.6
.1677	7.392E-2	.1204	.3599	.6979	2.241	1.674	116.0
							120.0

TABLE XV (Continued)

SCATTERING DIAGRAMS FOR 9.02  $\mu$  DIAMETER FIBERS

$$\theta = 1.02101766$$

$\phi=0$	$\phi=0.38335$	$\phi=0.77605$	$\phi=1.1678$	$\phi=1.5614$	$\phi=1.9541$	$\phi=2.3468$	$\phi=2.7395$
.9167	.1583	8.144E-2	.1601	.1437	.7706	3.208	.9894
.9368	.1604	9.032E-2	.1551	.1751	.5343	2.988	.8789
.9895	.1603	.1055	.1429	.2268	.3375	2.451	1.171
1.054	.1584	.1213	.1287	.2850	.2548	1.757	1.851
1.104	.1554	.1320	.1170	.3346	.3290	1.115	2.837
1.115	.1524	.1339	.1103	.3627	.5545	.7255	3.982
1.076	.1499	.1273	.1088	.3625	.8759	.7193	5.096
.9882	.1479	.1161	.1110	.3345	1.202	1.120	5.972
.8692	.1456	.1058	.1152	.2867	1.435	1.837	6.431
.7453	.1419	.1010	.1205	.2326	1.501	2.688	6.369
.6431	.1357	.1031	.1272	.1881	1.376	3.449	5.788
.5820	.1272	.1098	.1356	.1677	1.098	3.919	4.817
.5679	.1177	.1162	.1450	.1805	.7575	3.976	3.684
.5924	.1095	.1172	.1533	.2275	.4712	3.609	2.669
.6364	.1048	.1103	.1569	.3000	.3451	2.925	2.030
.6771	.1048	9.688E-2	.1526	.3815	.4381	2.119	1.933
.6956	.1089	8.158E-2	.1395	.4510	.7404	1.418	2.397
.6830	.1150	7.058E-2	.1203	.4889	1.172	1.024	3.289
.6422	.1202	6.847E-2	.1015	.4827	1.608	1.053	4.362
.5862	.1220	7.605E-2	9.154E-2	.4322	1.915	1.505	5.334
.5322	.1199	8.977E-2	9.740E-2	.3509	1.996	2.264	5.972
.4954	.1153	.1031	.1216	.2636	1.823	3.130	6.168
.4832	.1111	.1098	.1602	.2002	1.453	3.873	5.960
.4928	.1103	.1064	.2033	.1863	1.008	4.298	5.506
.5128	.1142	9.435E-2	.2378	.2351	.6412	4.296	5.003
.5270	.1217	7.925E-2	.2523	.3410	.4861	3.876	4.598
.5207	.1294	6.889E-2	.2413	.4796	.6117	3.157	4.319
.4853	.1330	6.951E-2	.2080	.6137	.9980	2.339	4.059
.4211	.1292	8.302E-2	.1635	.7034	1.538	1.644	3.645
.3369	.1175	.1059	.1236	.7198	2.072	1.255	2.959
.2465	.1007	.1304	.1033	.6548	2.436	1.275	2.085
.1648	8.405E-2	.1480	.1117	.5265	2.514	1.696	1.422
.1030	7.304E-2	.1522	.1483	.3756	2.280	2.409	1.706
6.657E-2	7.130E-2	.1422	.2034	.2540	1.809	3.237	3.906
5.447E-2	7.882E-2	.1224	.2608	.2092	1.252	3.983	9.004
6.103E-2	9.191E-2	.1010	.3034	.2676	.7958	4.475	17.70
7.845E-2	.1047	8.680E-2	.3189	.4246	.5991	4.607	30.13
9.948E-2	.1117	8.520E-2	.3037	.6428	.7454	4.357	45.68
.1190	.1102	9.680E-2	.2636	.8618	1.213	3.782	62.92
.1346	.1014	.1171	.2123	1.015	1.879	3.002	79.83
.1460	8.992E-2	.1388	.1664	1.055	2.556	2.172	94.13
.1536	8.170E-2	.1546	.1408	.9652	3.048	1.454	103.7
							107.0

TABLE XV (Continued)

SCATTERING DIAGRAMS FOR 9.02  $\mu$  DIAMETER FIBERS  
 $\theta = 0.94247784$

$\phi=0$	$\phi=0.38335$	$\phi=0.77605$	$\phi=1.1678$	$\phi=1.5614$	$\phi=1.9541$	$\phi=2.3468$	$\phi=2.7395$
2.403	.1799	8.520E-2	.1109	.3538	.3365	2.363	1.822
2.386	.1791	7.550E-2	.1473	.3135	.5545	1.836	1.458
2.334	.1740	7.703E-2	.1792	.2509	.8228	1.288	1.456
2.246	.1678	8.950E-2	.1972	.1840	1.071	.8749	1.859
2.119	.1634	.1083	.1963	.1328	1.233	.7208	2.623
1.954	.1625	.1263	.1777	.1138	1.262	.8835	3.617
1.756	.1645	.1365	.1478	.1355	1.146	1.336	4.650
1.537	.1675	.1350	.1159	.1952	.9178	1.975	5.514
1.310	.1680	.1223	9.109E-2	.2799	.6423	2.645	6.029
1.094	.1635	.1033	7.944E-2	.3690	.4033	3.176	6.084
.9039	.1526	8.514E-2	8.262E-2	.4396	.2786	3.434	5.667
.7513	.1364	7.444E-2	9.812E-2	.4733	.3174	3.352	4.860
.6413	.1182	7.467E-2	.1206	.4605	.5243	2.949	3.816
.5713	.1020	8.485E-2	.1443	.4042	.8557	2.326	2.718
.5321	9.208E-2	.1000	.1641	.3193	1.230	1.642	1.735
.5105	9.022E-2	.1137	.1770	.2297	1.549	1.072	.9854
.4925	9.593E-2	.1201	.1822	.1619	1.725	.7641	.5234
.4671	.1060	.1171	.1799	.1382	1.708	.8004	.3495
.4281	.1161	.1068	.1713	.1701	1.500	1.181	.4363
.3757	.1219	9.430E-2	.1578	.2544	1.159	1.823	.7624
.3150	.1212	8.549E-2	.1412	.3734	.7826	2.582	1.333
.2547	.1145	8.448E-2	.1244	.4985	.4830	3.287	2.185
.2040	.1048	9.158E-2	.1112	.5973	.3566	3.781	3.352
.1699	9.674E-2	.1031	.1058	.6429	.4545	3.959	4.830
.1557	9.409E-2	.1132	.1121	.6216	.7667	3.787	6.527
.1598	9.863E-2	.1163	.1316	.5375	1.222	3.307	8.235
.1768	.1090	.1097	.1625	.4135	1.708	2.626	9.647
.1989	.1214	9.561E-2	.1991	.2852	2.097	1.889	10.41
.2179	.1308	7.957E-2	.2328	.1925	2.286	1.246	10.25
.2274	.1332	6.913E-2	.2541	.1677	2.224	.8262	9.036
.2239	.1274	7.021E-2	.2560	.2264	1.927	.7093	6.917
.2079	.1153	8.452E-2	.2364	.3611	1.478	.9169	4.353
.1829	.1018	.1084	.1996	.5418	1.003	1.410	2.072
.1548	9.240E-2	.1342	.1559	.7236	.6417	2.098	.9551
.1297	9.098E-2	.1526	.1190	.8577	.5029	2.857	1.839
.1128	9.839E-2	.1565	.1019	.9063	.6393	3.550	5.311
.1070	.1116	.1440	.1128	.8538	1.028	4.050	11.51
.1124	.1252	.1194	.1522	.7131	1.578	4.267	20.06
.1263	.1331	9.168E-2	.2123	.5238	2.152	4.160	30.00
.1443	.1313	7.133E-2	.2782	.3424	2.600	3.752	40.01
.1615	.1196	6.681E-2	.3327	.2270	2.808	3.130	48.59
.1741	.1021	8.116E-2	.3606	.2204	2.720	2.432	54.38
							56.43

TABLE XV (Continued)

SCATTERING DIAGRAMS FOR 9.02  $\mu$  DIAMETER FIBERS  
 $\theta = 0.86393802$

$\phi=0$	$\phi=0.38335$	$\phi=0.77605$	$\phi=1.1678$	$\phi=1.5614$	$\phi=1.9541$	$\phi=2.3468$	$\phi=2.7395$
2.017	.1526	.1000	7.775E-2	.1935	1.093	1.216	2.320
1.994	.1521	8.727E-2	7.078E-2	.2526	1.052	.8138	1.592
1.925	.1520	7.793E-2	7.673E-2	.3126	.9145	.5631	1.025
1.813	.1541	7.582E-2	9.645E-2	.3611	.7142	.5250	.6924
1.664	.1594	8.235E-2	.1262	.3869	.5038	.7133	.6187
1.485	.1675	9.588E-2	.1588	.3831	.3406	1.092	.7899
1.288	.1764	.1121	.1851	.3492	.2729	1.584	1.159
1.085	.1835	.1256	.1972	.2920	.3269	2.086	1.664
.8908	.1861	.1315	.1908	.2249	.4996	2.495	2.237
.7169	.1825	.1273	.1669	.1653	.7578	2.726	2.818
.5751	.1729	.1140	.1318	.1304	1.045	2.732	3.354
.4727	.1590	9.586E-2	9.534E-2	.1331	1.296	2.515	3.800
.4119	.1439	7.878E-2	6.824E-2	.1779	1.450	2.124	4.112
.3893	.1309	6.871E-2	5.898E-2	.2591	1.471	1.642	4.251
.3969	.1227	6.935E-2	7.126E-2	.3611	1.350	1.174	4.181
.4235	.1203	8.093E-2	.1029	.4621	1.119	.8209	3.885
.4564	.1225	.1000	.1464	.5385	.8338	.6614	3.379
.4841	.1268	.1206	.1911	.5713	.5687	.7360	2.721
.4977	.1299	.1363	.2259	.5513	.3957	1.038	2.023
.4929	.1290	.1420	.2423	.4820	.3669	1.518	1.438
.4696	.1229	.1360	.2370	.3800	.5007	2.089	1.133
.4314	.1123	.1201	.2117	.2717	.7764	2.645	1.257
.3845	.1000	9.929E-2	.1735	.1867	1.137	3.081	1.891
.3358	8.981E-2	7.946E-2	.1320	.1508	1.504	3.314	3.016
.2911	8.498E-2	6.597E-2	9.745E-2	.1787	1.793	3.298	4.491
.2541	8.747E-2	6.164E-2	7.800E-2	.2701	1.936	3.035	6.067
.2258	9.692E-2	6.614E-2	7.803E-2	.4082	1.898	2.575	7.429
.2050	.1106	7.636E-2	9.742E-2	.5632	1.688	2.009	8.266
.1891	.1246	8.791E-2	.1319	.6995	1.354	1.452	8.357
.1750	.1346	9.678E-2	.1746	.7841	.9797	1.023	7.642
.1607	.1376	.1008	.2170	.7955	.6564	.8211	6.273
.1454	.1331	.1005	.2512	.7300	.4690	.9051	4.611
.1301	.1228	9.844E-2	.2714	.6032	.4717	1.280	3.182
.1168	.1104	9.772E-2	.2742	.4477	.6749	1.897	2.575
.1077	.1002	.1009	.2598	.3050	1.042	2.655	3.314
.1045	9.545E-2	.1084	.2311	.2157	1.497	3.425	5.732
.1075	9.711E-2	.1182	.1942	.2090	1.941	4.071	9.869
.1157	.1038	.1264	.1567	.2944	2.277	4.476	15.42
.1266	.1121	.1290	.1268	.4585	2.428	4.569	21.78
.1375	.1179	.1235	.1122	.6671	2.361	4.335	28.11
.1461	.1181	.1103	.1181	.8732	2.090	3.815	33.49
.1510	.1116	9.308E-2	.1462	1.027	1.677	3.103	37.10
							38.37

TABLE XV (Continued)

SCATTERING DIAGRAMS FOR 9.02- $\mu$  DIAMETER FIBERS  
 $\theta = 0.78539820$

$\phi=0$	$\phi=0.38335$	$\phi=0.77605$	$\phi=1.1678$	$\phi=1.5614$	$\phi=1.9541$	$\phi=2.3468$	$\phi=2.7395$
.9806	.1270	.1502	7.274E-2	.1402	.3655	.6560	2.996
.9675	.1362	.1482	8.419E-2	9.767E-2	.2679	.5121	2.725
.9294	.1513	.1402	9.734E-2	8.666E-2	.2448	.5198	2.333
.8698	.1715	.1298	.1100	.1106	.3069	.6862	1.873
.7941	.1944	.1209	.1215	.1662	.4474	.9892	1.413
.7088	.2172	.1165	.1319	.2438	.6424	1.380	1.029
.6209	.2363	.1178	.1423	.3296	.8553	1.794	.7983
.5371	.2490	.1237	.1532	.4079	1.044	2.159	.7799
.4630	.2539	.1312	.1642	.4647	1.171	2.411	1.009
.4026	.2510	.1367	.1735	.4899	1.209	2.507	1.485
.3580	.2419	.1367	.1784	.4792	1.150	2.427	2.164
.3295	.2293	.1298	.1761	.4350	1.007	2.188	2.967
.3157	.2163	.1166	.1649	.3663	.8095	1.831	3.783
.3139	.2052	.1003	.1454	.2869	.6009	1.422	4.492
.3210	.1974	8.541E-2	.1208	.2130	.4282	1.036	4.983
.3336	.1924	7.652E-2	9.677E-2	.1605	.3321	.7437	5.176
.3488	.1888	7.694E-2	8.003E-2	.1417	.3386	.6002	5.037
.3642	.1842	8.736E-2	7.701E-2	.1633	.4525	.6351	4.586
.3781	.1764	.1055	9.166E-2	.2243	.6563	.8465	3.894
.3893	.1639	.1265	.1240	.3163	.9131	1.201	3.066
.3971	.1471	.1444	.1696	.4243	1.173	1.641	3.475
.4008	.1278	.1536	.2202	.5295	1.387	2.094	1.463
.3997	.1089	.1507	.2651	.6125	1.510	2.485	.8641
.3931	9.385E-2	.1353	.2941	.6572	1.519	2.750	.4484
.3805	8.536E-2	.1109	.2997	.6543	1.410	2.848	.1977
.3616	8.473E-2	8.341E-2	.2794	.6035	1.207	2.764	6.679E-2
.3368	9.124E-2	5.968E-2	.2367	.5144	.9525	2.515	1.267E-2
.3071	.1022	4.603E-2	.1807	.4051	.6994	2.143	2.897E-2
.2743	.1140	4.621E-2	.1241	.2990	.5037	1.707	.1759
.2410	.1224	6.039E-2	8.039E-2	.2205	.4107	1.278	.5976
.2097	.1244	8.519E-2	6.086E-2	.1897	.4459	.9184	1.518
.1827	.1190	.1145	7.182E-2	.2182	.6098	.6813	3.217
.1615	.1072	.1414	.1129	.3056	.8770	.5993	5.978
.1468	9.218E-2	.1595	.1769	.4392	1.201	.6819	10.02
.1378	7.821E-2	.1652	.2516	.5959	1.522	.9161	15.46
.1333	6.952E-2	.1578	.3219	.7461	1.782	1.269	22.22
.1312	6.903E-2	.1400	.3733	.8603	1.930	1.696	30.02
.1297	7.746E-2	.1168	.3954	.9146	1.938	2.142	38.38
.1279	9.315E-2	9.385E-2	.3838	.8969	1.805	2.552	46.66
.1254	.1124	7.608E-2	.3411	.8101	1.555	2.875	54.15
.1233	.1309	6.656E-2	.2768	.6718	1.238	3.072	60.12
.1232	.1443	6.594E-2	.2046	.5116	.9165	3.116	63.98
							65.32

TABLE XV (Continued)

SCATTERING DIAGRAMS FOR 9.02  $\mu$  DIAMETER FIBERS  
 $\theta = 0.70685838$

$\phi=0$	$\phi=0.38335$	$\phi=0.77605$	$\phi=1.1678$	$\phi=1.5614$	$\phi=1.9541$	$\phi=2.3468$	$\phi=2.7395$
.5848	.1155	.1492	7.059E-2	.4421	.5981	.4164	2.940
.5842	.1339	.1562	4.088E-2	.4611	.7593	.4392	2.993
.5821	.1554	.1527	2.638E-2	.4460	.8962	.5601	2.892
.5786	.1770	.1397	3.003E-2	.3985	.9866	.7639	2.652
.5736	.1957	.1202	5.129E-2	.3263	1.015	1.022	2.304
.5673	.2092	9.903E-2	8.624E-2	.2423	.9784	1.298	1.892
.5597	.2161	8.095E-2	.1284	.1625	.8813	1.552	1.464
.5512	.2164	7.026E-2	.1705	.1028	.7410	1.746	1.063
.5424	.2115	6.944E-2	.2051	7.643E-2	.5821	1.853	.7286
.5340	.2038	7.871E-2	.2269	9.072E-2	.4329	1.856	.4840
.5267	.1963	9.606E-2	.2331	.1459	.3209	1.755	.3428
.5214	.1918	.1177	.2237	.2348	.2679	1.564	.3076
.5188	.1924	.1394	.2015	.3436	.2867	1.311	.3749
.5193	.1986	.1570	.1711	.4542	.3778	1.033	.5397
.5228	.2097	.1678	.1380	.5480	.5299	.7706	.7987
.5287	.2235	.1710	.1075	.6084	.7209	.5635	1.152
.5361	.2370	.1675	8.386E-2	.6248	.9217	.4443	1.601
.5432	.2470	.1301	6.989E-2	.5942	1.100	.4341	2.146
.5483	.2510	.1518	6.691E-2	.5221	1.229	.5400	2.776
.5495	.2476	.1455	7.481E-2	.4215	1.286	.7535	3.465
.5451	.2369	.1428	9.244E-2	.3109	1.262	1.052	4.168
.5339	.2206	.1436	.1179	.2113	1.162	1.401	4.816
.5153	.2015	.1463	.1491	.1418	1.001	1.759	5.328
.4898	.1827	.1483	.1832	.1168	.8086	2.084	5.617
.4585	.1670	.1467	.2175	.1430	.6160	2.334	5.608
.4230	.1562	.1395	.2485	.2184	.4578	2.477	5.256
.3856	.1505	.1264	.2727	.3319	.3629	2.496	4.565
.3483	.1487	.1090	.2869	.4660	.3503	2.387	3.601
.3130	.1483	9.079E-2	.2881	.5990	.4255	2.164	2.493
.2809	.1465	7.618E-2	.2750	.7090	.5800	1.854	1.432
.2526	.1409	6.960E-2	.2480	.7778	.7916	1.499	.6466
.2278	.1300	7.412E-2	.2100	.7941	1.028	1.146	.3764
.2058	.1143	9.054E-2	.1664	.7554	1.254	.8467	.8366
.1857	9.555E-2	.1168	.1246	.6688	1.434	.6426	2.179
.1667	7.706E-2	.1486	9.274E-2	.5497	1.539	.5668	4.461
.1485	6.258E-2	.1794	7.845E-2	.4196	1.553	.6351	7.622
.1312	5.545E-2	.2026	8.726E-2	.3023	1.473	.8443	11.48
.1158	5.771E-2	.2128	.1210	.2199	1.313	1.171	15.74
.1038	6.943E-2	.2068	.1772	.1890	1.099	1.577	20.03
9.682E-2	8.859E-2	.1847	.2489	.2181	.8652	2.010	23.94
9.613E-2	.1114	.1502	.3252	.3051	.6509	2.415	27.08
.1024	.1332	.1095	.3937	.4384	.4920	2.739	29.10
							29.81

TABLE XV (Continued).

SCATTERING DIAGRAMS FOR 9.02  $\mu$  DIAMETER FIBERS  
 $\theta = 0.62831856$

$\phi=0$	$\phi=0.38335$	$\phi=0.77605$	$\phi=1.1678$	$\phi=1.5614$	$\phi=1.9541$	$\phi=2.3468$	$\phi=2.7395$
.5305	.1096	.1345	.1730	.1323	.8144	.3309	1.032
.5317	.1204	.1431	.1434	.1758	.7305	.4116	1.389
.5356	.1286	.1473	.1118	.2274	.6121	.5608	1.777
.5418	.1329	.1444	8.233E-2	.2822	.4763	.7625	2.171
.5501	.1328	.1335	5.946E-2	.3347	.3428	.9939	2.538
.5600	.1290	.1152	4.734E-2	.3792	.2317	1.228	2.847
.5710	.1235	9.197E-2	4.897E-2	.4106	.1603	1.438	3.066
.5823	.1189	6.742E-2	6.553E-2	.4245	.1405	1.599	3.171
.5929	.1180	4.596E-2	9.598E-2	.4185	.1773	1.692	3.145
.6016	.1237	3.175E-2	.1369	.3926	.2678	1.706	2.984
.6075	.1376	2.794E-2	.1830	.3491	.4018	1.640	2.699
.6094	.1603	3.604E-2	.2279	.2931	.5627	1.503	2.315
.6064	.1909	5.557E-2	.2646	.2320	.7300	1.311	1.871
.5979	.2266	8.408E-2	.2874	.1744	.8820	1.088	1.414
.5837	.2640	.1176	.2924	.1294	.9987	.8607	.9969
.5642	.2985	.1514	.2782	.1051	1.064	.6560	.6660
.5400	.3259	.1807	.2464	.1075	1.071	.4983	.4601
.5123	.3428	.2014	.2015	.1391	1.018	.4059	.4010
.4828	.3470	.2111	.1499	.1983	.9120	.3892	.4901
.4530	.3381	.2092	9.925E-2	.2796	.7677	.4494	.7072
.4247	.3178	.1969	5.698E-2	.3736	.6055	.5789	1.012
.3993	.2892	.1768	2.941E-2	.4684	.4480	.7621	1.354
.3777	.2564	.1527	2.063E-2	.5513	.3178	.9778	1.673
.3604	.2243	.1286	3.195E-2	.6104	.2343	1.201	1.918
.3470	.1968	.1080	6.175E-2	.6367	.2110	1.408	2.054
.3367	.1772	9.349E-2	.1058	.6256	.2536	1.577	2.072
.3279	.1667	8.647E-2	.1582	.5775	.3595	1.690	1.994
.3190	.1652	8.710E-2	.2117	.4987	.5175	1.736	1.876
.3082	.1705	9.449E-2	.2597	.4003	.7096	1.712	1.804
.2940	.1795	.1070	.2961	.2966	.9132	1.621	1.885
.2755	.1887	.1229	.3171	.2037	1.103	1.472	2.233
.2524	.1946	.1405	.3208	.1366	1.257	1.280	2.953
.2256	.1949	.1584	.3077	.1072	1.356	1.063	4.123
.1963	.1887	.1757	.2804	.1222	1.387	.8398	5.780
.1666	.1765	.1916	.2430	.1822	1.348	.6293	7.907
.1390	.1604	.2057	.2005	.2810	1.242	.4503	10.42
.1157	.1433	.2171	.1584	.4068	1.085	.3193	13.21
9.857E-2	.1283	.2251	.1219	.5431	.8964	.2496	16.09
8.867E-2	.1182	.2282	9.537E-2	.6717	.7014	.2515	18.85
8.614E-2	.1144	.2253	8.197E-2	.7748	.5263	.3314	21.28
9.010E-2	.1170	.2152	8.364E-2	.8379	.3948	.4913	23.18
9.874E-2	.1246	.1976	.1008	.8519	.3260	.7278	24.39
							24.81

TABLE XV (Continued)

SCATTERING DIAGRAMS FOR 9.02  $\mu$  DIAMETER FIBERS

$$\theta = 0.54977874$$

$\phi=0$	$\phi=0.38335$	$\phi=0.77605$	$\phi=1.1678$	$\phi=1.5614$	$\phi=1.9541$	$\phi=2.3468$	$\phi=2.7395$
.4792	.1500	.1044	.2508	.2003	.2124	.1527	.2732
.4767	.1511	8.325E-2	.2351	.1556	.1519	.1903	.2130
.4694	.1471	6.589E-2	.2116	.1133	.1220	.2717	.2060
.4576	.1391	5.269E-2	.1825	7.786E-2	.1283	.3895	.2473
.4416	.1287	4.350E-2	.1507	5.299E-2	.1725	.5333	.3288
.4221	.1179	3.785E-2	.1193	4.163E-2	.2520	.6904	.4403
.3997	.1090	3.506E-2	9.166E-2	4.547E-2	.3602	.8474	.5711
.3754	.1043	3.444E-2	7.076E-2	6.480E-2	.4874	.9911	.7117
.3501	.1056	3.545E-2	5.912E-2	9.851E-2	.6209	1.109	.8546
.3248	.1139	3.773E-2	5.830E-2	.1441	.7474	1.193	1.921
.3003	.1297	4.120E-2	6.880E-2	.1980	.8536	1.235	1.131
.2778	.1522	4.596E-2	8.991E-2	.2557	.9283	1.232	1.263
.2579	.1801	5.226E-2	.1197	.3121	.9633	1.185	1.392
.2412	.2110	6.034E-2	.1553	.3622	.9546	1.097	1.519
.2283	.2422	7.030E-2	.1930	.4014	.9029	.9770	1.640
.2192	.2709	8.202E-2	.2288	.4257	.8136	.8336	1.751
.2137	.2944	9.505E-2	.2587	.4326	.6962	.6795	1.844
.2113	.3106	.1086	.2792	.4212	.5637	.5282	1.907
.2112	.3182	.1217	.2877	.3922	.4306	.3933	1.925
.2125	.3168	.1331	.2830	.3484	.3119	.2878	1.886
.2140	.3071	.1417	.2651	.2939	.2213	.2227	1.780
.2145	.2907	.1464	.2357	.2345	.1697	.2062	1.604
.2129	.2699	.1465	.1976	.1768	.1637	.2430	1.366
.2083	.2476	.1420	.1547	.1275	.2053	.3337	1.084
.2000	.2264	.1330	.1116	9.306E-2	.2915	.4743	.7929
.1880	.2089	.1207	7.306E-2	7.852E-2	.4143	.6565	.5377
.1723	.1969	.1063	4.311E-2	8.731E-2	.5618	.8679	.3763
.1539	.1915	9.183E-2	2.519E-2	.1205	.7197	1.093	.3728
.1337	.1927	7.903E-2	2.141E-2	.1766	.8721	1.315	.5928
.1132	.1996	6.990E-2	3.237E-2	.2516	1.004	1.515	1.096
9.408E-2	.2106	6.606E-2	5.709E-2	.3391	1.102	1.678	1.929
7.780E-2	.2235	6.868E-2	9.313E-2	.4311	1.156	1.790	3.119
6.582E-2	.2357	7.827E-2	.1368	.5185	1.162	1.840	4.667
5.916E-2	.2450	9.462E-2	.1838	.5925	1.118	1.824	6.545
5.833E-2	.2494	.1167	.2293	.6450	1.029	1.742	8.695
6.324E-2	.2476	.1431	.2686	.6702	.9054	1.603	11.02
7.321E-2	.2392	.1714	.2980	.6648	.7573	1.417	13.43
8.695E-2	.2245	.1992	.3145	.6289	.5999	1.200	15.78
.1027	.2043	.2239	.3165	.5661	.4485	.9708	17.95
.1188	.1804	.2431	.3041	.4830	.3175	.7476	19.79
.1330	.1545	.2547	.2786	.3890	.2191	.5481	21.20
.1438	.1286	.2575	.2428	.2950	.1625	.3866	22.09
							22.39



TABLE XV (Continued)

SCATTERING DIAGRAMS FOR 9.02  $\mu$  DIAMETER FIBERS  
 $\theta = 0.47123892$

$\phi=0$	$\phi=0.38335$	$\phi=0.77605$	$\phi=1.1678$	$\phi=1.5614$	$\phi=1.9541$	$\phi=2.3468$	$\phi=2.7395$
1.533E-2	.1182	.1570	.2021	.2527	.1947	9.884E-2	1.481
1.583E-2	.1282	.1372	.2119	.2918	.2681	9.662E-2	1.372
1.731E-2	.1393	.1178	.2154	.3244	.3490	.1223	1.229
1.965E-2	.1516	9.965E-2	.2124	.3481	.4315	.1747	1.061
2.267E-2	.1648	8.365E-2	.2029	.3609	.5097	.2504	.8788
2.615E-2	.1788	7.050E-2	.1875	.3618	.5777	.3446	.6937
2.984E-2	.1935	6.067E-2	.1675	.3506	.6303	.4514	.5188
3.346E-2	.2087	5.436E-2	.1445	.3281	.6636	.5639	.3662
3.677E-2	.2239	5.152E-2	.1204	.2957	.6749	.6750	.2463
3.954E-2	.2388	5.187E-2	9.741E-2	.2559	.6633	.7776	.1672
4.160E-2	.2530	5.494E-2	7.768E-2	.2116	.6294	.8555	.1334
4.283E-2	.2660	6.012E-2	6.324E-2	.1662	.5759	.9333	.1459
4.321E-2	.2774	6.670E-2	5.571E-2	.1234	.5068	.9768	.2015
4.276E-2	.2868	7.396E-2	5.620E-2	8.668E-2	.4274	.9938	.2933
4.160E-2	.2937	8.119E-2	6.518E-2	5.915E-2	.3439	.9833	.4112
3.990E-2	.2978	8.778E-2	8.242E-2	4.344E-2	.2629	.9462	.5432
3.787E-2	.2990	9.318E-2	.1069	4.134E-2	.1909	.8850	.6762
3.575E-2	.2972	9.700E-2	.1371	5.365E-2	.1338	.8033	.7983
3.379E-2	.2926	9.894E-2	.1709	8.012E-2	9.655E-2	.7063	.8995
3.222E-2	.2854	9.886E-2	.2056	.1194	8.243E-2	.5995	.9741
3.122E-2	.2762	9.673E-2	.2387	.1691	9.326E-2	.4894	1.021
3.094E-2	.2656	9.261E-2	.2675	.2261	.1289	.3824	1.046
3.145E-2	.2542	8.669E-2	.2896	.2864	.1874	.2849	1.060
3.278E-2	.2430	7.924E-2	.3031	.3457	.2651	.2027	1.081
3.489E-2	.2327	7.064E-2	.3070	.3997	.3569	.1412	1.132
3.766E-2	.2240	6.133E-2	.3007	.4442	.4563	.1047	1.238
4.097E-2	.2175	5.186E-2	.2845	.4758	.5566	9.631E-2	1.427
4.467E-2	.2134	4.282E-2	.2597	.4920	.6506	.1180	1.727
4.859E-2	.2119	3.489E-2	.2281	.4911	.7316	.1704	2.158
5.260E-2	.2129	2.876E-2	.1922	.4732	.7939	.2526	2.739
5.658E-2	.2159	2.511E-2	.1548	.4395	.8330	.3620	3.478
6.047E-2	.2203	2.457E-2	.1188	.3923	.8460	.4948	4.372
6.424E-2	.2253	2.766E-2	8.722E-2	.3353	.8318	.6456	5.409
6.793E-2	.2300	3.472E-2	6.260E-2	.2732	.7916	.8076	6.563
7.161E-2	.2335	4.586E-2	4.704E-2	.2109	.7280	.9732	7.799
7.542E-2	.2349	6.090E-2	4.198E-2	.1538	.6458	1.133	9.072
7.949E-2	.2334	7.939E-2	4.802E-2	.1067	.5507	1.281	10.33
8.399E-2	.2286	.1005	6.495E-2	7.414E-2	.4496	1.406	11.52
8.908E-2	.2203	.1232	9.173E-2	5.932E-2	.3500	1.501	12.58
9.494E-2	.2085	.1462	.1265	6.426E-2	.2590	1.559	13.48
.1016	.1935	.1680	.1669	8.947E-2	.1833	1.577	14.15
.1094	.1761	.1871	.2100	.1338	.1285	1.550	14.56
							14.71

TABLE XV (Continued)

SCATTERING DIAGRAMS FOR 9.02  $\mu$  DIAMETER FIBERS  
 $\theta = 0.39269910$

$\phi=0$	$\phi=0.38335$	$\phi=0.77605$	$\phi=1.1678$	$\phi=1.5614$	$\phi=1.9541$	$\phi=2.3468$	$\phi=2.7395$
.1172	.3459	5.505E-2	.1130	.1378	.3383	.2515	.2569
.1186	.3289	5.361E-2	.1467	9.586E-2	.3446	.2138	.3194
.1226	.3087	5.430E-2	.1828	6.366E-2	.3433	.1819	.3934
.1292	.2858	5.667E-2	.2195	4.326E-2	.3349	.1582	.4785
.1377	.2608	6.022E-2	.2548	3.587E-2	.3202	.1448	.5736
.1479	.2345	6.440E-2	.2864	4.190E-2	.3000	.1433	.6769
.1591	.2074	6.872E-2	.3125	6.090E-2	.2756	.1545	.7857
.1707	.1805	7.275E-2	.3313	9.163E-2	.2481	.1788	.8964
.1821	.1545	7.616E-2	.3415	.1321	.2190	.2156	1.004
.1927	.1302	7.877E-2	.3423	.1797	.1894	.2635	1.104
.2020	.1083	8.056E-2	.3336	.2316	.1604	.3207	1.191
.2096	8.945E-2	8.163E-2	.3157	.2844	.1330	.3845	1.260
.2152	7.414E-2	8.222E-2	.2897	.3348	.1083	.4520	1.303
.2186	6.284E-2	8.266E-2	.2572	.3797	8.697E-2	.5199	1.318
.2200	5.580E-2	8.331E-2	.2203	.4165	6.955E-2	.5849	1.301
.2195	5.315E-2	8.454E-2	.1814	.4429	5.662E-2	.6438	1.250
.2174	5.481E-2	8.668E-2	.1433	.4572	4.858E-2	.6937	1.165
.2142	6.053E-2	8.993E-2	.1085	.4588	4.572E-2	.7321	1.048
.2103	6.990E-2	9.438E-2	7.977E-2	.4477	4.825E-2	.7575	.9061
.2065	8.233E-2	9.994E-2	5.920E-2	.4245	5.629E-2	.7685	.7446
.2032	9.710E-2	.1063	4.860E-2	.3907	6.984E-2	.7650	.5741
.2010	.1133	.1131	4.913E-2	.3484	8.877E-2	.7474	.4061
.2005	.1302	.1199	6.122E-2	.3002	.1128	.7169	.2537
.2022	.1468	.1258	8.460E-2	.2488	.1416	.6750	.1306
.2062	.1621	.1303	.1182	.1972	.1745	.6241	5.067E-2
.2128	.1754	.1327	.1603	.1483	.2106	.5666	2.663E-2
.2219	.1860	.1324	.2085	.1047	.2491	.5051	6.969E-2
.2335	.1932	.1292	.2602	6.865E-2	.2885	.4423	.1884
.2473	.1967	.1228	.3121	4.186E-2	.3277	.3805	.3882
.2627	.1964	.1133	.3613	2.546E-2	.3650	.3220	.6705
.2793	.1922	.1012	.4045	1.993E-2	.3989	.2683	1.032
.2965	.1846	8.715E-2	.4392	2.509E-2	.4279	.2211	1.467
.3135	.1739	7.211E-2	.4631	4.017E-2	.4504	.1811	1.963
.3297	.1607	5.724E-2	.4747	6.386E-2	.4654	.1490	2.505
.3443	.1459	4.384E-2	.4731	9.441E-2	.4717	.1252	3.075
.3568	.1302	3.325E-2	.4583	.1297	.4690	.1098	3.651
.3664	.1145	2.675E-2	.4311	.1677	.4570	.1030	4.211
.3727	9.958E-2	2.544E-2	.3933	.2061	.4363	.1048	4.733
.3754	8.606E-2	3.018E-2	.3469	.2427	.4078	.1156	5.195
.3741	7.455E-2	4.146E-2	.2950	.2756	.3730	.1357	5.578
.3687	6.544E-2	5.936E-2	.2406	.3032	.3337	.1655	5.863
.3592	5.894E-2	8.350E-2	.1871	.3244	.2924	.2057	6.040
							6.100

TABLE XV (Continued)

SCATTERING DIAGRAMS FOR 9.02  $\mu$  DIAMETER FIBERS  
 $\theta = 0.31415928$ 

$\phi=0$	$\phi=0.38335$	$\phi=0.77605$	$\phi=1.1678$	$\phi=1.5614$	$\phi=1.9541$	$\phi=2.3468$	$\phi=2.7395$
.1661	1.959E-2	1.750E-2	4.188E-2	.1612	.2883	.3254	.2835
.1659	1.739E-2	1.517E-2	4.758E-2	.1828	.2832	.3000	.2478
.1653	1.543E-2	1.277E-2	5.571E-2	.2034	.2738	.2715	.2129
.1642	1.374E-2	1.049E-2	6.607E-2	.2222	.2607	.2409	.1792
.1627	1.236E-2	8.556E-3	7.839E-2	.2384	.2442	.2089	.1471
.1607	1.131E-2	7.178E-3	9.232E-2	.2514	.2250	.1768	.1171
.1583	1.060E-2	6.578E-3	.1074	.2607	.2036	.1456	8.953E-2
.1553	1.022E-2	6.965E-3	.1232	.2659	.1808	.1164	6.501E-2
.1519	1.013E-2	8.517E-3	.1393	.2666	.1572	9.033E-2	4.423E-2
.1480	1.030E-2	1.137E-2	.1552	.2628	.1336	6.837E-2	2.805E-2
.1436	1.068E-2	1.563E-2	.1702	.2545	.1107	5.142E-2	1.754E-2
.1388	1.119E-2	2.133E-2	.1840	.2420	8.918E-2	4.024E-2	1.400E-2
.1336	1.178E-2	2.844E-2	.1961	.2256	6.957E-2	3.541E-2	1.896E-2
.1280	1.238E-2	3.686E-2	.2061	.2059	5.246E-2	3.731E-2	3.421E-2
.1221	1.293E-2	4.645E-2	.2136	.1836	3.836E-2	4.608E-2	6.172E-2
.1160	1.339E-2	5.696E-2	.2184	.1595	2.765E-2	6.165E-2	.1036
.1098	1.372E-2	6.814E-2	.2203	.1344	2.066E-2	8.372E-2	.1622
.1036	1.390E-2	7.965E-2	.2192	.1092	1.760E-2	.1117	.2398
9.746E-2	1.393E-2	9.114E-2	.2151	8.492E-2	1.861E-2	.1449	.3386
9.142E-2	1.383E-2	.1022	.2081	6.238E-2	2.372E-2	.1825	.4608
8.562E-2	1.363E-2	.1125	.1984	4.245E-2	3.287E-2	.2232	.6081
8.011E-2	1.338E-2	.1217	.1862	2.589E-2	4.591E-2	.2660	.7821
7.496E-2	1.313E-2	.1294	.1721	1.332E-2	6.259E-2	.3095	.9838
7.020E-2	1.295E-2	.1354	.1563	5.229E-3	8.257E-2	.3525	1.213
6.587E-2	1.288E-2	.1394	.1395	1.919E-3	.1054	.3938	1.471
6.195E-2	1.299E-2	.1412	.1221	3.538E-3	.1307	.4321	1.755
5.845E-2	1.331E-2	.1409	.1049	1.004E-2	.1578	.4664	2.064
5.531E-2	1.386E-2	.1384	8.836E-2	2.120E-2	.1862	.4958	2.396
5.250E-2	1.466E-2	.1338	7.307E-2	3.663E-2	.2150	.5194	2.746
4.995E-2	1.569E-2	.1273	5.965E-2	5.579E-2	.2438	.5369	2.397
4.760E-2	1.690E-2	.1192	4.860E-2	7.799E-2	.2717	.5478	2.747
4.539E-2	1.824E-2	.1098	4.040E-2	.1024	.2979	.5521	3.111
4.325E-2	1.962E-2	9.957E-2	3.541E-2	.1283	.3218	.5498	3.486
4.112E-2	2.095E-2	8.882E-2	3.390E-2	.1547	.3427	.5412	3.864
3.895E-2	2.213E-2	7.807E-2	3.603E-2	.1807	.3600	.5268	4.240
3.672E-2	2.306E-2	6.779E-2	4.183E-2	.2055	.3731	.5071	4.607
3.439E-2	2.364E-2	5.844E-2	5.120E-2	.2281	.3815	.4828	4.958
3.198E-2	2.381E-2	5.045E-2	6.391E-2	.2480	.3849	.4547	5.288
2.949E-2	2.349E-2	4.420E-2	7.961E-2	.2645	.3831	.4236	5.589
2.696E-2	2.268E-2	4.001E-2	9.781E-2	.2770	.3761	.3902	5.855
2.443E-2	2.137E-2	3.813E-2	.1179	.2852	.3639	.3553	6.082
2.195E-2	1.961E-2	3.873E-2	.1393	.2890	.3469	.3195	6.263
							6.395
							6.476
							6.503

TABLE XV (Continued)

SCATTERING DIAGRAMS FOR 9.02  $\mu$  DIAMETER FIBERS

$$\theta = 0.23561946$$

$\phi=0$	$\phi=0.38335$	$\phi=0.77605$	$\phi=1.1678$	$\phi=1.5614$	$\phi=1.9541$	$\phi=2.3468$	$\phi=2.7395$
.1050	6.041E-2	5.669E-2	.1267	.1212	8.466E-2	.1264	7.152E-2
.1050	6.108E-2	4.851E-2	.1134	.1057	7.646E-2	.1336	7.434E-2
.1052	6.232E-2	4.118E-2	.1006	9.065E-2	6.859E-2	.1402	7.638E-2
.1054	6.413E-2	3.488E-2	8.874E-2	7.619E-2	6.119E-2	.1460	7.780E-2
.1058	6.653E-2	2.977E-2	7.785E-2	6.266E-2	5.436E-2	.1507	7.885E-2
.1062	6.950E-2	2.598E-2	6.826E-2	5.034E-2	4.817E-2	.1543	7.985E-2
.1067	7.304E-2	2.365E-2	6.017E-2	3.946E-2	4.268E-2	.1566	8.123E-2
.1072	7.711E-2	2.286E-2	5.378E-2	3.020E-2	3.793E-2	.1575	8.346E-2
.1077	8.169E-2	2.367E-2	4.922E-2	2.275E-2	3.392E-2	.1569	8.710E-2
.1082	8.674E-2	2.613E-2	4.659E-2	1.720E-2	3.063E-2	.1548	9.277E-2
.1087	9.219E-2	3.024E-2	4.597E-2	1.363E-2	2.803E-2	.1512	.1011
.1091	9.800E-2	3.598E-2	4.736E-2	1.207E-2	2.607E-2	.1460	.1128
.1095	.1040	4.327E-2	5.075E-2	1.249E-2	2.468E-2	.1395	.1286
.1097	.1103	5.203E-2	5.606E-2	1.483E-2	2.380E-2	.1316	.1491
.1098	.1167	6.212E-2	6.319E-2	1.896E-2	2.335E-2	.1226	.1751
.1098	.1231	7.339E-2	7.199E-2	2.474E-2	2.325E-2	.1127	.2071
.1096	.1295	8.566E-2	8.226E-2	3.198E-2	2.344E-2	.1020	.2456
.1091	.1357	9.871E-2	9.380E-2	4.046E-2	2.386E-2	9.081E-2	.2911
.1085	.1415	.1123	.1063	4.993E-2	2.445E-2	7.938E-2	.3440
.1076	.1470	.1262	.1196	6.013E-2	2.517E-2	6.796E-2	.4044
.1064	.1520	.1402	.1333	7.078E-2	2.599E-2	5.685E-2	.4723
.1050	.1564	.1539	.1471	8.160E-2	2.693E-2	4.629E-2	.5478
.1034	.1601	.1672	.1608	9.233E-2	2.797E-2	3.655E-2	.6306
.1015	.1631	.1798	.1741	.1026	2.914E-2	2.784E-2	.7201
9.946E-2	.1651	.1914	.1865	.1124	3.049E-2	2.036E-2	.8160
9.713E-2	.1663	.2018	.1979	.1213	3.206E-2	1.427E-2	.9173
9.460E-2	.1664	.2108	.2080	.1291	3.391E-2	9.702E-3	1.023
9.190E-2	.1656	.2182	.2166	.1357	3.610E-2	6.703E-3	1.132
8.906E-2	.1636	.2239	.2234	.1410	3.869E-2	5.306E-3	1.244
8.612E-2	.1606	.2277	.2282	.1449	4.176E-2	5.479E-3	1.357
8.312E-2	.1566	.2296	.2311	.1472	4.535E-2	7.145E-3	1.469
8.010E-2	.1515	.2296	.2318	.1480	4.951E-2	1.017E-2	1.580
7.712E-2	.1454	.2275	.2304	.1474	5.428E-2	1.440E-2	1.688
7.421E-2	.1385	.2236	.2268	.1453	5.965E-2	1.963E-2	1.791
7.145E-2	.1308	.2178	.2211	.1419	6.563E-2	2.561E-2	1.887
6.887E-2	.1223	.2103	.2135	.1372	7.218E-2	3.210E-2	1.976
6.654E-2	.1133	.2012	.2040	.1315	7.925E-2	3.883E-2	2.056
6.450E-2	.1039	.1908	.1928	.1249	8.675E-2	4.555E-2	2.127
6.281E-2	9.428E-2	.1792	.1803	.1175	9.458E-2	5.201E-2	2.185
6.151E-2	8.453E-2	.1667	.1665	.1096	.1026	5.799E-2	2.232
6.065E-2	7.490E-2	.1536	.1519	.1014	.1107	6.331E-2	2.266
6.027E-2	6.555E-2	.1402	.1367	9.304E-2	.1187	6.784E-2	2.287
							2.294

TABLE XV (Continued)

SCATTERING DIAGRAMS FOR 9.02- $\mu$  DIAMETER FIBERS  
 $\theta = 0.15707964$

$\phi=0$	$\phi=0.38335$	$\phi=0.77605$	$\phi=1.1678$	$\phi=1.5614$	$\phi=1.9541$	$\phi=2.3468$	$\phi=2.7395$
7.343E-2	1.194E-2	5.009E-2	4.389E-2	.1106	.3049	.2216	9.688E-2
7.323E-2	1.319E-2	5.186E-2	4.232E-2	.1132	.3280	.2027	9.265E-2
7.264E-2	1.451E-2	5.348E-2	4.073E-2	.1154	.3514	.1851	8.823E-2
7.167E-2	1.589E-2	5.494E-2	3.911E-2	.1170	.3751	.1687	8.368E-2
7.032E-2	1.734E-2	5.626E-2	3.750E-2	.1182	.3987	.1538	7.905E-2
6.862E-2	1.885E-2	5.742E-2	3.591E-2	.1188	.4221	.1403	7.440E-2
6.660E-2	2.043E-2	5.844E-2	3.436E-2	.1190	.4451	.1282	6.977E-2
6.426E-2	2.208E-2	5.931E-2	3.287E-2	.1186	.4674	.1177	6.520E-2
6.166E-2	2.380E-2	6.006E-2	3.146E-2	.1176	.4889	.1086	6.075E-2
5.881E-2	2.559E-2	6.068E-2	3.016E-2	.1162	.5094	.1009	5.646E-2
5.577E-2	2.747E-2	6.118E-2	2.899E-2	.1144	.5285	9.466E-2	5.237E-2
5.256E-2	2.941E-2	6.157E-2	2.797E-2	.1121	.5463	8.972E-2	4.850E-2
4.923E-2	3.144E-2	6.187E-2	2.714E-2	.1095	.5624	8.604E-2	4.489E-2
4.581E-2	3.355E-2	6.208E-2	2.651E-2	.1066	.5767	8.354E-2	4.156E-2
4.235E-2	3.574E-2	6.220E-2	2.610E-2	.1035	.5891	8.213E-2	3.853E-2
3.889E-2	3.800E-2	6.226E-2	2.595E-2	.1002	.5994	8.170E-2	3.582E-2
3.547E-2	4.034E-2	6.225E-2	2.606E-2	9.693E-2	.6076	8.214E-2	3.344E-2
3.211E-2	4.273E-2	6.219E-2	2.646E-2	9.369E-2	.6136	8.334E-2	3.139E-2
2.886E-2	4.898E-3	6.208E-2	2.716E-2	9.061E-2	.6172	8.518E-2	2.968E-2
2.575E-2	6.458E-3	6.192E-2	2.818E-2	8.780E-2	.6185	8.755E-2	2.830E-2
2.280E-2	6.380E-3	6.173E-2	2.953E-2	8.539E-2	.6174	9.032E-2	2.725E-2
2.004E-2	6.651E-3	6.149E-2	3.121E-2	8.350E-2	.6140	9.337E-2	2.651E-2
1.749E-2	7.256E-3	6.122E-2	3.322E-2	8.223E-2	.6083	9.661E-2	2.608E-2
1.516E-2	8.177E-3	6.090E-2	3.557E-2	8.170E-2	.6003	9.991E-2	2.594E-2
1.307E-2	9.391E-3	6.055E-2	3.825E-2	8.204E-2	.5902	.1031	2.608E-2
1.123E-2	1.087E-2	6.016E-2	4.124E-2	8.335E-2	.5780	.1063	2.646E-2
9.641E-3	1.259E-2	5.973E-2	4.454E-2	8.574E-2	.5639	.1092	2.707E-2
8.301E-3	1.454E-2	5.925E-2	4.813E-2	8.930E-2	.5479	.1119	2.788E-2
7.210E-3	1.666E-2	5.871E-2	5.197E-2	9.411E-2	.5303	.1142	2.888E-2
6.363E-3	1.894E-2	5.812E-2	5.605E-2	.1002	.5113	.1161	3.004E-2
5.752E-3	2.135E-2	5.747E-2	6.032E-2	.1077	.4910	.1175	3.133E-2
5.365E-3	2.385E-2	5.676E-2	6.476E-2	.1167	.4696	.1185	3.273E-2
5.190E-3	2.641E-2	5.597E-2	6.931E-2	.1271	.4473	.1189	3.421E-2
5.213E-3	2.901E-2	5.511E-2	7.394E-2	.1390	.4244	.1189	3.576E-2
5.420E-3	3.162E-2	5.417E-2	7.860E-2	.1524	.4010	.1183	3.735E-2
5.796E-3	3.421E-2	5.316E-2	8.323E-2	.1672	.3774	.1172	3.896E-2
6.325E-3	3.676E-2	5.206E-2	8.779E-2	.1834	.3537	.1156	4.057E-2
6.991E-3	3.925E-2	5.088E-2	9.222E-2	.2009	.3303	.1134	4.217E-2
7.782E-3	4.165E-2	4.962E-2	9.647E-2	.2197	.3071	.1109	4.374E-2
8.684E-3	4.394E-2	4.829E-2	.1004	.2396	.2845	.1079	4.526E-2
9.686E-3	4.613E-2	4.688E-2	.1042	.2605	.2626	.1045	4.674E-2
1.077E-2	4.818E-2	4.541E-2	.1076	.2823	.2416	.1008	4.815E-2
							4.949E-2

TABLE XV (Continued)

SCATTERING DIAGRAMS FOR 9.02  $\mu$  DIAMETER FIBERS

$\theta = 0.07853982$

$\phi=0$	$\phi=0.38335$	$\phi=0.77605$	$\phi=1.1678$	$\phi=1.5614$	$\phi=1.9541$	$\phi=2.3468$	$\phi=2.7395$
1.507E-2	1.119E-2	9.236E-3	1.680E-2	1.133E-2	5.566E-3	2.039E-2	5.879E-2
1.507E-2	1.105E-2	9.337E-3	1.693E-2	1.099E-2	5.767E-3	2.083E-2	6.034E-2
1.506E-2	1.092E-2	9.445E-3	1.704E-2	1.066E-2	5.983E-3	2.128E-2	6.190E-2
1.505E-2	1.078E-2	9.561E-3	1.715E-2	1.032E-2	6.214E-3	2.174E-2	6.349E-2
1.503E-2	1.065E-2	9.685E-3	1.724E-2	9.991E-3	6.458E-3	2.221E-2	6.508E-2
1.500E-2	1.052E-2	9.816E-3	1.733E-2	9.658E-3	6.715E-3	2.269E-2	6.669E-2
1.497E-2	1.039E-2	9.954E-3	1.740E-2	9.328E-3	6.985E-3	2.319E-2	6.831E-2
1.494E-2	1.027E-2	1.010E-2	1.746E-2	9.003E-3	7.266E-3	2.371E-2	6.994E-2
1.489E-2	1.015E-2	1.025E-2	1.750E-2	8.681E-3	7.559E-3	2.424E-2	7.157E-2
1.485E-2	1.003E-2	1.041E-2	1.754E-2	8.366E-3	7.862E-3	2.478E-2	7.320E-2
1.479E-2	9.916E-3	1.057E-2	1.756E-2	8.058E-3	8.175E-3	2.535E-2	7.483E-2
1.474E-2	9.804E-3	1.074E-2	1.756E-2	7.757E-3	8.497E-3	2.593E-2	7.646E-2
1.467E-2	9.695E-3	1.092E-2	1.755E-2	7.464E-3	8.827E-3	2.654E-2	7.808E-2
1.461E-2	9.591E-3	1.110E-2	1.753E-2	7.181E-3	9.164E-3	2.717E-2	7.968E-2
1.453E-2	9.490E-3	1.129E-2	1.749E-2	6.908E-3	9.509E-3	2.782E-2	8.128E-2
1.446E-2	9.395E-3	1.148E-2	1.744E-2	6.646E-3	9.860E-3	2.850E-2	8.285E-2
1.437E-2	9.304E-3	1.168E-2	1.738E-2	6.396E-3	1.021E-2	2.921E-2	8.440E-2
1.429E-2	9.218E-3	1.188E-2	1.730E-2	6.158E-3	1.057E-2	2.994E-2	8.593E-2
1.420E-2	9.137E-3	1.209E-2	1.720E-2	5.933E-3	1.094E-2	3.070E-2	8.744E-2
1.410E-2	9.062E-3	1.230E-2	1.710E-2	5.723E-3	1.131E-2	3.149E-2	8.891E-2
1.400E-2	8.992E-3	1.251E-2	1.697E-2	5.526E-3	1.168E-2	3.231E-2	9.035E-2
1.390E-2	8.928E-3	1.272E-2	1.683E-2	5.345E-3	1.206E-2	3.316E-2	9.175E-2
1.379E-2	8.871E-3	1.294E-2	1.668E-2	5.180E-3	1.244E-2	3.405E-2	9.311E-2
1.368E-2	8.820E-3	1.315E-2	1.652E-2	5.031E-3	1.282E-2	3.496E-2	9.442E-2
1.357E-2	8.775E-3	1.337E-2	1.634E-2	4.898E-3	1.320E-2	3.591E-2	9.569E-2
1.345E-2	8.737E-3	1.359E-2	1.615E-2	4.782E-3	1.358E-2	3.690E-2	9.691E-2
1.333E-2	8.705E-3	1.381E-2	1.594E-2	4.684E-3	1.397E-2	3.792E-2	9.808E-2
1.321E-2	8.681E-3	1.402E-2	1.572E-2	4.604E-3	1.436E-2	3.897E-2	9.919E-2
1.309E-2	8.664E-3	1.424E-2	1.549E-2	4.541E-3	1.474E-2	4.006E-2	.1002
1.296E-2	8.654E-3	1.445E-2	1.525E-2	4.497E-3	1.513E-2	4.119E-2	.1012
1.283E-2	8.652E-3	1.466E-2	1.500E-2	4.471E-3	1.552E-2	4.235E-2	.1021
1.270E-2	8.657E-3	1.487E-2	1.474E-2	4.463E-3	1.591E-2	4.354E-2	.1030
1.256E-2	8.670E-3	1.508E-2	1.446E-2	4.474E-3	1.630E-2	4.477E-2	.1038
1.243E-2	8.691E-3	1.528E-2	1.418E-2	4.503E-3	1.669E-2	4.603E-2	.1045
1.229E-2	8.719E-3	1.547E-2	1.389E-2	4.551E-3	1.709E-2	4.733E-2	.1052
1.216E-2	8.756E-3	1.566E-2	1.359E-2	4.617E-3	1.749E-2	4.866E-2	.1058
1.202E-2	8.801E-3	1.589E-2	1.328E-2	4.700E-3	1.789E-2	5.002E-2	.1063
1.188E-2	8.853E-3	1.603E-2	1.297E-2	4.802E-3	1.829E-2	5.141E-2	.1067
1.174E-2	8.914E-3	1.620E-2	1.265E-2	4.921E-3	1.870E-2	5.284E-2	.1070
1.160E-2	8.982E-3	1.636E-2	1.232E-2	5.058E-3	1.911E-2	5.429E-2	.1073
1.146E-2	9.059E-3	1.652E-2	1.200E-2	5.211E-3	1.953E-2	5.576E-2	.1075
1.133E-2	9.144E-3	1.666E-2	1.166E-2	5.381E-3	1.996E-2	5.727E-2	.1076

.1077

TABLE XVI

SCATTERING DIAGRAMS FOR 5.69  $\mu$  DIAMETER FIBERS  
 $\theta = 1.57079640$

$\phi=0$	$\phi=0.38335$	$\phi=0.77605$	$\phi=1.1678$	$\phi=1.5614$	$\phi=1.9541$	$\phi=2.3468$	$\phi=2.7395$
.3893	.1951	5.253E-2	.1234	.1458	.5337	1.368	2.163
.3724	.1284	3.965E-2	.1424	.1281	.6127	1.707	1.737
.3256	7.670E-2	3.413E-2	.1534	.1145	.6920	2.051	1.493
.2587	4.548E-2	3.509E-2	.1552	.1091	.7568	2.345	1.489
.1859	3.702E-2	4.072E-2	.1483	.1140	.7952	2.543	1.754
.1223	4.981E-2	4.880E-2	.1350	.1289	.8010	2.611	2.282
8.058E-2	7.906E-2	5.733E-2	.1188	.1509	.7751	2.540	3.032
6.820E-2	.1176	6.489E-2	.1036	.1753	.7262	2.340	3.930
8.618E-2	.1577	7.090E-2	9.290E-2	.1969	.6690	2.046	4.874
.1291	.1918	7.547E-2	8.918E-2	.2113	.6210	1.709	5.749
.1871	.2145	7.915E-2	9.334E-2	.2160	.5988	1.388	6.439
.2481	.2230	8.253E-2	.1046	.2116	.6143	1.139	6.848
.3012	.2174	8.590E-2	.1208	.2011	.6715	1.008	6.910
.3393	.2002	8.897E-2	.1388	.1895	.7655	1.021	6.605
.3611	.1757	9.096E-2	.1552	.1825	.8826	1.180	5.963
.3704	.1486	9.076E-2	.1674	.1846	1.003	1.462	5.059
.3758	.1236	8.733E-2	.1737	.1983	1.105	1.823	4.009
.3877	.1036	8.018E-2	.1741	.2227	1.170	2.205	2.948
.4159	9.006E-2	6.968E-2	.1697	.2541	1.185	2.547	2.009
.4664	8.251E-2	5.722E-2	.1630	.2866	1.148	2.792	1.304
.5400	7.917E-2	4.503E-2	.1564	.3137	1.066	2.900	.9028
.6316	7.752E-2	3.583E-2	.1522	.3302	.9607	2.853	.8221
.7312	7.518E-2	3.221E-2	.1515	.3336	.8554	2.659	1.026
.8259	7.057E-2	3.600E-2	.1544	.3249	.7786	2.351	1.438
.9025	6.341E-2	4.774E-2	.1594	.3087	.7546	1.980	1.959
.9507	5.481E-2	6.641E-2	.1643	.2922	.7989	1.609	2.499
.9646	4.698E-2	8.947E-2	.1667	.2834	.9146	1.305	3.005
.9444	4.264E-2	.1133	.1645	.2886	1.091	1.123	3.487
.8957	4.430E-2	.1337	.1572	.3114	1.304	1.105	4.032
.8281	5.349E-2	.1472	.1455	.3505	1.522	1.266	4.805
.7533	7.030E-2	.1510	.1317	.4007	1.709	1.597	6.030
.6823	9.315E-2	.1444	.1188	.4533	1.831	2.065	7.954
.6231	.1190	.1284	.1102	.4984	1.867	2.615	10.80
.5794	.1438	.1059	.1083	.5273	1.806	3.179	14.73
.5501	.1637	8.100E-2	.1141	.5350	1.659	3.688	19.79
.5304	.1752	5.832E-2	.1267	.5214	1.451	4.075	25.86
.5128	.1762	4.211E-2	.1434	.4919	1.220	4.290	32.68
.4895	.1667	3.538E-2	.1601	.4562	1.010	4.305	39.83
.4545	.1481	3.937E-2	.1728	.4264	.8661	4.116	46.79
.4047	.1236	5.333E-2	.1781	.4141	.8211	3.748	53.00
.3413	9.708E-2	7.468E-2	.1745	.4273	.8941	3.252	57.91
.2690	7.232E-2	9.953E-2	.1628	.4685	1.083	2.696	61.06
							62.14

TABLE XVI (Continued)

SCATTERING DIAGRAMS FOR 5.69  $\mu$  DIAMETER FIBERS  
 $\theta = 1.49225658$

$\phi=0$	$\phi=0.38335$	$\phi=0.77605$	$\phi=1.1678$	$\phi=1.5614$	$\phi=1.9541$	$\phi=2.3468$	$\phi=2.7395$
.5108	.2020	5.778E-2	.2346	.3865	.4688	1.448	1.783
.4879	.1426	7.087E-2	.2115	.3411	.4891	1.893	1.547
.4251	8.682E-2	.1035	.1823	.2766	.5259	2.337	1.459
.3388	4.535E-2	.1483	.1529	.2089	.5716	2.704	1.558
.2514	2.714E-2	.1948	.1287	.1552	.6162	2.931	1.864
.1864	3.760E-2	.2324	.1133	.1296	.6497	2.976	2.379
.1619	7.735E-2	.2530	.1083	.1397	.6652	2.834	3.074
.1864	.1419	.2523	.1129	.1845	.6610	2.534	3.894
.2569	.2221	.2308	.1248	.2544	.6413	2.138	4.758
.3593	.3059	.1935	.1409	.3335	.6156	1.724	5.567
.4725	.3799	.1478	.1579	.4034	.5962	1.378	6.219
.5731	.4324	.1022	.1733	.4480	.5954	1.170	6.621
.6414	.4550	6.369E-2	.1847	.4572	.6221	1.146	6.709
.6662	.4446	3.645E-2	.1909	.4299	.6791	1.314	6.456
.6473	.4036	2.141E-2	.1910	.3737	.7618	1.647	5.884
.5953	.3393	1.660E-2	.1847	.3033	.8584	2.084	5.062
.5291	.2626	1.835E-2	.1722	.2369	.9521	2.546	4.094
.4712	.1854	2.281E-2	.1548	.1914	1.024	2.948	3.111
.4423	.1182	2.729E-2	.1343	.1781	1.059	3.217	2.242
.4561	6.842E-2	3.099E-2	.1142	.2004	1.047	3.307	1.592
.5167	3.869E-2	3.498E-2	9.823E-2	.2528	.9908	3.202	1.228
.6170	2.731E-2	4.148E-2	9.057E-2	.3227	.8996	2.924	1.161
.7410	2.914E-2	5.265E-2	9.448E-2	.3937	.7956	2.525	1.349
.8668	3.747E-2	6.941E-2	.1113	.4495	.7064	2.074	1.707
.9717	4.612E-2	9.074E-2	.1397	.4785	.6608	1.651	2.131
1.036	5.123E-2	.1135	.1755	.4763	.6822	1.324	2.526
1.050	5.220E-2	.1335	.2119	.4465	.7835	1.145	2.841
1.010	5.162E-2	.1461	.2411	.3995	.9622	1.141	3.093
.9232	5.410E-2	.1481	.2562	.3496	1.199	1.307	3.386
.8037	6.450E-2	.1390	.2529	.3113	1.462	1.617	3.906
.6700	8.598E-2	.1210	.2312	.2954	1.708	2.024	4.906
.5407	.1185	9.909E-2	.1960	.3067	1.893	2.471	6.662
.4313	.1585	7.953E-2	.1562	.3428	1.981	2.900	9.432
.3518	.1991	6.868E-2	.1229	.3951	1.951	3.262	13.39
.3052	.2320	7.103E-2	.1067	.4517	1.805	3.516	18.59
.2879	.2497	8.805E-2	.1151	.5000	1.568	3.641	24.92
.2913	.2473	.1177	.1498	.5309	1.285	3.628	32.09
.3040	.2246	.1549	.2062	.5402	1.015	3.484	39.67
.3143	.1859	.1926	.2735	.5299	.8191	3.228	47.07
.3125	.1399	.2237	.3376	.5075	.7487	2.888	53.70
.2929	9.704E-2	.2425	.3841	.4833	.8342	2.503	58.94
.2548	6.729E-2	.2460	.4019	.4678	1.077	2.118	62.31
							63.47



TABLE XVI (Continued)

SCATTERING DIAGRAMS FOR 5.69  $\mu$  DIAMETER FIBERS  
 $\theta = 1.41371676$

$\phi=0$	$\phi=0.38335$	$\phi=0.77605$	$\phi=1.1678$	$\phi=1.5614$	$\phi=1.9541$	$\phi=2.3468$	$\phi=2.7395$
.4877	.1519	6.824E-2	.1191	.2757	.6422	1.489	2.250
.4761	.1349	8.731E-2	.1183	.2598	.6264	1.821	1.898
.4437	.1233	.1097	.1151	.2350	.5990	2.135	1.698
.3977	.1210	.1324	.1106	.2067	.5668	2.380	1.706
.3480	.1310	.1519	.1063	.1816	.5370	2.514	1.953
.3053	.1535	.1652	.1038	.1661	.5162	2.516	2.441
.2789	.1864	.1700	.1042	.1651	.5099	2.386	3.136
.2747	.2251	.1656	.1084	.1806	.5221	2.149	3.971
.2939	.2634	.1527	.1166	.2112	.5543	1.849	4.853
.3332	.2949	.1334	.1285	.2519	.6061	1.540	5.670
.3856	.3139	.1108	.1429	.2955	.6748	1.281	6.311
.4424	.3168	8.849E-2	.1582	.3336	.7554	1.120	6.681
.4950	.3024	6.957E-2	.1727	.3588	.8409	1.090	6.716
.5373	.2724	5.651E-2	.1846	.3660	.9230	1.198	6.399
.5666	.2309	5.056E-2	.1922	.3541	.9923	1.428	5.757
.5847	.1835	5.164E-2	.1949	.3259	1.040	1.742	4.868
.5967	.1363	5.851E-2	.1925	.2879	1.059	2.087	3.841
.6101	9.489E-2	6.911E-2	.1858	.2489	1.046	2.403	2.805
.6323	6.320E-2	8.102E-2	.1766	.2184	1.001	2.636	1.882
.6688	4.333E-2	9.192E-2	.1668	.2043	.9327	2.747	1.172
.7217	3.523E-2	9.997E-2	.1590	.2111	.8512	2.714	.7330
.7885	3.709E-2	.1040	.1550	.2392	.7736	2.542	.5727
.8623	4.593E-2	.1038	.1561	.2845	.7189	2.259	.6542
.9331	5.835E-2	9.974E-2	.1627	.3394	.7049	1.909	.9073
.9895	7.127E-2	9.254E-2	.1737	.3940	.7450	1.547	1.251
1.021	8.243E-2	8.337E-2	.1872	.4387	.8451	1.232	1.622
1.020	9.063E-2	7.337E-2	.2005	.4658	1.001	1.014	1.998
.9848	9.567E-2	6.355E-2	.2110	.4713	1.197	.9311	2.424
.9156	9.809E-2	5.475E-2	.2162	.4557	1.411	1.001	3.013
.8201	9.870E-2	4.761E-2	.2150	.4238	1.612	1.224	3.947
.7082	9.822E-2	4.261E-2	.2076	.3838	1.768	1.578	5.452
.5920	9.700E-2	4.012E-2	.1960	.3455	1.854	2.027	7.760
.4825	9.490E-2	4.039E-2	.1830	.3183	1.852	2.523	11.07
.3887	9.147E-2	4.355E-2	.1725	.3094	1.760	3.011	15.50
.3157	8.622E-2	4.956E-2	.1680	.3224	1.593	3.440	21.06
.2646	7.896E-2	5.814E-2	.1717	.3567	1.379	3.763	27.58
.2328	7.008E-2	6.870E-2	.1845	.4079	1.158	3.944	34.79
.2150	6.070E-2	8.040E-2	.2048	.4685	.9725	3.964	42.24
.2046	5.255E-2	9.217E-2	.2292	.5296	.8632	3.820	49.43
.1958	4.769E-2	.1028	.2531	.5829	.8589	3.532	55.78
.1846	4.801E-2	.1113	.2714	.6215	.9711	3.136	60.76
.1696	5.479E-2	.1169	.2797	.6414	1.190	2.687	63.95
							65.05

TABLE XVI (Continued)

SCATTERING DIAGRAMS FOR 5.69  $\mu$  DIAMETER FIBERS

$\theta = 1.33517694$

$\phi=0$	$\phi=0.38335$	$\phi=0.77605$	$\phi=1.1678$	$\phi=1.5614$	$\phi=1.9541$	$\phi=2.3468$	$\phi=2.7395$
.5437	.2688	8.604E-2	.2697	.2786	1.086	1.792	2.320
.5466	.2721	5.498E-2	.2770	.2802	1.078	1.977	2.055
.5559	.2637	4.239E-2	.2574	.3210	.9903	2.059	1.876
.5735	.2419	5.326E-2	.2163	.3926	.8376	2.031	1.828
.6014	.2085	8.646E-2	.1652	.4792	.6499	1.908	1.946
.6406	.1686	.1349	.1185	.5614	.4660	1.720	2.248
.6901	.1302	.1875	8.962E-2	.6219	.3258	1.509	2.728
.7466	.1021	.2319	8.709E-2	.6498	.2618	1.320	3.354
.8047	9.214E-2	.2580	.1122	.6428	.2926	1.193	4.072
.8580	.1045	.2602	.1587	.6081	.4178	1.155	4.804
.9006	.1389	.2392	.2138	.5597	.6185	1.217	5.463
.9284	.1897	.2015	.2624	.5141	.8597	1.374	5.958
.9410	.2468	.1573	.2905	.4860	1.097	1.604	6.215
.9411	.2984	.1179	.2899	.4842	1.287	1.874	6.182
.9347	.3331	9.242E-2	.2603	.5089	1.393	2.149	5.846
.9288	.3431	8.542E-2	.2096	.5527	1.394	2.390	5.234
.9300	.3261	9.589E-2	.1519	.6022	1.288	2.570	4.410
.9424	.2857	.1177	.1039	.6429	1.094	2.669	3.470
.9659	.2309	.1420	8.008E-2	.6630	.8482	2.679	2.523
.9960	.1735	.1594	8.882E-2	.6575	.5953	2.604	1.677
1.025	.1256	.1632	.1297	.6296	.3844	2.459	1.013
1.042	9.596E-2	.1516	.1938	.5901	.2566	2.263	.5783
1.040	8.838E-2	.1276	.2655	.5540	.2391	2.040	.3741
1.010	.1007	9.880E-2	.3267	.5366	.3392	1.816	.3659
.9504	.1257	7.422E-2	.3621	.5483	.5431	1.614	.4961
.8641	.1532	6.216E-2	.3632	.5913	.8187	1.455	.7089
.7582	.1731	6.728E-2	.3306	.6584	1.120	1.357	.9796
.6430	.1781	8.904E-2	.2744	.7341	1.398	1.331	1.340
.5296	.1657	.1217	.2116	.7986	1.605	1.384	1.895
.4277	.1390	.1562	.1615	.8329	1.708	1.515	2.828
.3440	.1056	.1823	.1405	.8242	1.693	1.718	4.377
.2814	7.541E-2	.1920	.1579	.7700	1.566	1.978	6.808
.2392	5.744E-2	.1822	.2131	.6798	1.352	2.273	10.36
.2140	5.745E-2	.1554	.2956	.5735	1.096	2.578	15.20
.2015	7.598E-2	.1196	.3874	.4771	.8471	2.864	21.35
.1973	.1081	8.601E-2	.4681	.4167	.6538	3.099	28.69
.1987	.1449	6.574E-2	.5199	.4118	.5551	3.258	36.88
.2043	.1757	6.683E-2	.5323	.4702	.5728	3.321	45.45
.2136	.1914	9.151E-2	.5047	.5850	.7074	3.279	53.78
.2265	.1869	.1353	.4471	.7357	.9382	3.134	61.19
.2418	.1630	.1883	.3769	.8915	1.227	2.904	67.04
.2572	.1259	.2373	.3147	1.018	1.528	2.619	70.79
							72.09

TABLE XVI (Continued)

SCATTERING DIAGRAMS FOR 5.69  $\mu$  DIAMETER FIBERS  
 $\theta = 1.25663712$ 

$\phi=0$	$\phi=0.38335$	$\phi=0.77605$	$\phi=1.1678$	$\phi=1.5614$	$\phi=1.9541$	$\phi=2.3468$	$\phi=2.7395$
.5006	.3647	.1014	.1116	.1594	.8493	1.600	2.547
.5045	.3386	9.333E-2	.1169	.1709	.7684	1.738	2.167
.5164	.3024	8.633E-2	.1234	.1918	.6729	1.806	1.925
.5361	.2604	8.146E-2	.1293	.2210	.5800	1.793	1.872
.5636	.2171	7.906E-2	.1327	.2559	.5070	1.700	2.033
.5980	.1767	7.874E-2	.1324	.2931	.4692	1.541	2.403
.6379	.1421	7.955E-2	.1279	.3283	.4763	1.340	2.947
.6810	.1149	8.030E-2	.1197	.3573	.5313	1.129	3.599
.7242	9.542E-2	7.986E-2	.1095	.3765	.6295	.9446	4.278
.7634	8.227E-2	7.757E-2	9.933E-2	.3833	.7588	.8165	4.891
.7949	7.362E-2	7.340E-2	9.147E-2	.3770	.9016	.7703	5.355
.8147	6.738E-2	6.801E-2	8.797E-2	.3589	1.037	.8195	5.603
.8201	6.182E-2	6.260E-2	9.005E-2	.3324	1.145	.9645	5.598
.8097	5.598E-2	5.858E-2	9.789E-2	.3024	1.210	1.192	5.335
.7835	4.988E-2	5.728E-2	.1104	.2752	1.222	1.477	4.845
.7435	4.439E-2	5.952E-2	.1258	.2571	1.179	1.786	4.184
.6930	4.098E-2	6.538E-2	.1413	.2535	1.089	2.081	3.429
.6363	4.118E-2	7.416E-2	.1542	.2681	.9680	2.327	2.658
.5779	4.613E-2	8.446E-2	.1623	.3018	.8361	2.490	1.942
.5219	5.618E-2	9.451E-2	.1639	.3526	.7175	2.551	1.333
.4714	7.066E-2	.1025	.1589	.4152	.6344	2.501	.8566
.4282	8.790E-2	.1070	.1483	.4823	.6035	2.346	.5124
.3923	.1055	.1075	.1340	.5448	.6336	2.104	.2841
.3625	.1208	.1043	.1188	.5942	.7233	1.808	.1503
.3369	.1315	9.836E-2	.1058	.6230	.8615	1.496	.1011
.3131	.1359	9.148E-2	9.755E-2	.6272	1.028	1.213	.1549
.2892	.1336	8.565E-2	9.600E-2	.6061	1.200	1.000	.3713
.2642	.1252	8.264E-2	.1019	.5635	1.349	.8959	.8569
.2385	.1127	8.357E-2	.1151	.5073	1.454	.9238	1.762
.2137	9.845E-2	8.873E-2	.1338	.4477	1.498	1.095	3.268
.1925	8.529E-2	9.742E-2	.1559	.3966	1.475	1.405	5.561
.1778	7.564E-2	.1081	.1783	.3650	1.390	1.828	8.805
.1726	7.111E-2	.1190	.1982	.3616	1.259	2.328	13.10
.1786	7.219E-2	.1281	.2131	.3906	1.106	2.853	18.48
.1964	7.823E-2	.1337	.2213	.4512	.9590	3.346	24.85
.2245	8.762E-2	.1352	.2222	.5375	.8448	3.752	32.00
.2596	9.818E-2	.1327	.2161	.6385	.7867	4.024	39.60
.2973	.1076	.1271	.2046	.7406	.7984	4.128	47.23
.3325	.1140	.1203	.1900	.8291	.8821	4.054	54.40
.3601	.1164	.1140	.1752	.8908	1.028	3.813	60.63
.3760	.1144	.1098	.1634	.9162	1.215	3.442	65.46
.3777	.1090	.1090	.1574	.9016	1.417	2.997	68.52
							69.57

TABLE XVI (Continued)

SCATTERING DIAGRAMS FOR 5.69  $\mu$  DIAMETER FIBERS  
 $\theta = 1.17809730$

$\phi=0$	$\phi=0.38335$	$\phi=0.77605$	$\phi=1.1678$	$\phi=1.5614$	$\phi=1.9541$	$\phi=2.3468$	$\phi=2.7395$
.2532	9.575E-2	7.079E-2	7.749E-2	.1698	.5789	1.784	2.081
.2670	7.613E-2	6.417E-2	8.354E-2	.1734	.4196	1.819	1.685
.3060	6.043E-2	5.910E-2	8.893E-2	.1831	.2962	1.765	1.399
.3640	4.895E-2	5.704E-2	9.265E-2	.1997	.2342	1.631	1.258
.4319	4.198E-2	5.877E-2	9.411E-2	.2227	.2486	1.437	1.276
.4991	3.974E-2	6.425E-2	9.326E-2	.2503	.3408	1.209	1.452
.5555	4.229E-2	7.258E-2	9.071E-2	.2789	.4983	.9799	1.762
.5932	4.936E-2	8.222E-2	8.760E-2	.3038	.6966	.7823	2.167
.6076	6.023E-2	9.131E-2	8.533E-2	.3202	.9033	.6462	2.618
.5980	7.372E-2	9.814E-2	8.526E-2	.3238	1.083	.5948	3.062
.5677	8.822E-2	.1014	8.838E-2	.3123	1.207	.6413	3.451
.5228	.1018	.1008	9.499E-2	.2862	1.254	.7876	3.745
.4714	.1128	9.671E-2	.1046	.2493	1.215	1.023	3.921
.4221	.1196	9.011E-2	.1161	.2084	1.099	1.328	3.971
.3821	.1215	8.265E-2	.1279	.1724	.9261	1.672	3.902
.3564	.1184	7.598E-2	.1380	.1510	.7267	2.019	3.735
.3474	.1112	7.151E-2	.1450	.1525	.5366	2.334	3.496
.3542	.1013	7.005E-2	.1480	.1816	.3895	2.584	3.211
.3738	9.089E-2	7.171E-2	.1470	.2386	.3120	2.742	2.903
.4013	8.165E-2	7.591E-2	.1427	.3180	.3188	2.793	2.584
.4314	7.521E-2	8.158E-2	.1367	.4093	.4104	2.736	2.260
.4589	7.240E-2	8.744E-2	.1309	.4985	.5731	2.582	1.930
.4802	7.317E-2	9.231E-2	.1272	.5702	.7813	2.353	1.597
.4930	7.665E-2	9.536E-2	.1271	.6110	1.002	2.084	1.273
.4969	8.140E-2	9.627E-2	.1313	.6119	1.200	1.814	.9909
.4926	8.572E-2	9.521E-2	.1396	.5713	1.345	1.586	.8130
.4820	8.812E-2	9.278E-2	.1512	.4951	1.415	1.436	.8353
.4671	8.767E-2	8.973E-2	.1646	.3971	1.399	1.392	1.186
.4499	8.418E-2	8.678E-2	.1781	.2965	1.301	1.472	2.019
.4316	7.830E-2	8.439E-2	.1899	.2146	1.138	1.676	3.497
.4127	7.131E-2	8.269E-2	.1991	.1708	.9361	1.988	5.775
.3931	6.479E-2	8.145E-2	.2050	.1792	.7279	2.380	8.972
.3723	6.024E-2	8.027E-2	.2076	.2444	.5469	2.809	13.14
.3497	5.871E-2	7.869E-2	.2074	.3610	.4226	3.228	18.28
.3246	6.047E-2	7.641E-2	.2051	.5134	.3760	3.587	24.26
.2971	6.503E-2	7.347E-2	.2014	.6782	.4167	3.843	30.87
.2674	7.116E-2	7.024E-2	.1968	.8284	.5421	3.963	37.81
.2363	7.727E-2	6.735E-2	.1916	.9381	.7374	3.929	44.70
.2049	8.176E-2	6.558E-2	.1859	.9878	.9784	3.742	51.13
.1742	8.343E-2	6.560E-2	.1801	.9678	1.234	3.422	56.68
.1453	8.179E-2	6.774E-2	.1748	.8811	1.473	3.005	60.95
.1189	7.721E-2	7.190E-2	.1709	.7431	1.664	2.539	63.65
							64.58

TABLE XVI (Continued)

SCATTERING DIAGRAMS FOR 5.69  $\mu$  DIAMETER FIBERS  
 $\theta = 1.02101766$

$\phi=0$	$\phi=0.38335$	$\phi=0.77605$	$\phi=1.1678$	$\phi=1.5614$	$\phi=1.9541$	$\phi=2.3468$	$\phi=2.7395$
1.262	.1633	5.761E-2	7.537E-2	.1399	.2938	1.856	1.643
1.257	.1640	6.780E-2	7.861E-2	.1170	.4213	1.726	1.274
1.244	.1599	7.824E-2	8.311E-2	.1016	.5641	1.529	.9512
1.220	.1507	8.725E-2	8.778E-2	9.593E-2	.7047	1.291	.6933
1.187	.1368	9.336E-2	9.140E-2	.1011	.8251	1.046	.5162
1.142	.1194	9.558E-2	9.284E-2	.1170	.9088	.8280	.4293
1.086	.1004	9.359E-2	9.135E-2	.1425	.9441	.6688	.4371
1.019	8.172E-2	8.776E-2	8.679E-2	.1753	.9253	.5951	.5410
.9427	6.536E-2	7.912E-2	7.971E-2	.2124	.8540	.6236	.7398
.8572	5.308E-2	6.918E-2	7.132E-2	.2503	.7392	.7591	1.031
.7654	4.605E-2	5.966E-2	6.333E-2	.2855	.5966	.9935	1.410
.6705	4.468E-2	5.223E-2	5.765E-2	.3144	.4461	1.306	1.872
.5756	4.859E-2	4.820E-2	5.604E-2	.3343	.3098	1.668	2.405
.4843	5.666E-2	4.831E-2	5.973E-2	.3428	.2084	2.041	2.995
.3997	6.722E-2	5.260E-2	6.914E-2	.3389	.1588	2.385	3.620
.3247	7.834E-2	6.043E-2	8.371E-2	.3226	.1715	2.664	4.249
.2612	8.814E-2	7.058E-2	.1019	.2952	.2487	2.847	4.845
.2105	9.508E-2	8.142E-2	.1214	.2596	.3842	2.914	5.362
.1729	9.820E-2	9.124E-2	.1396	.2199	.5636	2.856	5.754
.1478	9.729E-2	9.853E-2	.1535	.1810	.7662	2.680	5.974
.1340	9.283E-2	.1021	.1611	.1487	.9679	2.406	5.986
.1295	8.591E-2	.1017	.1610	.1283	1.143	2.065	5.765
.1320	7.802E-2	9.733E-2	.1530	.1246	1.271	1.696	5.310
.1392	7.072E-2	8.986E-2	.1384	.1407	1.335	1.342	4.647
.1486	6.539E-2	8.062E-2	.1194	.1775	1.327	1.042	3.829
.1580	6.296E-2	7.114E-2	9.942E-2	.2333	1.248	.8327	2.940
.1658	6.373E-2	6.296E-2	8.179E-2	.3035	1.109	.7373	2.090
.1707	6.738E-2	5.729E-2	6.996E-2	.3813	.9298	.7683	1.408
.1721	7.299E-2	5.489E-2	6.651E-2	.4578	.7335	.9235	1.030
.1697	7.922E-2	5.588E-2	7.284E-2	.5236	.5484	1.187	1.087
.1642	8.463E-2	5.981E-2	8.889E-2	.5696	.4017	1.532	1.689
.1564	8.790E-2	6.575E-2	.1131	.5888	.3158	1.922	2.915
.1475	8.810E-2	7.246E-2	.1427	.5773	.3063	2.316	4.793
.1389	8.489E-2	7.867E-2	.1739	.5353	.3792	2.675	7.300
.1319	7.859E-2	8.331E-2	.2028	.4673	.5304	2.961	10.35
.1276	7.010E-2	8.572E-2	.2257	.3821	.7454	3.149	13.81
.1267	6.079E-2	8.574E-2	.2396	.2916	1.001	3.220	17.49
.1293	5.224E-2	8.376E-2	.2428	.2096	1.270	3.170	21.17
.1349	4.595E-2	8.058E-2	.2353	.1497	1.520	3.005	24.62
.1426	4.308E-2	7.724E-2	.2183	.1233	1.724	2.743	27.59
.1510	4.423E-2	7.479E-2	.1943	.1381	1.856	2.408	29.88
.1585	4.932E-2	7.404E-2	.1669	.1962	1.901	2.031	31.33
							31.82

TABLE XVI (Continued)

SCATTERING DIAGRAMS FOR 5.69  $\mu$  DIAMETER FIBERS  
 $\theta = 1.09955748$

$\phi=0$	$\phi=0.38335$	$\phi=0.77605$	$\phi=1.1678$	$\phi=1.5614$	$\phi=1.9541$	$\phi=2.3468$	$\phi=2.7395$
.2982	9.750E-2	7.127E-2	9.364E-2	.3908	.6045	1.752	2.456
.3174	9.834E-2	7.674E-2	9.697E-2	.3981	.6427	1.850	1.934
.3723	.1018	8.148E-2	9.796E-2	.3825	.6814	1.876	1.457
.4557	.1074	8.378E-2	9.627E-2	.3470	.7184	1.825	1.076
.5565	.1138	8.247E-2	9.236E-2	.2984	.7525	1.703	.8286
.6619	.1193	7.721E-2	8.743E-2	.2460	.7834	1.525	.7349
.7592	.1225	6.861E-2	8.303E-2	.2000	.8114	1.314	.7962
.8380	.1223	5.812E-2	8.070E-2	.1697	.8366	1.097	.9958
.8910	.1183	4.773E-2	8.153E-2	.1618	.8587	.9045	1.303
.9158	.1110	3.958E-2	8.580E-2	.1796	.8766	.7617	1.679
.9142	.1017	3.549E-2	9.287E-2	.2215	.8886	.6895	2.085
.8920	9.203E-2	3.653E-2	.1012	.2822	.8928	.7001	2.483
.8576	8.369E-2	4.282E-2	.1089	.3527	.8876	.7955	2.847
.8201	7.820E-2	5.340E-2	.1138	.4225	.8727	.9671	3.161
.7879	7.639E-2	6.649E-2	.1144	.4812	.8496	1.197	3.418
.7672	7.830E-2	7.979E-2	.1099	.5202	.8221	1.460	3.621
.7606	8.316E-2	9.094E-2	.1010	.5343	.7960	1.726	3.775
.7673	8.962E-2	9.807E-2	8.972E-2	.5225	.7783	1.964	3.880
.7830	9.600E-2	.1001	7.876E-2	.4885	.7766	2.147	3.934
.8013	.1007	9.713E-2	7.153E-2	.4395	.7972	2.252	3.924
.8146	.1028	9.016E-2	7.112E-2	.3853	.8436	2.267	3.831
.8155	.1018	8.115E-2	7.962E-2	.3364	.9158	2.190	3.635
.7987	9.813E-2	7.244E-2	9.757E-2	.3022	1.009	2.030	3.322
.7612	9.278E-2	6.631E-2	.1236	.2895	1.114	1.809	2.894
.7035	8.729E-2	6.453E-2	.1545	.3013	1.219	1.557	2.382
.6289	8.317E-2	6.791E-2	.1858	.3366	1.310	1.309	1.850
.5429	8.164E-2	7.622E-2	.2123	.3903	1.372	1.103	1.400
.4527	8.331E-2	8.816E-2	.2293	.4547	1.395	.9773	1.172
.3655	8.800E-2	.1017	.2335	.5205	1.372	.9574	1.331
.2874	9.476E-2	.1144	.2238	.5790	1.305	1.061	2.056
.2229	.1021	.1242	.2016	.6229	1.201	1.292	3.514
.1743	.1083	.1294	.1710	.6479	1.073	1.637	5.838
.1414	.1119	.1293	.1380	.6530	.9419	2.067	9.103
.1220	.1118	.1243	.1097	.6407	.8266	2.542	13.30
.1129	.1078	.1156	9.277E-2	.6160	.7480	3.012	18.34
.1102	.1004	.1052	9.237E-2	.5856	.7221	3.425	24.03
.1102	9.089E-2	9.527E-2	.1110	.5564	.7580	3.734	30.09
.1103	8.104E-2	8.746E-2	.1480	.5345	.8564	3.899	36.17
.1091	7.262E-2	8.303E-2	.1991	.5241	1.009	3.899	41.88
.1063	6.708E-2	8.231E-2	.2575	.5271	1.198	3.729	46.83
.1025	6.520E-2	8.473E-2	.3145	.5432	1.403	3.407	50.66
9.921E-2	6.690E-2	8.905E-2	.3614	.5701	1.596	2.966	53.08
							53.91

TABLE XVI (Continued)

SCATTERING DIAGRAMS FOR 5.69  $\mu$  DIAMETER FIBERS  
 $\theta = 0.94247784$

$\phi=0$	$\phi=0.38335$	$\phi=0.77605$	$\phi=1.1678$	$\phi=1.5614$	$\phi=1.9541$	$\phi=2.3468$	$\phi=2.7395$
.6719	6.925E-2	4.678E-2	9.647E-2	.3259	.7775	1.063	1.023
.6651	9.892E-2	4.258E-2	6.101E-2	.3374	.7868	.9232	.9035
.6451	.1343	5.577E-2	4.312E-2	.3434	.7556	.8032	.7965
.6137	.1700	8.433E-2	4.741E-2	.3459	.6874	.7202	.7071
.5736	.2007	.1236	7.489E-2	.3470	.5909	.6864	.6412
.5281	.2221	.1672	.1227	.3482	.4785	.7091	.6058
.4808	.2316	.2079	.1846	.3503	.3651	.7893	.6095
.4355	.2286	.2391	.2517	.3527	.2657	.9221	.6626
.3954	.2148	.2560	.3141	.3541	.1939	1.096	.7768
.3629	.1938	.2562	.3623	.3524	.1601	1.298	.9639
.3397	.1701	.2402	.3889	.3457	.1700	1.509	1.234
.3262	.1489	.2114	.3900	.3328	.2238	1.710	1.595
.3216	.1348	.1752	.3655	.3136	.3165	1.885	2.048
.3244	.1309	.1384	.3192	.2899	.4381	2.018	2.586
.3321	.1382	.1075	.2586	.2649	.5751	2.101	3.192
.3422	.1558	8.803E-2	.1935	.2432	.7120	2.127	3.840
.3521	.1805	8.291E-2	.1340	.2295	.8331	2.099	4.492
.3596	.2077	9.262E-2	8.972E-2	.2287	.9247	2.021	5.102
.3634	.2318	.1147	6.753E-2	.2440	.9764	1.904	5.618
.3629	.2480	.1445	7.099E-2	.2764	.9824	1.763	5.989
.3589	.2522	.1757	9.961E-2	.3244	.9426	1.611	6.169
.3524	.2427	.2021	.1490	.3837	.8620	1.465	6.124
.3454	.2198	.2180	.2120	.4476	.7508	1.337	5.837
.3397	.1867	.2201	.2792	.5078	.6229	1.240	5.315
.3367	.1480	.2076	.3410	.5556	.4944	1.180	4.589
.3373	.1099	.1827	.3891	.5836	.3818	1.160	3.717
.3414	7.856E-2	.1499	.4174	.5864	.3003	1.179	2.782
.3475	5.899E-2	.1155	.4231	.5620	.2619	1.232	1.883
.3536	5.458E-2	8.635E-2	.4070	.5125	.2738	1.311	1.129
.3568	6.610E-2	6.833E-2	.3729	.4435	.3380	1.406	.6301
.3542	9.163E-2	6.556E-2	.3271	.3643	.4507	1.505	.4820
.3432	.1268	7.937E-2	.2772	.2859	.6026	1.596	.7585
.3223	.1655	.1079	.2308	.2201	.7800	1.671	1.500
.2913	.2011	.1468	.1942	.1775	.9664	1.721	2.706
.2516	.2272	.1891	.1717	.1660	1.143	1.741	4.335
.2061	.2391	.2274	.1651	.1894	1.295	1.729	6.299
.1588	.2345	.2544	.1735	.2468	1.406	1.685	8.476
.1147	.2140	.2650	.1941	.3326	1.466	1.613	10.71
7.863E-2	.1810	.2566	.2223	.4368	1.472	1.517	12.85
5.439E-2	.1409	.2300	.2534	.5469	1.425	1.403	14.72
4.464E-2	.1007	.1895	.2830	.6488	1.332	1.278	16.18
5.006E-2	6.742E-2	.1422	.3077	.7292	1.206	1.150	17.10
							17.42

TABLE XVI (Continued)

SCATTERING DIAGRAMS FOR 5.69  $\mu$  DIAMETER FIBERS  
 $\theta = 0.86393802$

$\phi=0$	$\phi=0.38335$	$\phi=0.77605$	$\phi=1.1678$	$\phi=1.5614$	$\phi=1.9541$	$\phi=2.3468$	$\phi=2.7395$
1.498	.1546	6.101E-2	.1352	.2394	.7008	1.240	2.835
1.490	.1600	5.599E-2	.1359	.2386	.6573	1.047	2.697
1.466	.1632	5.348E-2	.1308	.2320	.5948	.8514	2.488
1.427	.1636	5.370E-2	.1206	.2203	.5199	.6728	2.221
1.373	.1611	5.643E-2	.1066	.2045	.4406	.5297	1.913
1.306	.1560	6.107E-2	9.073E-2	.1864	.3663	.4376	1.589
1.225	.1486	6.669E-2	7.471E-2	.1677	.3061	.4067	1.275
1.134	.1399	7.226E-2	6.060E-2	.1509	.2686	.4416	1.000
1.034	.1307	7.674E-2	5.007E-2	.1382	.2603	.5406	.7922
.9271	.1220	7.932E-2	4.439E-2	.1316	.2852	.6957	.6775
.8160	.1146	7.950E-2	4.424E-2	.1328	.3440	.8935	.6764
.7040	.1091	7.721E-2	4.965E-2	.1428	.4339	1.116	.8011
.5939	.1058	7.283E-2	6.006E-2	.1619	.5490	1.345	1.053
.4887	.1046	6.710E-2	7.438E-2	.1894	.6799	1.558	1.424
.3914	.1051	6.104E-2	9.113E-2	.2239	.8156	1.737	1.891
.3041	.1066	5.578E-2	.1086	.2630	.9435	1.866	2.422
.2290	.1083	5.236E-2	.1253	.3037	1.051	1.933	2.975
.1671	.1093	5.157E-2	.1395	.3427	1.129	1.933	3.503
.1191	.1087	5.379E-2	.1502	.3768	1.168	1.864	3.957
8.488E-2	.1061	5.891E-2	.1566	.4027	1.163	1.734	4.293
6.335E-2	.1011	6.636E-2	.1584	.4181	1.116	1.553	4.473
5.309E-2	9.397E-2	7.511E-2	.1557	.4213	1.030	1.336	4.475
5.211E-2	8.504E-2	8.389E-2	.1491	.4119	.9134	1.102	4.292
5.814E-2	7.519E-2	9.130E-2	.1394	.3908	.7786	.8692	3.940
6.878E-2	6.542E-2	9.610E-2	.1278	.3600	.6402	.6565	3.450
8.172E-2	5.679E-2	9.734E-2	.1153	.3227	.5136	.4811	2.875
9.492E-2	5.031E-2	9.458E-2	.1033	.2831	.4137	.3572	2.282
.1067	4.673E-2	8.792E-2	9.277E-2	.2459	.3533	.2948	1.748
.1161	4.646E-2	7.809E-2	8.473E-2	.2158	.3412	.2998	1.352
.1224	4.949E-2	6.631E-2	7.996E-2	.1972	.3821	.3735	1.167
.1255	5.538E-2	5.416E-2	7.901E-2	.1937	.4750	.5128	1.257
.1260	6.333E-2	4.337E-2	8.218E-2	.2076	.6138	.7107	1.662
.1246	7.226E-2	3.559E-2	8.954E-2	.2397	.7872	.9567	2.400
.1222	8.096E-2	3.214E-2	.1008	.2887	.9802	1.237	3.459
.1199	8.826E-2	3.381E-2	.1157	.3519	1.175	1.539	4.797
.1186	9.321E-2	4.075E-2	.1333	.4248	1.354	1.844	6.347
.1189	9.519E-2	5.245E-2	.1527	.5015	1.501	2.136	8.017
.1214	9.398E-2	6.774E-2	.1729	.5754	1.599	2.400	9.700
.1260	8.986E-2	8.495E-2	.1925	.6399	1.641	2.620	11.28
.1323	8.347E-2	.1021	.2101	.6888	1.622	2.783	12.65
.1398	7.578E-2	.1173	.2245	.7169	1.542	2.877	13.70
.1475	6.792E-2	.1288	.2346	.7212	1.411	2.896	14.37
							14.60



TABLE XVI (Continued)

SCATTERING DIAGRAMS FOR 5.69  $\mu$  DIAMETER FIBERS  
 $\theta = 0.78539820$

$\phi=0$	$\phi=0.38335$	$\phi=0.77605$	$\phi=1.1678$	$\phi=1.5614$	$\phi=1.9541$	$\phi=2.3468$	$\phi=2.7395$
.4511	.1746	8.925E-2	5.761E-2	9.022E-2	.1674	.4661	2.477
.4489	.1695	8.056E-2	7.842E-2	8.653E-2	.1407	.3670	2.337
.4424	.1624	7.340E-2	.1006	8.992E-2	.1384	.2979	2.140
.4316	.1533	6.859E-2	.1223	.1012	.1624	.2654	1.899
.4168	.1425	6.664E-2	.1413	.1207	.2120	.2733	1.628
.3984	.1306	6.765E-2	.1561	.1478	.2843	.3226	1.346
.3767	.1183	7.130E-2	.1654	.1812	.3742	.4114	1.072
.3523	.1064	7.691E-2	.1685	.2190	.4751	.5349	.8220
.3260	9.574E-2	8.354E-2	.1655	.2583	.5790	.6859	.6120
.2985	8.697E-2	9.009E-2	.1569	.2963	.6775	.8553	.4540
.2708	8.068E-2	9.549E-2	.1437	.3296	.7626	1.032	.3558
.2437	7.715E-2	9.883E-2	.1274	.3551	.8271	1.206	.3199
.2182	7.636E-2	9.951E-2	.1097	.3705	.8654	1.366	.3439
.1953	7.801E-2	9.731E-2	9.227E-2	.3739	.8744	1.501	.4210
.1757	8.151E-2	9.248E-2	7.655E-2	.3645	.8532	1.603	.5403
.1601	8.606E-2	8.566E-2	6.388E-2	.3429	.8035	1.666	.6889
.1487	9.077E-2	7.784E-2	5.516E-2	.3105	.7299	1.686	.8530
.1419	9.475E-2	7.023E-2	5.091E-2	.2703	.6388	1.661	1.020
.1394	9.719E-2	6.410E-2	5.120E-2	.2260	.5384	1.593	1.180
.1409	9.754E-2	6.058E-2	5.577E-2	.1819	.4379	1.487	1.329
.1457	9.551E-2	6.051E-2	6.408E-2	.1426	.3469	1.350	1.468
.1529	9.116E-2	6.434E-2	7.536E-2	.1127	.2739	1.191	1.604
.1618	8.488E-2	7.199E-2	8.880E-2	9.589E-2	.2266	1.022	1.752
.1712	7.735E-2	8.286E-2	.1035	9.504E-2	.2103	.8532	1.934
.1803	6.946E-2	9.589E-2	.1188	.1116	.2278	.6979	2.175
.1884	6.221E-2	.1096	.1340	.1455	.2791	.5678	2.504
.1947	5.657E-2	.1225	.1485	.1950	.3615	.4736	2.951
.1989	5.336E-2	.1328	.1618	.2568	.4695	.4242	3.543
.2010	5.312E-2	.1392	.1737	.3264	.5953	.4258	4.303
.2010	5.608E-2	.1407	.1837	.3983	.7296	.4816	5.244
.1993	6.206E-2	.1366	.1915	.4666	.8622	.5915	6.372
.1964	7.053E-2	.1271	.1967	.5254	.9829	.7518	7.677
.1929	8.063E-2	.1130	.1991	.5695	1.082	.9553	9.140
.1892	9.132E-2	9.550E-2	.1983	.5949	1.152	1.191	10.72
.1859	.1014	7.635E-2	.1940	.5991	1.188	1.447	12.38
.1834	.1098	5.753E-2	.1862	.5815	1.186	1.708	14.07
.1817	.1156	4.105E-2	.1752	.5435	1.147	1.959	15.71
.1808	.1183	2.871E-2	.1614	.4885	1.074	2.182	17.25
.1804	.1175	2.193E-2	.1456	.4215	.9724	2.364	18.62
.1802	.1135	2.156E-2	.1290	.3489	.8505	2.491	19.75
.1795	.1068	2.781E-2	.1131	.2776	.7184	2.555	20.60
.1778	9.840E-2	4.020E-2	9.965E-2	.2149	.5866	2.551	21.13
							21.31

TABLE XVI (Continued)

SCATTERING DIAGRAMS FOR 5.69  $\mu$  DIAMETER FIBERS  
 $\theta = 0.70685838$

$\phi=0$	$\phi=0.38335$	$\phi=0.77605$	$\phi=1.1678$	$\phi=1.5614$	$\phi=1.9541$	$\phi=2.3468$	$\phi=2.7395$
.6433	9.335E-2	7.597E-2	.2172	.3070	.2428	.5142	1.661
.6419	8.846E-2	7.953E-2	.2139	.3346	.2993	.4410	1.686
.6377	8.608E-2	8.748E-2	.2032	.3546	.3640	.3797	1.678
.6307	8.619E-2	9.851E-2	.1858	.3657	.4329	.3349	1.642
.6210	8.855E-2	.1110	.1631	.3673	.5016	.3109	1.579
.6086	9.270E-2	.1236	.1369	.3592	.5657	.3106	1.497
.5936	9.805E-2	.1347	.1096	.3421	.6209	.3358	1.401
.5761	.1039	.1430	8.380E-2	.3172	.6638	.3869	1.296
.5563	.1095	.1479	6.191E-2	.2861	.6916	.4627	1.186
.5344	.1143	.1488	4.620E-2	.2510	.7025	.5605	1.076
.5106	.1177	.1459	3.844E-2	.2145	.6960	.6761	.9681
.4853	.1196	.1395	3.974E-2	.1793	.6727	.8039	.8621
.4587	.1197	.1305	5.046E-2	.1481	.6342	.9376	.7582
.4313	.1185	.1198	7.013E-2	.1234	.5833	1.069	.6557
.4036	.1163	.1085	9.752E-2	.1075	.5236	1.193	.5536
.3759	.1141	9.765E-2	.1307	.1020	.4592	1.300	.4523
.3489	.1125	8.794E-2	.1672	.1080	.3945	1.385	.3536
.3230	.1126	8.001E-2	.2044	.1257	.3341	1.442	.2623
.2987	.1153	7.408E-2	.2394	.1545	.2822	1.467	.1863
.2765	.1211	7.009E-2	.2695	.1931	.2424	1.458	.1375
.2566	.1306	6.768E-2	.2924	.2395	.2179	1.416	.1316
.2395	.1438	6.630E-2	.3066	.2908	.2105	1.343	.1881
.2252	.1603	6.530E-2	.3108	.3438	.2214	1.243	.3292
.2137	.1795	6.410E-2	.3050	.3952	.2503	1.124	.5792
.2050	.2003	6.222E-2	.2897	.4415	.2962	.9917	.9626
.1988	.2212	5.945E-2	.2662	.4795	.3569	.8559	1.502
.1946	.2409	5.588E-2	.2364	.5065	.4291	.7259	2.218
.1921	.2576	5.189E-2	.2027	.5205	.5092	.6107	3.125
.1907	.2699	4.817E-2	.1676	.5206	.5929	.5186	4.229
.1896	.2767	4.561E-2	.1340	.5067	.6757	.4564	5.529
.1883	.2772	4.517E-2	.1043	.4796	.7531	.4290	7.012
.1863	.2711	4.780E-2	8.079E-2	.4415	.8209	.4388	8.658
.1830	.2585	5.424E-2	6.523E-2	.3950	.8752	.4859	10.43
.1781	.2403	6.490E-2	5.880E-2	.3439	.9132	.5677	12.29
.1716	.2178	7.979E-2	6.204E-2	.2919	.9326	.6792	14.18
.1633	.1923	9.844E-2	7.481E-2	.2433	.9323	.8135	16.06
.1536	.1659	.1198	9.632E-2	.2019	.9124	.9622	17.85
.1428	.1404	.1427	.1252	.1714	.8740	1.116	19.50
.1314	.1176	.1653	.1596	.1544	.8192	1.265	20.94
.1202	9.889E-2	.1857	.1974	.1529	.7514	1.401	22.12
.1096	8.542E-2	.2022	.2362	.1676	.6747	1.516	23.00
.1005	7.777E-2	.2131	.2735	.1981	.5939	1.604	23.55
							23.73

TABLE XVI (Continued)

SCATTERING DIAGRAMS FOR 5.69  $\mu$  DIAMETER FIBERS  
 $\theta = 0.62831856$

$\phi=0$	$\phi=0.38335$	$\phi=0.77605$	$\phi=1.1678$	$\phi=1.5614$	$\phi=1.9541$	$\phi=2.3468$	$\phi=2.7395$
.2131	6.104E-2	.1260	.1900	.2003	.5465	.3042	.7507
.2124	6.109E-2	9.950E-2	.1921	.1663	.5889	.2858	.8649
.2105	6.613E-2	7.413E-2	.1943	.1317	.6162	.2861	.9873
.2072	7.663E-2	5.166E-2	.1969	9.900E-2	.6268	.3060	1.117
.2027	9.263E-2	3.355E-2	.1999	7.053E-2	.6203	.3456	1.252
.1968	.1138	2.091E-2	.2032	4.859E-2	.5972	.4037	1.390
.1896	.1394	1.444E-2	.2066	3.517E-2	.5590	.4784	1.527
.1811	.1682	1.437E-2	.2099	3.179E-2	.5081	.5665	1.659
.1714	.1989	2.046E-2	.2126	3.936E-2	.4476	.6644	1.779
.1605	.2296	3.203E-2	.2145	5.814E-2	.3813	.7676	1.882
.1485	.2587	4.806E-2	.2149	8.763E-2	.3131	.8712	1.961
.1357	.2844	6.726E-2	.2136	.1266	.2473	.9704	2.011
.1221	.3050	8.819E-2	.2102	.1731	.1876	1.060	2.025
.1082	.3192	.1093	.2044	.2247	.1378	1.136	2.001
9.430E-2	.3261	.1294	.1962	.2785	.1010	1.194	1.935
8.069E-2	.3252	.1472	.1857	.3311	7.944E-2	1.231	1.829
6.787E-2	.3166	.1617	.1732	.3794	7.465E-2	1.246	1.685
5.627E-2	.3009	.1724	.1592	.4203	8.727E-2	1.237	1.511
4.636E-2	.2791	.1791	.1443	.4510	.1170	1.204	1.314
3.854E-2	.2528	.1817	.1294	.4694	.1626	1.150	1.109
3.318E-2	.2237	.1807	.1154	.4741	.2223	1.076	.9097
3.054E-2	.1940	.1767	.1033	.4646	.2932	.9871	.7332
3.077E-2	.1656	.1706	9.399E-2	.4412	.3721	.8859	.5981
3.385E-2	.1403	.1632	8.828E-2	.4054	.4555	.7775	.5232
3.963E-2	.1199	.1555	8.691E-2	.3591	.5395	.6669	.5264
4.778E-2	.1056	.1482	9.036E-2	.3055	.6204	.5586	.6238
5.780E-2	9.806E-2	.1422	9.884E-2	.2478	.6944	.4571	.8285
6.906E-2	9.746E-2	.1379	.1122	.1899	.7583	.3660	1.149
8.082E-2	.1034	.1356	.1301	.1357	.8093	.2885	1.590
9.228E-2	.1151	.1354	.1517	8.903E-2	.8452	.2266	2.151
.1026	.1311	.1372	.1759	5.305E-2	.8647	.1818	2.823
.1111	.1498	.1407	.2015	3.053E-2	.8670	.1545	3.594
.1170	.1692	.1456	.2269	2.334E-2	.8523	.1445	4.444
.1201	.1874	.1514	.2505	3.241E-2	.8218	.1509	5.350
.1199	.2027	.1576	.2707	5.763E-2	.7771	.1725	6.282
.1166	.2134	.1638	.2860	9.789E-2	.7209	.2079	7.211
.1104	.2184	.1695	.2952	.1511	.6562	.2556	8.104
.1020	.2170	.1746	.2972	.2143	.5866	.3144	8.927
9.217E-2	.2090	.1790	.2917	.2840	.5162	.3834	9.649
8.197E-2	.1949	.1826	.2785	.3562	.4488	.4617	10.24
7.257E-2	.1754	.1855	.2581	.4267	.3887	.5491	10.68
6.520E-2	.1519	.1878	.2315	.4914	.3393	.6454	10.95
							11.05

TABLE XVI (Continued)

SCATTERING DIAGRAMS FOR 5.69  $\mu$  DIAMETER FIBERS

$\theta = 0.54977874$

$\phi=0$	$\phi=0.38335$	$\phi=0.77605$	$\phi=1.1678$	$\phi=1.5614$	$\phi=1.9541$	$\phi=2.3468$	$\phi=2.7395$
.3057	.2266	.1059	9.483E-2	.1016	.4926	.1733	.4165
.3054	.2188	.1171	7.524E-2	.1233	.4854	.1387	.5170
.3045	.2090	.1271	5.814E-2	.1462	.4700	.1136	.6317
.3030	.1975	.1352	4.429E-2	.1696	.4471	9.912E-2	.7567
.3009	.1848	.1410	3.425E-2	.1928	.4175	9.568E-2	.8876
.2980	.1713	.1442	2.845E-2	.2149	.3826	.1036	1.019
.2945	.1573	.1445	2.709E-2	.2352	.3440	.1228	1.146
.2903	.1434	.1419	3.018E-2	.2529	.3035	.1529	1.262
.2853	.1301	.1365	3.751E-2	.2675	.2630	.1929	1.363
.2795	.1176	.1286	4.871E-2	.2784	.2246	.2420	1.444
.2729	.1064	.1187	6.321E-2	.2851	.1900	.2986	1.501
.2656	9.672E-2	.1073	8.033E-2	.2874	.1611	.3613	1.531
.2576	8.864E-2	9.510E-2	9.927E-2	.2852	.1396	.4284	1.532
.2490	8.227E-2	8.283E-2	.1191	.2785	.1267	.4979	1.503
.2399	7.756E-2	7.129E-2	.1390	.2675	.1232	.5679	1.447
.2304	7.437E-2	6.126E-2	.1581	.2528	.1298	.6365	1.365
.2208	7.248E-2	5.344E-2	.1755	.2349	.1465	.7016	1.263
.2112	7.159E-2	4.844E-2	.1905	.2145	.1729	.7614	1.145
.2018	7.137E-2	4.674E-2	.2024	.1925	.2083	.8140	1.018
.1930	7.147E-2	4.864E-2	.2108	.1699	.2513	.8577	.8915
.1849	7.154E-2	5.428E-2	.2154	.1477	.3005	.8912	.7725
.1778	7.128E-2	6.358E-2	.2159	.1271	.3539	.9132	.6702
.1719	7.041E-2	7.625E-2	.2124	.1092	.4094	.9228	.5932
.1674	6.877E-2	9.185E-2	.2051	9.503E-2	.4650	.9196	.5497
.1646	6.626E-2	.1097	.1944	8.539E-2	.5182	.9032	.5466
.1634	6.288E-2	.1291	.1806	8.113E-2	.5670	.8742	.5896
.1639	5.875E-2	.1492	.1645	8.281E-2	.6093	.8331	.6827
.1662	5.408E-2	.1690	.1467	9.080E-2	.6435	.7811	.8279
.1700	4.915E-2	.1876	.1279	.1051	.6681	.7201	1.025
.1754	4.430E-2	.2042	.1090	.1257	.6822	.6519	1.271
.1820	3.994E-2	.2178	9.077E-2	.1521	.6850	.5792	1.562
.1895	3.645E-2	.2279	7.388E-2	.1834	.6765	.5049	1.891
.1976	3.423E-2	.2339	5.907E-2	.2189	.6570	.4320	2.249
.2060	3.361E-2	.2354	4.696E-2	.2571	.6273	.3639	2.626
.2140	3.485E-2	.2325	3.806E-2	.2968	.5885	.3039	3.009
.2215	3.811E-2	.2250	3.278E-2	.3365	.5422	.2552	3.387
.2278	4.343E-2	.2134	3.137E-2	.3746	.4900	.2209	3.747
.2327	5.075E-2	.1982	3.396E-2	.4096	.4342	.2034	4.076
.2358	5.984E-2	.1800	4.055E-2	.4399	.3767	.2050	4.363
.2369	7.039E-2	.1596	5.096E-2	.4643	.3197	.2269	4.598
.2358	8.194E-2	.1379	6.491E-2	.4818	.2655	.2698	4.772
.2324	9.399E-2	.1160	8.199E-2	.4913	.2161	.3335	4.880
							4.916

TABLE XVI (Continued)

SCATTERING DIAGRAMS FOR 5.69  $\mu$  DIAMETER FIBERS

$\theta = 0.47123892$

$\phi=0$	$\phi=0.38335$	$\phi=0.77605$	$\phi=1.1678$	$\phi=1.5614$	$\phi=1.9541$	$\phi=2.3468$	$\phi=2.7395$
3.212E-3	7.334E-2	.1417	.1652	.2099	.2419	.1926	3.045E-2
3.607E-3	7.429E-2	.1552	.1631	.2119	.2108	.1707	1.948E-2
4.781E-3	7.529E-2	.1688	.1589	.2109	.1798	.1554	1.210E-2
6.692E-3	7.639E-2	.1821	.1528	.2066	.1500	.1473	7.994E-3
9.277E-3	7.767E-2	.1945	.1450	.1991	.1225	.1468	6.977E-3
1.245E-2	7.916E-2	.2055	.1360	.1884	9.855E-2	.1542	9.047E-3
1.610E-2	8.093E-2	.2146	.1261	.1750	7.887E-2	.1693	1.444E-2
2.012E-2	8.301E-2	.2215	.1156	.1591	6.434E-2	.1920	2.370E-2
2.439E-2	8.543E-2	.2257	.1049	.1413	5.561E-2	.2217	3.768E-2
2.876E-2	8.820E-2	.2270	9.432E-2	.1223	5.315E-2	.2576	5.760E-2
3.313E-2	9.131E-2	.2254	8.410E-2	.1027	5.722E-2	.2988	8.505E-2
3.736E-2	9.470E-2	.2206	7.448E-2	8.339E-2	6.789E-2	.3441	.1219
4.136E-2	9.832E-2	.2128	6.564E-2	6.510E-2	8.502E-2	.3922	.1705
4.503E-2	.1020	.2022	5.771E-2	4.869E-2	.1082	.4417	.2334
4.830E-2	.1058	.1892	5.077E-2	3.493E-2	.1370	.4911	.3132
5.114E-2	.1094	.1741	4.484E-2	2.454E-2	.1707	.5390	.4128
5.350E-2	.1128	.1574	3.994E-2	1.814E-2	.2084	.5839	.5351
5.540E-2	.1158	.1397	3.604E-2	1.620E-2	.2491	.6243	.6827
5.684E-2	.1182	.1217	3.310E-2	1.907E-2	.2918	.6591	.8583
5.786E-2	.1200	.1039	3.110E-2	2.690E-2	.3353	.6871	1.064
5.853E-2	.1209	8.709E-2	3.000E-2	3.966E-2	.3784	.7075	1.301
5.889E-2	.1209	7.168E-2	2.978E-2	5.715E-2	.4200	.7197	1.572
5.904E-2	.1201	5.830E-2	3.045E-2	7.895E-2	.4590	.7232	1.875
5.904E-2	.1182	4.737E-2	3.204E-2	.1045	.4942	.7179	2.212
5.897E-2	.1155	3.925E-2	3.458E-2	.1331	.5248	.7040	2.581
5.891E-2	.1120	3.417E-2	3.815E-2	.1638	.5499	.6819	2.980
5.891E-2	.1078	3.225E-2	4.281E-2	.1957	.5688	.6523	3.405
5.902E-2	.1032	3.344E-2	4.864E-2	.2279	.5811	.6161	3.853
5.929E-2	9.834E-2	3.762E-2	5.568E-2	.2591	.5864	.5743	4.319
5.973E-2	9.351E-2	4.451E-2	6.397E-2	.2884	.5847	.5281	4.798
6.036E-2	8.902E-2	5.375E-2	7.352E-2	.3148	.5759	.4788	5.283
6.116E-2	8.517E-2	6.489E-2	8.426E-2	.3374	.5605	.4278	5.768
6.212E-2	8.226E-2	7.739E-2	9.611E-2	.3554	.5389	.3763	6.244
6.321E-2	8.058E-2	9.071E-2	.1088	.3682	.5117	.3255	6.705
6.439E-2	8.038E-2	.1042	.1223	.3753	.4799	.2767	7.143
6.562E-2	8.187E-2	.1175	.1362	.3765	.4444	.2308	7.551
6.686E-2	8.520E-2	.1298	.1500	.3718	.4062	.1885	7.920
6.808E-2	9.042E-2	.1409	.1636	.3613	.3668	.1504	8.246
6.925E-2	9.754E-2	.1502	.1763	.3454	.3272	.1170	8.521
7.036E-2	.1064	.1574	.1877	.3247	.2887	8.845E-2	8.741
7.140E-2	.1170	.1624	.1974	.2999	.2527	6.461E-2	8.901
7.239E-2	.1288	.1650	.2049	.2720	.2203	4.538E-2	8.998
							9.031

TABLE XVI (Continued)

SCATTERING DIAGRAMS FOR 5.69  $\mu$  DIAMETER FIBERS  
 $\theta = 0.39269910$

$\phi=0$	$\phi=0.38335$	$\phi=0.77605$	$\phi=1.1678$	$\phi=1.5614$	$\phi=1.9541$	$\phi=2.3468$	$\phi=2.7395$
.2710	7.448E-2	1.159E-2	3.207E-2	5.710E-2	6.210E-2	.1472	.6512
.2705	7.864E-2	1.278E-2	2.697E-2	4.405E-2	4.616E-2	.1260	.6054
.2688	8.298E-2	1.400E-2	2.219E-2	3.237E-2	3.286E-2	.1063	.5551
.2661	8.739E-2	1.520E-2	1.793E-2	2.241E-2	2.255E-2	8.852E-2	.5014
.2623	9.176E-2	1.634E-2	1.434E-2	1.449E-2	1.552E-2	7.292E-2	.4453
.2575	9.598E-2	1.740E-2	1.162E-2	8.907E-3	1.195E-2	5.990E-2	.3881
.2519	9.993E-2	1.838E-2	9.909E-3	5.877E-3	1.196E-2	4.974E-2	.3312
.2453	.1034	1.927E-2	9.347E-3	5.575E-3	1.559E-2	4.273E-2	.2760
.2380	.1065	2.009E-2	1.004E-2	8.107E-3	2.279E-2	3.910E-2	.2241
.2301	.1090	2.088E-2	1.210E-2	1.351E-2	3.342E-2	3.905E-2	.1771
.2216	.1108	2.167E-2	1.556E-2	2.175E-2	4.728E-2	4.275E-2	.1365
.2126	.1119	2.251E-2	2.044E-2	3.272E-2	6.408E-2	5.030E-2	.1038
.2032	.1122	2.345E-2	2.674E-2	4.624E-2	8.349E-2	6.179E-2	8.059E-2
.1936	.1116	2.454E-2	3.440E-2	6.207E-2	.1051	7.723E-2	6.820E-2
.1838	.1102	2.581E-2	4.332E-2	7.989E-2	.1284	9.659E-2	6.791E-2
.1740	.1079	2.732E-2	5.339E-2	9.932E-2	.1531	.1198	8.086E-2
.1642	.1048	2.909E-2	6.444E-2	.1199	.1785	.1467	.1079
.1544	.1009	3.114E-2	7.627E-2	.1413	.2042	.1771	.1499
.1449	9.630E-2	3.348E-2	8.867E-2	.1630	.2296	.2108	.2072
.1356	9.104E-2	3.609E-2	.1013	.1844	.2543	.2475	.2801
.1266	8.524E-2	3.897E-2	.1141	.2051	.2778	.2867	.3685
.1180	7.901E-2	4.206E-2	.1267	.2245	.2996	.3281	.4720
.1098	7.247E-2	4.530E-2	.1388	.2423	.3193	.3712	.5901
.1021	6.575E-2	4.864E-2	.1500	.2579	.3366	.4154	.7218
9.499E-2	5.897E-2	5.198E-2	.1603	.2710	.3511	.4601	.8658
8.835E-2	5.228E-2	5.523E-2	.1692	.2812	.3626	.5047	1.020
8.229E-2	4.578E-2	5.830E-2	.1766	.2884	.3709	.5486	1.184
7.683E-2	3.959E-2	6.108E-2	.1822	.2922	.3759	.5911	1.356
7.201E-2	3.381E-2	6.348E-2	.1860	.2926	.3775	.6314	1.532
6.785E-2	2.852E-2	6.540E-2	.1877	.2896	.3758	.6689	1.711
6.436E-2	2.380E-2	6.674E-2	.1873	.2832	.3708	.7028	1.891
6.157E-2	1.970E-2	6.745E-2	.1847	.2736	.3627	.7324	2.068
5.947E-2	1.624E-2	6.745E-2	.1800	.2609	.3516	.7571	2.241
5.809E-2	1.344E-2	6.671E-2	.1733	.2456	.3378	.7764	2.406
5.741E-2	1.129E-2	6.522E-2	.1647	.2280	.3215	.7896	2.562
5.743E-2	9.757E-3	6.298E-2	.1543	.2085	.3031	.7964	2.706
5.813E-2	8.804E-3	6.001E-2	.1424	.1875	.2829	.7964	2.835
5.948E-2	8.374E-3	5.639E-2	.1292	.1657	.2614	.7895	2.948
6.146E-2	8.403E-3	5.219E-2	.1152	.1435	.2389	.7754	3.043
6.401E-2	8.816E-3	4.752E-2	.1005	.1215	.2158	.7542	3.119
6.708E-2	9.537E-3	4.251E-2	8.577E-2	.1002	.1925	.7262	3.174
7.059E-2	1.048E-2	3.730E-2	7.114E-2	8.030E-2	.1695	.6917	3.207
							3.218

TABLE XVI (Continued)

SCATTERING DIAGRAMS FOR 5.69  $\mu$  DIAMETER FIBERS $\theta = 0.31415928$ 

$\phi=0$	$\phi=0.38335$	$\phi=0.77605$	$\phi=1.1678$	$\phi=1.5614$	$\phi=1.9541$	$\phi=2.3468$	$\phi=2.7395$
6.484E-2	6.512E-2	.1704	.1837	7.877E-2	2.677E-2	.1519	.1757
6.498E-2	6.264E-2	.1713	.1909	8.820E-2	2.551E-2	.1429	.1842
6.540E-2	6.024E-2	.1712	.1970	9.765E-2	2.507E-2	.1334	.1935
6.608E-2	5.795E-2	.1702	.2018	.1069	2.547E-2	.1235	.2038
6.702E-2	5.578E-2	.1682	.2052	.1160	2.672E-2	.1135	.2155
6.821E-2	5.376E-2	.1653	.2072	.1246	2.881E-2	.1033	.2287
6.961E-2	5.192E-2	.1614	.2077	.1328	3.174E-2	9.319E-2	.2438
7.121E-2	5.027E-2	.1567	.2067	.1403	3.547E-2	8.321E-2	.2611
7.298E-2	4.884E-2	.1511	.2041	.1471	3.998E-2	7.352E-2	.2811
7.488E-2	4.765E-2	.1448	.2001	.1532	4.524E-2	6.426E-2	.3038
7.688E-2	4.674E-2	.1379	.1947	.1584	5.119E-2	5.555E-2	.3298
7.896E-2	4.611E-2	.1304	.1880	.1627	5.778E-2	4.750E-2	.3592
8.107E-2	4.580E-2	.1225	.1800	.1661	6.495E-2	4.022E-2	.3923
8.317E-2	4.584E-2	.1144	.1709	.1685	7.264E-2	3.382E-2	.4294
8.524E-2	4.624E-2	.1062	.1609	.1700	8.076E-2	2.837E-2	.4705
8.724E-2	4.703E-2	9.810E-2	.1501	.1705	8.923E-2	2.396E-2	.5157
8.912E-2	4.823E-2	9.014E-2	.1387	.1700	9.797E-2	2.063E-2	.5653
9.087E-2	4.985E-2	8.254E-2	.1269	.1686	.1068	1.843E-2	.6191
9.246E-2	5.192E-2	7.546E-2	.1148	.1663	.1158	1.738E-2	.6770
9.384E-2	5.444E-2	6.905E-2	.1028	.1632	.1248	1.749E-2	.7389
9.502E-2	5.742E-2	6.344E-2	9.090E-2	.1593	.1337	1.873E-2	.8047
9.595E-2	6.087E-2	5.877E-2	7.934E-2	.1546	.1423	2.107E-2	.8740
9.664E-2	6.478E-2	5.515E-2	6.832E-2	.1493	.1507	2.447E-2	.9464
9.707E-2	6.914E-2	5.267E-2	5.799E-2	.1433	.1586	2.886E-2	1.021
9.722E-2	7.394E-2	5.140E-2	4.852E-2	.1369	.1661	3.416E-2	1.098
9.711E-2	7.914E-2	5.140E-2	4.004E-2	.1300	.1729	4.026E-2	1.177
9.672E-2	8.472E-2	5.269E-2	3.268E-2	.1228	.1791	4.707E-2	1.257
9.607E-2	9.064E-2	5.528E-2	2.652E-2	.1153	.1845	5.447E-2	1.338
9.516E-2	9.684E-2	5.915E-2	2.164E-2	.1076	.1891	6.234E-2	1.417
9.400E-2	.1032	6.424E-2	1.810E-2	9.990E-2	.1929	7.056E-2	1.496
9.261E-2	.1098	7.049E-2	1.592E-2	9.214E-2	.1957	7.901E-2	1.573
9.099E-2	.1165	7.781E-2	1.511E-2	8.446E-2	.1975	8.759E-2	1.648
8.918E-2	.1231	8.606E-2	1.567E-2	7.694E-2	.1983	9.619E-2	1.719
8.720E-2	.1297	9.512E-2	1.753E-2	6.966E-2	.1980	.1047	1.786
8.505E-2	.1362	.1048	2.066E-2	6.272E-2	.1967	.1131	1.848
8.278E-2	.1423	.1150	2.497E-2	5.617E-2	.1944	.1213	1.904
8.039E-2	.1481	.1254	3.037E-2	5.009E-2	.1911	.1293	1.954
7.792E-2	.1535	.1360	3.674E-2	4.454E-2	.1867	.1371	1.998
7.538E-2	.1583	.1465	4.398E-2	3.959E-2	.1814	.1448	2.035
7.281E-2	.1624	.1567	5.194E-2	3.530E-2	.1752	.1523	2.063
7.023E-2	.1659	.1664	6.049E-2	3.170E-2	.1682	.1599	2.084
6.766E-2	.1685	.1755	6.948E-2	2.885E-2	.1604	.1676	2.097
							2.101

TABLE XVI (Continued)

SCATTERING DIAGRAMS FOR 5.69  $\mu$  DIAMETER FIBERS  
 $\theta = 0.23561946$

$\phi=0$	$\phi=0.38335$	$\phi=0.77605$	$\phi=1.1678$	$\phi=1.5614$	$\phi=1.9541$	$\phi=2.3468$	$\phi=2.7395$
6.882E-3	2.591E-2	1.176E-2	4.714E-2	6.152E-2	1.928E-2	.1978	1.371E-2
6.891E-3	2.622E-2	1.266E-2	4.518E-2	6.571E-2	1.587E-2	.2031	1.740E-2
6.918E-3	2.646E-2	1.367E-2	4.310E-2	6.984E-2	1.279E-2	.2077	2.277E-2
6.965E-3	2.663E-2	1.482E-2	4.092E-2	7.390E-2	1.008E-2	.2118	2.987E-2
7.031E-3	2.672E-2	1.608E-2	3.865E-2	7.783E-2	7.752E-3	.2152	3.874E-2
7.117E-3	2.674E-2	1.746E-2	3.632E-2	8.161E-2	5.838E-3	.2180	4.940E-2
7.225E-3	2.668E-2	1.895E-2	3.394E-2	8.522E-2	4.362E-3	.2200	6.188E-2
7.355E-3	2.654E-2	2.054E-2	3.154E-2	8.861E-2	3.345E-3	.2213	7.617E-2
7.510E-3	2.632E-2	2.222E-2	2.915E-2	9.177E-2	2.805E-3	.2219	9.226E-2
7.689E-3	2.603E-2	2.399E-2	2.677E-2	9.465E-2	2.758E-3	.2217	.1101
7.896E-3	2.566E-2	2.583E-2	2.445E-2	9.725E-2	3.215E-3	.2207	.1297
8.131E-3	2.521E-2	2.773E-2	2.219E-2	9.953E-2	4.184E-3	.2189	.1510
8.396E-3	2.470E-2	2.968E-2	2.003E-2	.1014	5.672E-3	.2163	.1739
8.692E-3	2.412E-2	3.167E-2	1.799E-2	.1030	7.680E-3	.2129	.1983
9.021E-3	2.348E-2	3.368E-2	1.608E-2	.1042	1.020E-2	.2088	.2242
9.383E-3	2.278E-2	3.571E-2	1.434E-2	.1051	1.325E-2	.2038	.2514
9.780E-3	2.203E-2	3.772E-2	1.278E-2	.1055	1.680E-2	.1981	.2798
1.021E-2	2.124E-2	3.972E-2	1.142E-2	.1055	2.084E-2	.1917	.3093
1.067E-2	2.041E-2	4.167E-2	1.029E-2	.1052	2.537E-2	.1847	.3396
1.118E-2	1.956E-2	4.358E-2	9.396E-3	.1044	3.037E-2	.1770	.3708
1.171E-2	1.868E-2	4.543E-2	8.754E-3	.1032	3.581E-2	.1687	.4025
1.228E-2	1.779E-2	4.719E-2	8.380E-3	.1016	4.168E-2	.1598	.4347
1.288E-2	1.689E-2	4.885E-2	8.285E-3	9.973E-3	4.794E-2	.1506	.4671
1.352E-2	1.600E-2	5.040E-2	8.480E-3	9.741E-3	5.457E-2	.1409	.4995
1.417E-2	1.513E-2	5.183E-2	8.970E-3	9.473E-3	6.154E-2	.1309	.5319
1.486E-2	1.428E-2	5.313E-2	9.760E-3	9.172E-3	6.881E-2	.1207	.5638
1.557E-2	1.346E-2	5.427E-2	1.085E-2	8.839E-3	7.635E-2	.1104	.5953
1.629E-2	1.269E-2	5.525E-2	1.225E-2	8.478E-3	8.412E-2	.1000	.6260
1.703E-2	1.197E-2	5.606E-2	1.394E-2	8.091E-3	9.208E-2	8.972E-2	.6559
1.778E-2	1.131E-2	5.669E-2	1.593E-2	7.681E-3	.1001	7.957E-2	.6846
1.853E-2	1.072E-2	5.713E-2	1.821E-2	7.252E-3	.1084	6.970E-2	.7120
1.928E-2	1.022E-2	5.738E-2	2.076E-2	6.806E-3	.1166	6.022E-2	.7380
2.003E-2	9.800E-3	5.743E-2	2.357E-2	6.348E-3	.1249	5.125E-2	.7623
2.077E-2	9.476E-3	5.727E-2	2.663E-2	5.881E-3	.1332	4.288E-2	.7849
2.148E-2	9.253E-3	5.692E-2	2.992E-2	5.409E-3	.1413	3.526E-2	.8055
2.218E-2	9.140E-3	5.635E-2	3.341E-2	4.936E-3	.1494	2.847E-2	.8240
2.284E-2	9.141E-3	5.559E-2	3.709E-2	4.466E-3	.1572	2.265E-2	.8403
2.347E-2	9.261E-3	5.463E-2	4.092E-2	4.003E-3	.1649	1.790E-2	.8543
2.406E-2	9.506E-3	5.348E-2	4.489E-2	3.550E-3	.1722	1.432E-2	.8659
2.461E-2	9.877E-3	5.215E-2	4.897E-2	3.113E-3	.1792	1.202E-2	.8750
2.510E-2	1.037E-2	5.064E-2	5.312E-2	2.694E-3	.1859	1.110E-2	.8815
2.554E-2	1.100E-2	4.897E-2	5.731E-2	2.298E-3	.1921	1.163E-2	.8855
							.8868



TABLE XVI (Continued)

SCATTERING DIAGRAMS FOR 5.69  $\mu$  DIAMETER FIBERS  
 $\theta = 0.15707964$

$\phi=0$	$\phi=0.38335$	$\phi=0.77605$	$\phi=1.1678$	$\phi=1.5614$	$\phi=1.9541$	$\phi=2.3468$	$\phi=2.7395$
2.712E-2	3.660E-2	1.638E-2	2.623E-2	4.752E-2	6.247E-3	4.291E-2	9.019E-2
2.713E-2	3.641E-2	1.608E-2	2.711E-2	4.665E-2	6.642E-3	4.312E-2	9.364E-2
2.718E-2	3.619E-2	1.581E-2	2.803E-2	4.570E-2	7.126E-3	4.330E-2	9.721E-2
2.727E-2	3.592E-2	1.557E-2	2.897E-2	4.467E-2	7.696E-3	4.344E-2	.1008
2.739E-2	3.563E-2	1.534E-2	2.993E-2	4.358E-2	8.349E-3	4.356E-2	.1046
2.754E-2	3.530E-2	1.514E-2	3.091E-2	4.241E-2	9.080E-3	4.366E-2	.1085
2.772E-2	3.493E-2	1.496E-2	3.191E-2	4.119E-2	9.884E-3	4.374E-2	.1124
2.793E-2	3.454E-2	1.480E-2	3.292E-2	3.990E-2	1.075E-2	4.382E-2	.1164
2.817E-2	3.412E-2	1.467E-2	3.394E-2	3.857E-2	1.169E-2	4.389E-2	.1205
2.844E-2	3.367E-2	1.455E-2	3.498E-2	3.719E-2	1.269E-2	4.397E-2	.1246
2.873E-2	3.319E-2	1.447E-2	3.601E-2	3.577E-2	1.373E-2	4.406E-2	.1288
2.905E-2	3.269E-2	1.440E-2	3.705E-2	3.431E-2	1.483E-2	4.417E-2	.1331
2.938E-2	3.217E-2	1.436E-2	3.809E-2	3.282E-2	1.596E-2	4.430E-2	.1373
2.974E-2	3.163E-2	1.434E-2	3.912E-2	3.132E-2	1.713E-2	4.447E-2	.1416
3.011E-2	3.107E-2	1.435E-2	4.014E-2	2.980E-2	1.833E-2	4.467E-2	.1458
3.050E-2	3.050E-2	1.438E-2	4.114E-2	2.827E-2	1.955E-2	4.492E-2	.1501
3.089E-2	2.991E-2	1.443E-2	4.212E-2	2.674E-2	2.079E-2	4.523E-2	.1543
3.130E-2	2.932E-2	1.451E-2	4.308E-2	2.522E-2	2.203E-2	4.560E-2	.1586
3.171E-2	2.871E-2	1.461E-2	4.401E-2	2.371E-2	2.328E-2	4.603E-2	.1627
3.212E-2	2.810E-2	1.474E-2	4.490E-2	2.222E-2	2.453E-2	4.655E-2	.1668
3.253E-2	2.748E-2	1.490E-2	4.576E-2	2.076E-2	2.577E-2	4.714E-2	.1709
3.294E-2	2.687E-2	1.509E-2	4.658E-2	1.933E-2	2.699E-2	4.782E-2	.1748
3.335E-2	2.625E-2	1.530E-2	4.734E-2	1.795E-2	2.819E-2	4.860E-2	.1787
3.374E-2	2.563E-2	1.554E-2	4.806E-2	1.661E-2	2.937E-2	4.948E-2	.1825
3.413E-2	2.502E-2	1.581E-2	4.872E-2	1.532E-2	3.052E-2	5.046E-2	.1862
3.450E-2	2.442E-2	1.611E-2	4.932E-2	1.410E-2	3.163E-2	5.156E-2	.1897
3.485E-2	2.382E-2	1.644E-2	4.985E-2	1.294E-2	3.271E-2	5.278E-2	.1931
3.518E-2	2.323E-2	1.680E-2	5.032E-2	1.185E-2	3.374E-2	5.411E-2	.1963
3.549E-2	2.266E-2	1.719E-2	5.072E-2	1.083E-2	3.473E-2	5.557E-2	.1994
3.578E-2	2.209E-2	1.762E-2	5.104E-2	9.904E-3	3.566E-2	5.716E-2	.2024
3.604E-2	2.154E-2	1.808E-2	5.128E-2	9.053E-3	3.655E-2	5.889E-2	.2051
3.628E-2	2.101E-2	1.857E-2	5.144E-2	8.291E-3	3.738E-2	6.074E-2	.2077
3.648E-2	2.049E-2	1.910E-2	5.152E-2	7.619E-3	3.816E-2	6.274E-2	.2100
3.665E-2	1.999E-2	1.966E-2	5.151E-2	7.041E-3	3.888E-2	6.487E-2	.2122
3.679E-2	1.950E-2	2.026E-2	5.142E-2	6.559E-3	3.955E-2	6.714E-2	.2142
3.690E-2	1.904E-2	2.089E-2	5.124E-2	6.174E-3	4.015E-2	6.955E-2	.2159
3.697E-2	1.860E-2	2.155E-2	5.097E-2	5.888E-3	4.070E-2	7.210E-2	.2174
3.700E-2	1.817E-2	2.225E-2	5.062E-2	5.702E-3	4.120E-2	7.478E-2	.2187
3.699E-2	1.777E-2	2.298E-2	5.017E-2	5.615E-3	4.164E-2	7.761E-2	.2198
3.695E-2	1.739E-2	2.374E-2	4.964E-2	5.627E-3	4.203E-2	8.056E-2	.2206
3.687E-2	1.703E-2	2.454E-2	4.901E-2	5.738E-3	4.237E-2	8.365E-2	.2212
3.676E-2	1.669E-2	2.537E-2	4.831E-2	5.945E-3	4.267E-2	8.686E-2	.2216
							.2217

TABLE XVI (Continued)

SCATTERING DIAGRAMS FOR 5.69  $\mu$  DIAMETER FIBERS  
 $\theta = 0.07853982$

$\phi=0$	$\phi=0.38335$	$\phi=0.77605$	$\phi=1.1678$	$\phi=1.5614$	$\phi=1.9541$	$\phi=2.3468$	$\phi=2.7395$
6.070E-3	6.985E-3	9.931E-3	1.209E-2	9.092E-3	4.083E-3	9.595E-3	2.945E-2
6.070E-3	7.033E-3	1.001E-2	1.209E-2	8.960E-3	4.037E-3	9.938E-3	2.995E-2
6.072E-3	7.082E-3	1.009E-2	1.208E-2	8.825E-3	3.997E-3	1.029E-2	3.045E-2
6.074E-3	7.133E-3	1.017E-2	1.207E-2	8.690E-3	3.964E-3	1.065E-2	3.094E-2
6.077E-3	7.184E-3	1.025E-2	1.206E-2	8.553E-3	3.939E-3	1.102E-2	3.143E-2
6.081E-3	7.238E-3	1.033E-2	1.205E-2	8.415E-3	3.920E-3	1.140E-2	3.192E-2
6.086E-3	7.292E-3	1.041E-2	1.203E-2	8.276E-3	3.908E-3	1.179E-2	3.239E-2
6.092E-3	7.348E-3	1.048E-2	1.200E-2	8.135E-3	3.905E-3	1.219E-2	3.286E-2
6.099E-3	7.406E-3	1.056E-2	1.198E-2	7.995E-3	3.908E-3	1.260E-2	3.332E-2
6.107E-3	7.464E-3	1.064E-2	1.195E-2	7.853E-3	3.920E-3	1.301E-2	3.377E-2
6.116E-3	7.524E-3	1.071E-2	1.191E-2	7.711E-3	3.940E-3	1.344E-2	3.422E-2
6.126E-3	7.585E-3	1.079E-2	1.188E-2	7.569E-3	3.968E-3	1.387E-2	3.465E-2
6.137E-3	7.648E-3	1.086E-2	1.184E-2	7.427E-3	4.004E-3	1.431E-2	3.508E-2
6.149E-3	7.711E-3	1.093E-2	1.179E-2	7.285E-3	4.050E-3	1.476E-2	3.550E-2
6.161E-3	7.776E-3	1.100E-2	1.174E-2	7.143E-3	4.103E-3	1.521E-2	3.591E-2
6.175E-3	7.842E-3	1.107E-2	1.169E-2	7.002E-3	4.166E-3	1.567E-2	3.630E-2
6.190E-3	7.909E-3	1.114E-2	1.164E-2	6.861E-3	4.238E-3	1.614E-2	3.669E-2
6.206E-3	7.978E-3	1.120E-2	1.158E-2	6.721E-3	4.319E-3	1.661E-2	3.706E-2
6.223E-3	8.047E-3	1.126E-2	1.152E-2	6.582E-3	4.410E-3	1.709E-2	3.743E-2
6.241E-3	8.118E-3	1.133E-2	1.145E-2	6.444E-3	4.510E-3	1.758E-2	3.778E-2
6.260E-3	8.189E-3	1.139E-2	1.138E-2	6.308E-3	4.619E-3	1.807E-2	3.812E-2
6.280E-3	8.262E-3	1.145E-2	1.131E-2	6.173E-3	4.739E-3	1.857E-2	3.845E-2
6.302E-3	8.335E-3	1.150E-2	1.123E-2	6.040E-3	4.868E-3	1.907E-2	3.876E-2
6.324E-3	8.410E-3	1.156E-2	1.116E-2	5.909E-3	5.007E-3	1.957E-2	3.906E-2
6.348E-3	8.485E-3	1.161E-2	1.107E-2	5.780E-3	5.156E-3	2.008E-2	3.935E-2
6.372E-3	8.561E-3	1.166E-2	1.099E-2	5.654E-3	5.315E-3	2.059E-2	3.962E-2
6.398E-3	8.638E-3	1.170E-2	1.090E-2	5.530E-3	5.484E-3	2.111E-2	3.988E-2
6.426E-3	8.716E-3	1.175E-2	1.081E-2	5.409E-3	5.664E-3	2.163E-2	4.013E-2
6.454E-3	8.795E-3	1.179E-2	1.071E-2	5.292E-3	5.853E-3	2.215E-2	4.036E-2
6.483E-3	8.874E-3	1.183E-2	1.061E-2	5.177E-3	6.054E-3	2.267E-2	4.057E-2
6.514E-3	8.953E-3	1.187E-2	1.051E-2	5.066E-3	6.264E-3	2.320E-2	4.077E-2
6.546E-3	9.033E-3	1.190E-2	1.041E-2	4.958E-3	6.485E-3	2.372E-2	4.096E-2
6.580E-3	9.114E-3	1.194E-2	1.030E-2	4.855E-3	6.716E-3	2.425E-2	4.113E-2
6.614E-3	9.195E-3	1.196E-2	1.019E-2	4.755E-3	6.958E-3	2.477E-2	4.128E-2
6.650E-3	9.276E-3	1.199E-2	1.008E-2	4.660E-3	7.210E-3	2.530E-2	4.142E-2
6.687E-3	9.358E-3	1.201E-2	9.965E-3	4.570E-3	7.472E-3	2.583E-2	4.154E-2
6.726E-3	9.440E-3	1.203E-2	9.847E-3	4.484E-3	7.745E-3	2.635E-2	4.165E-2
6.766E-3	9.522E-3	1.205E-2	9.726E-3	4.403E-3	8.028E-3	2.687E-2	4.174E-2
6.807E-3	9.604E-3	1.207E-2	9.604E-3	4.328E-3	8.321E-3	2.739E-2	4.181E-2
6.849E-3	9.686E-3	1.208E-2	9.479E-3	4.258E-3	8.624E-3	2.791E-2	4.187E-2
6.893E-3	9.767E-3	1.208E-2	9.352E-3	4.194E-3	8.938E-3	2.843E-2	4.191E-2
6.938E-3	9.849E-3	1.209E-2	9.223E-3	4.135E-3	9.261E-3	2.894E-2	4.193E-2
							4.194E-2

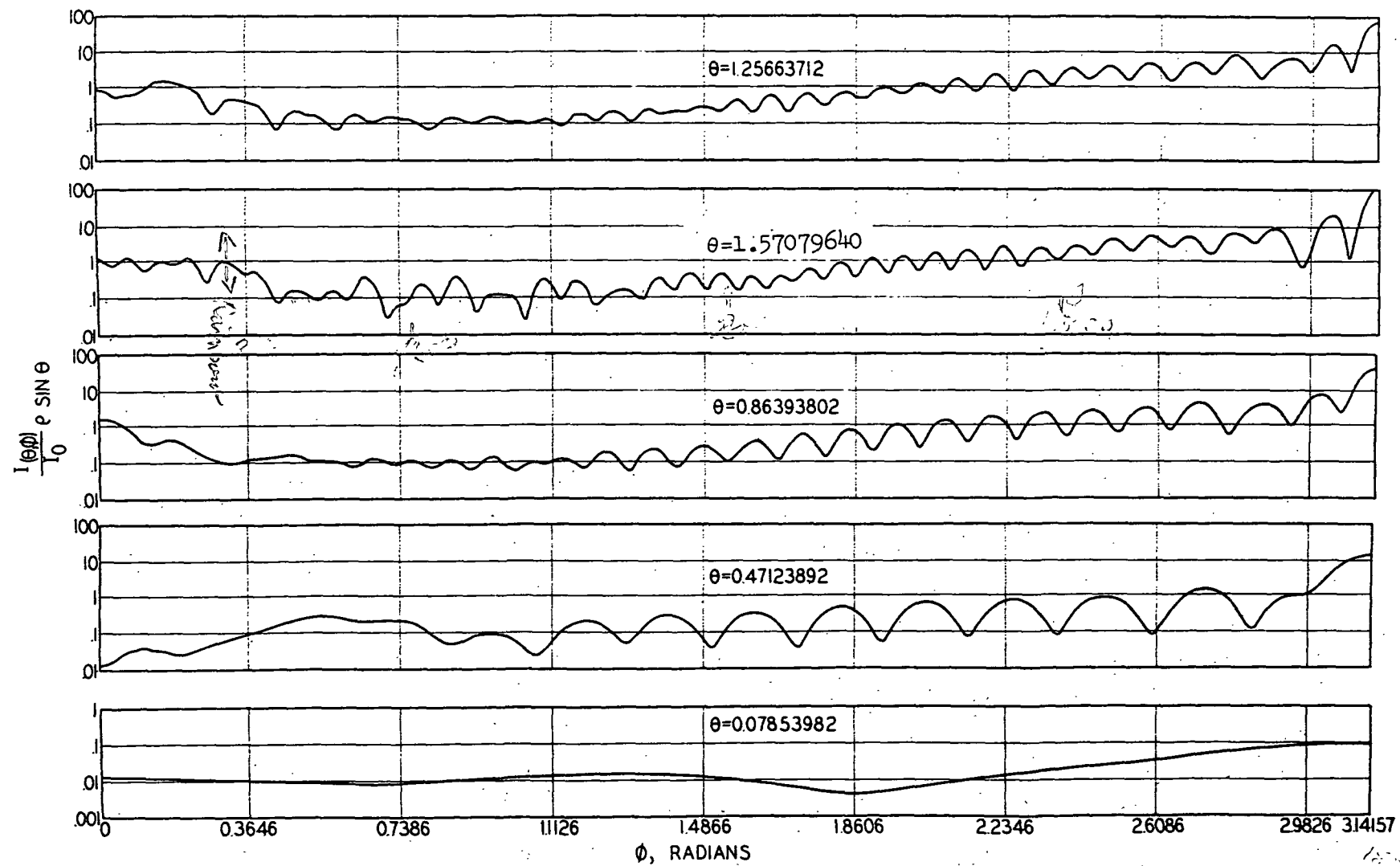


Figure 25. Scattering Diagrams for the 9.02  $\mu$  Diameter Fiber

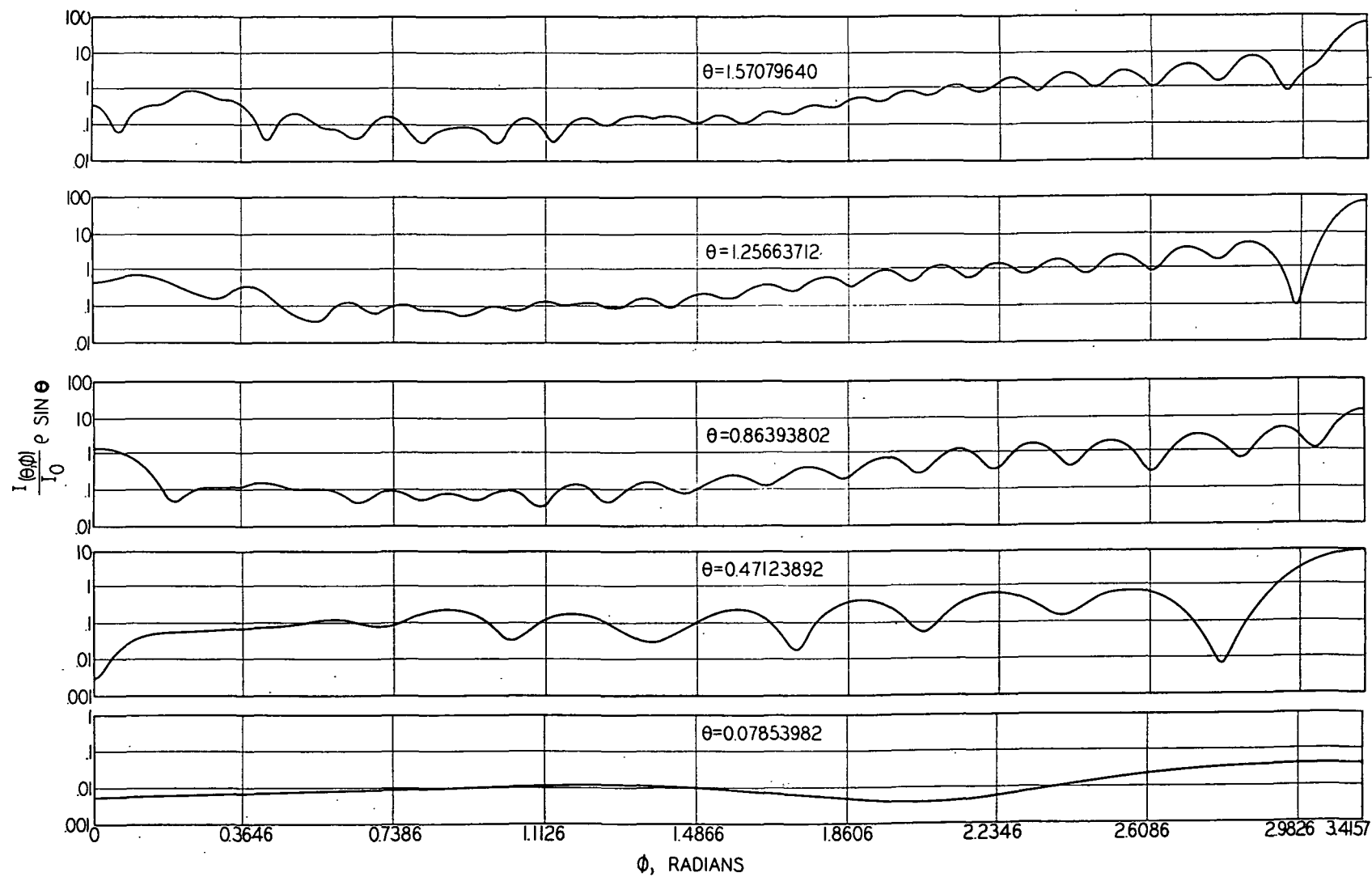


Figure 26. Scattering Diagrams for the 5.69  $\mu$  Diameter Fiber

### APPENDIX III

#### THE DISTRIBUTION OF LIGHT REFLECTED FROM A SINGLE FIBER

The light scattered backwards from a single fiber was calculated as a function of the angle  $\gamma$ . The angle  $\gamma$  is defined as the angle in a plane perpendicular to the fiber axis where  $\gamma = 0$  indicates direct back scattering. Thus, the angle  $\gamma$  defines a plane passing through the fiber axis. If the fiber were in a sheet with the fiber axis in the sheet plane,  $\gamma = 0$  would be the normal to the sheet and  $\gamma = \pi/2$  would be the grazing angles. The form of the distribution would be similar for a single layer of fibers arranged randomly in a plane, except that the distribution would be axially symmetrical about the normal to the layer, whereas there is no axial symmetry in the case of the single fiber.

The total light scattered per unit incident intensity was calculated for fourteen equal intervals of  $\gamma$  assuming isotropic illumination of the fiber. The total intensity back scattered per unit length of fiber is simply the sum of the intensities in each angle interval. Thus, two separate calculations were made to find the total light back-scattered from a unit length of fiber, one by summing the intensities in each interval and one from the integration procedure described previously in Appendix I. This served as a check on the accuracy of the two computations, both of which were performed on the IBM 1620 computer. The results agreed which indicated that the programs used for the computations and the methods which were used for the calculations were no doubt satisfactory in both cases. The results of these computations are tabulated in Table XVII and are shown in Fig. 27.

It would be difficult to relate the distribution of the light reflected from a single layer to the light distribution reflected from a multilayer sheet. The top layer of the multilayer sheet would reflect the incident, isotropic illumination

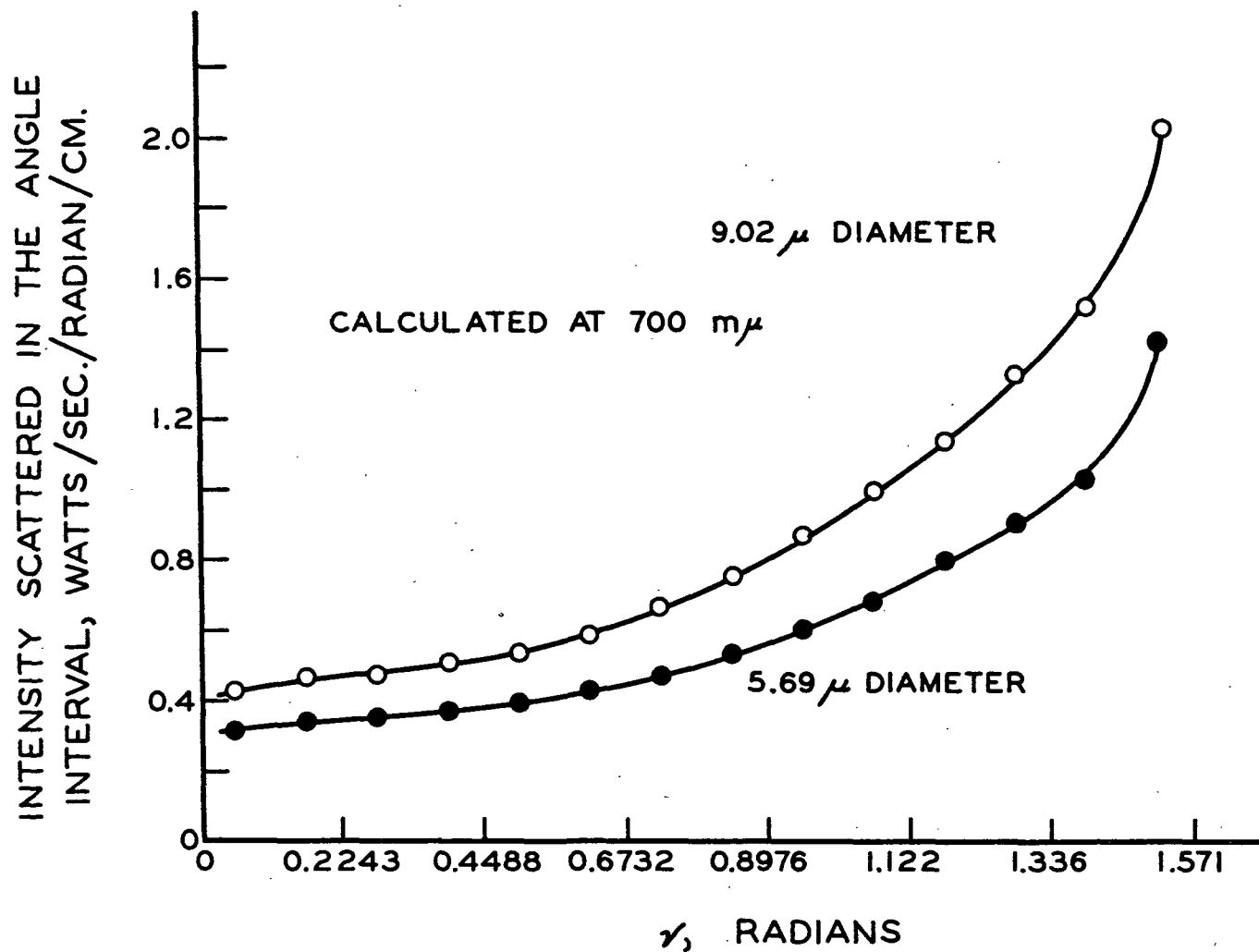
as shown in Fig. 27, but it would also transmit the light reflected from the layer below. No attempt was made to determine this distribution. The most that can be said is that the nonisotropic distribution from a single fiber definitely does not indicate that the reflectance from a multilayer sheet would be isotropic.

TABLE XVII

DISTRIBUTION OF LIGHT SCATTERED FROM A SINGLE FIBER

$\gamma$ , Radians Angle Interval	Intensity <sup>a</sup>	
	5.69 $\mu$ diameter	9.02 $\mu$ diameter
0.0 0.1121	0.3134	0.4268
0.1121 0.2243	0.3408	0.4626
0.2243 0.3366	0.3538	0.4793
0.3366 0.4488	0.3729	0.5068
0.4488 0.5610	0.3972	0.5465
0.5610 0.6732	0.4304	0.5984
0.6732 0.7854	0.4780	0.6719
0.7854 0.8976	0.5345	0.7614
0.8976 1.010	0.6065	0.8742
1.010 1.122	0.6828	1.0021
1.122 1.234	0.7909	1.1496
1.234 1.346	0.8976	1.3235
1.346 1.458	1.0267	1.5220
1.458 1.571	1.5076	2.0496

<sup>a</sup>The quantities tabulated are the intensities of the light scattered from a single fiber in the angle interval 0.1121 radians wide.



The quantity plotted is the intensity in the angle interval 0.1121 radians wide.

Figure 27. Distribution of Light Scattered from a Single Fiber